Aalto University
School of Engineering

Master's degree in Mineral and Environmental Engineering

Mateusz Janiszewski

Geotechnical risk assessment in the Pyhäsalmi mine with a focus on seismic risk

Master's Thesis

Espoo

Supervisor: Professor Mikael Rinne

Aalto University
School of Engineering

Aalto University, P.O. BOX 11000, 00076
AALTO
www.aalto.fi

Abstract of Master's thesis

Author Mateusz Janiszewski

Title of thesis Geotechnical risk assessment in the Pyhäsalmi mine with a focus on seismic risk

Department Civil and Environmental Engineering

Professorship Rock Engineering **Code of professorship** RAK-32

Thesis supervisor Prof. Mikael Rinne

Thesis advisor Wen Zhijie

Date 05.08.2014 **Number of pages** 79 +37 **Language** English

Abstract

Due to a constant depletion of shallower deposits underground mining is pushing production to larger depths resulting in more difficult ground conditions and an increase of rock stresses. Mining at larger depth effects in an increase in seismic activity, therefore seismic risk is becoming more important and requires special attention. This necessitates development of frameworks and guidelines to tackle those risks more efficiently.

The scope of this study was to apply and test the Geotechnical Risk Assessment guideline for underground mines developed at Aalto University as part of the project: Innovative Technologies and Concepts for the Intelligent Deep Mine of the Future (I2mine), work package 3 - "Rock mechanics and ground control", under the 7th framework of the European Union. The goal was to use seismic monitoring data from the Pyhäsalmi mine in order to quantify the seismic risk, using proposed guideline as a framework for evaluation. Furthermore, the research was aimed to give answers on: what is the applicability of the guideline, what are the main issues encountered during its usage and how to improve it.

Geotechnical Hazard Potential was evaluated using a proposed methodology. Next, seismic risk in the Pyhäsalmi mine was assessed. Seismic events from the database were clustered into logical groups in order to speed up the analysis. Then, the maximum predicted size of a seismic event was found for each cluster group. Seismic risk was assessed based on the largest possible seismic event attributable with a particular damage that is expected. The final risk was evaluated using two methodologies: one that is currently used in the mining industry and second under the development.

The level of seismic risk in the Pyhäsalmi mine was found to be low. The biggest risk was found in areas located at the northern ore-waste contact zone. Installation of additional ground support was recommended in order to lower the risk. The Geotechnical Risk Assessment guideline was found to be suitable framework for risk assessment purposes, which supports in selection of appropriate assessment approach and aids in selection of tools that are used throughout the evaluation. Its applicability was found to be high, however minor changes were recommended in order to use its full functionality.

Keywords Mining, risk assessment, seismic hazard, Pyhäsalmi mine

Foreword

Foremost, I would like to express my sincere gratitude to my supervisor Prof. Mikael Rinne for his continuous support and guidance that helped me throughout this study. Besides my supervisor, I would like to thank my advisor Wen Zhijie for his enthusiasm, knowledge and insightful observations in all the time of research. Completion of this thesis would not have been possible without their commitment and effort.

My sincere thanks also goes to Pekka Bergström from the Pyhäsalmi mine who supported me with collection of all the required data and gave answers to many questions during research and writing of this thesis.

I thank my colleagues from the Rock Engineering department at Aalto University for their assistance and all the stimulating discussions we had for the last months. In particular, I am grateful to Otto Hedström for solving many organizational glitches that would take much more time without his assistance.

Finally, I would like to thank my parents for supporting me spiritually during my whole life.

Espoo 05.08.2014

Mateusz Janiszewski

Table of contents

List of figures

List of tables

Nomenclature

AEC	Absorbed Energy Capacity
ASTH	Apparent Stress Time History
EVP	Excavation Vulnerability Potential
F-M diagram	The Gutenberg-Richter Frequency Magnitude Diagram
GHP	Geotechnical Hazard Potential
GRA	Geotechnical Risk Assessment
I^2mine	Innovative Technologies and Concepts for the Intelligent Deep Mine of the Future
MAG, M_L	Local magnitude
PASRA	Probabilistic Approach for Seismic Risk Assessment
PPV	Peak Particle Velocity
QSHRAF	Quantitative Seismic Hazard and Risk Assessment Approach developed by the Australian Centre for Geomechanics
QTCLUST	Quality Threshold Clustering algorithm
REC	Released Energy Capacity
RDP	Rockburst Damage Potential
SHS	Seismic Hazard Scale
SLINK	Single Linkage Hierarchical Clustering algorithm
SRR	Seismic Risk Rating

1 Introduction

These days, shallower deposits are being depleted and underground mines are pushing to larger depths. This results in much more difficult rock stress conditions that pose more geotechnical risks on mining operations. Larger stresses are also attributable with an increase in seismic activity, therefore seismic risk becomes more significant and necessitates special attention. Development of frameworks and guidelines for underground mines is required to assess and manage those risks. This study is part of the I^2mine project (Innovative Technologies and Concepts for the Intelligent Deep Mine of the Future) work package 3 - "Rock mechanics and ground control", under the 7th framework of the European Union, which aims for new approaches in rock mechanics and ground control to prevent geotechnical related accidents and financial losses in underground mines with increasing mining depths in the future.

1.1 Motivation

The main reason of this study is to investigate practical application of the Geotechnical Risk Assessment guideline for underground mines proposed by Ritesh Kumar Mishra in his Master thesis at Aalto University. A preliminary study to test this guideline was made at the Garpenberg mine in the fall of 2013 (Froehlich, 2014). The study revealed that the analysis of seismic events appears to be a valuable tool to analyze geotechnical risks. The study at the Pyhäsalmi mine aims to improve this method by applying more extensive database.

1.2 Objectives

The main objective is to apply the Geotechnical Risk Assessment guideline using data from the Pyhäsalmi mine. The study focuses on the seismic hazard by evaluation of both the probability and the consequence of an undesirable event. The goal is to establish a risk ranking for different areas under investigation by analyzing the seismic events database and other factors influencing the risk. The research question posed in this thesis is:

- What is the level of seismic risk in the Pyhäsalmi mine and which areas in the mine require special attention in terms of risk related to seismic events?

The second objective is to suggest on how to improve the Geotechnical Risk Assessment guideline using the experience of testing it with real data from the mine. The research questions associated with the second objective are:

- What is the applicability of the guideline and what are the main issues encountered during its usage?
- Which features of the guideline can be changed to improve it?

1.3 Structure

The thesis is divided into seven main parts. Chapter 2 gives an overview of the Pyhäsalmi mine and describes: geological and rock mechanical conditions, basic information on mining method and ground support used in the mine, and seismic monitoring system. Next, chapter 3 provides a theoretical background for this study and briefly defines three aspects: the Geotechnical Risk Assessment guideline and its main aspects that are used in this thesis, mine seismicity and basic definitions related to it and data clustering procedure with a focus on clustering of seismic events. Then, chapter 4 describes the process of geotechnical risk assessment performed in the Pyhäsalmi mine according to the guideline, as well as evaluation of geotechnical hazard potential. Selection of risk assessment approach and hazard identification is presented. Next, chapter 5 focuses on seismic risk assessment using two methods: one that is used in the mining industry and second new approach under the development. Chapter 6 gives a discussion on seismic risk assessment in the Pyhäsalmi mine and strengths and weaknesses of the Geotechnical Risk Assessment guideline encountered during this study. Finally, chapters 7 and 8 present final conclusions and recommendations for future work.

2 General description of the Pyhäsalmi mine

The Pyhäsalmi mine (63º39’31’’N - 26º02’48’’E) is located in central Finland about 450km north from Helsinki (Figure 2-1). It is an underground copper, zinc and pyrite mine owned by First Quantum Minerals. It is the oldest Finnish metal mine in operation and one of the oldest in Europe. Pyhäsalmi is the deepest mine in Europe, with the depth reaching 1445m.

Figure 2-1. Location of the Pyhäsalmi mine. Source: Google Maps

The orebody with reserves of 30Mt was discovered in 1958, and production of ore started in 1962 with an open pit mining and continued until 1976 when it was switched to underground mining. In late 1990’s the deposit was close to depletion and deep drilling program lead to a discovery of the orebody extension below the 1050m level and doubling of ore reserves. Production in the “new mine” started in 2001 with a projected mine life of about 14 years. The access to the mine provides a 1450m deep, 5m-diameter shaft installed during the expansion and an extended ramp (Figure 2-2).

As at December 31, 2012, the proven reserves amounted to 8,5Mt of ore, and measured resources estimated to further 8Mt. In the year 2013 the ore milled amounted 1,3Mt, resulting in production of 14 800t of copper, 21 600t of zinc and 825 800t of pyrite. (First Quantum Minerals, 2013).

The mine has outstanding safety records, as well as high efficiency. Currently it employs 210 people directly and 50 through subcontractors (Trzaska, et al., 2010; First Quantum Minerals, 2013). At present production commences on the levels between -1050 and -1350. At the current metal prices, the end of mining is expected in 2019, with lower tonnage already in 2018 (Pyhäsalmi Mine Oy, 2013).

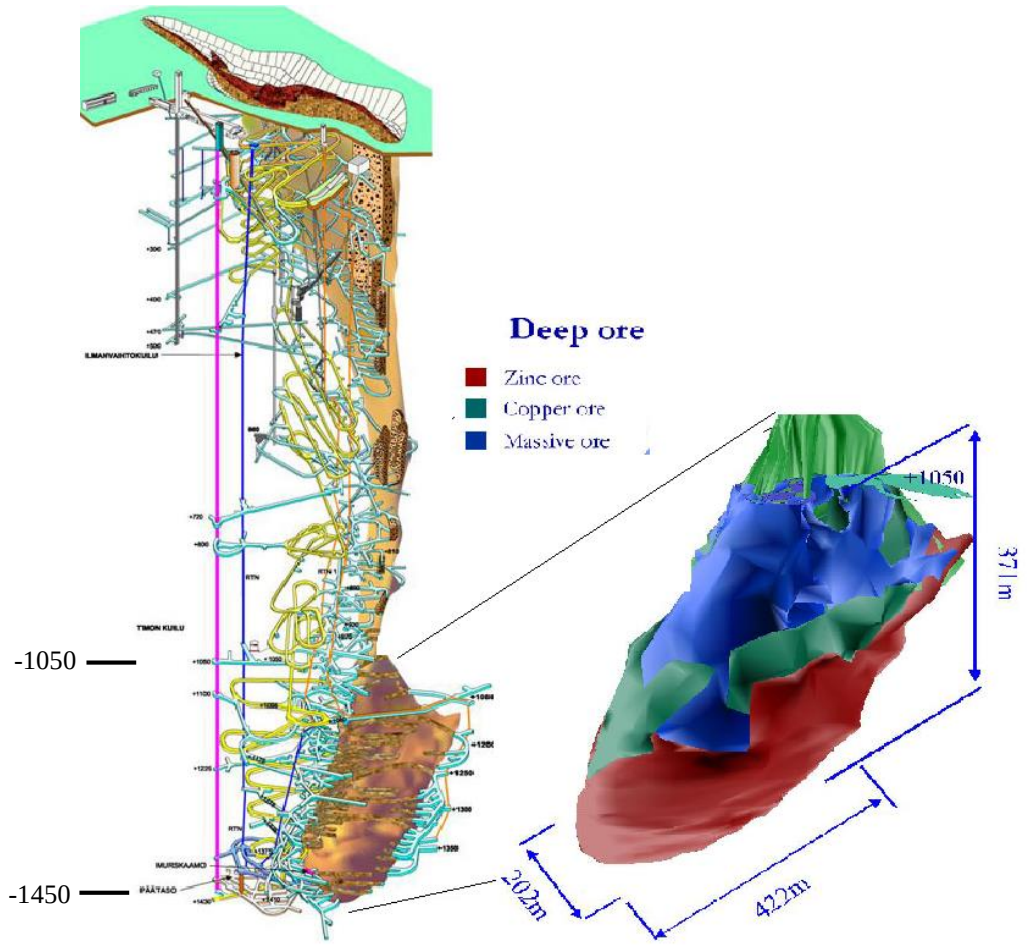

Figure 2-2. Pyhäsalmi mine underground layout and deep ore dimensions (Numminen, 2012).

2.1 Geology

The bedrock in the area of the Pyhäsalmi mine is part of the Svecofennian domain between the Central Finland Granitoid Complex in the southwest and the Archean Basement Complex in the east. Structurally it belongs to a crossing zone of the Raahe-Ladoga Zone trending NW and the Oulujärvi Shear Zone trending SE. In terms of lithology it belongs to the Savo Schist Belt trending NW (Puustjärvi, 2006).

The Pyhäsalmi orebody is a typical Zn-Cu volcanogenic massive sulfide deposit situated in the hinge of a large syncline, surrounded by volcanites and an alteration halo. The ore extents from the surface (outcropping with an area of 650m length and 80m width) down to 1410m depth (Figure 2-2). The deposit consists of massive ore containing 70% of medium- to coarse-grained sulfides. Originally it had no fractures or schistocity. The composition varies both horizontally and vertically. In some places the ore is finely banded with common thin porphyritic bands. Sporadically inclusion of week and altered

rock lenses can be found in massive sulfides. The contact between the ore and waste rock is sharp. Around the massive ore there is a pyrite dissemination characterized by brecciated structure (Puustjärvi, 2006). The main minerals are: pyrite, chalcopyrite and sphalerite, and the average grades are: 1.2% Cu, 2.5% Zn and 43% S (Numminen, 2012). The host rocks are mostly felsic pyroclastic rocks and porphyries rich in quartz that were hydrothermally altered, metamorphosed, deformed and recrystallized. Other rock types are mafic volcanic rocks, mainly coarse-grained tuff breccias and lavas, and volcanic and felsic dykes (Puustjärvi, 2006).

The schistocity in host rocks is clear and leads to development of cracks that are most dominant in the schistocity direction. Although there are no distinctive faults in the active mining area that could be activated by mining, pegmatite veins that are present near the ore contact zone have been identified as fault planes and might be important (Oye & Roth, 2005).

2.2 Mining method

The mining method currently utilized in the Pyhäsalmi mine is non-entry, bulk open stoping. The mining sequence is carried from the middle of the orebody (at the bottom) and continues upwards. Typically around 25 stopes are mined each year, with up to 5 in production at the same time. The dimensions of primary and secondary stopes, as well as the mining sequence is given on Figure 2-3.

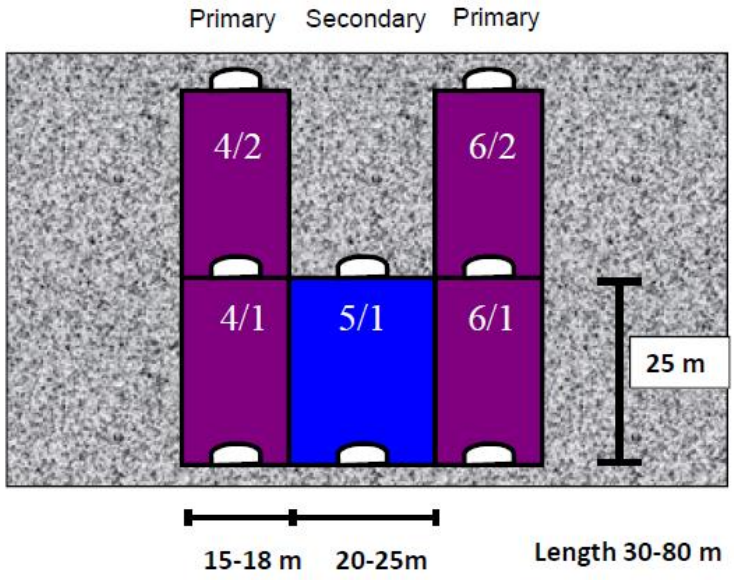

Figure 2-3. Stope size and mining sequence at the Pyhäsalmi mine. Mining sequence: 1) Mine out stopes 4/1 and 6/1; 2) Consolidated backfill of stopes 4/1 and 6/1; 3) Mine out stopes 4/2 and 6/2; 4) Consolidated backfill of stopes 4/2 and 6/2; 5) Mine out stope 5/1; 6) Rock filling 5/1; 7) Repeat sequence for next stope (Gleeson, 2010).

The size of stopes varies from 50 000t to 200 000t (in 2013 the average size of around 55 000t). Primary stopes are backfilled with hydraulic backfill and consolidated using material consisting of coarse tailings sand, slaked lime and slag which is pumped underground as a slurry. Secondary stopes are backfilled either with hydraulic backfill or with rock fill from a nearby quarry (Gleeson, 2010). The mine operates five days per week - on weekdays with morning and evening shift. Stope blasting is performed with emulsion explosives. For safety reasons (mainly because of sulfuric fumes after the blast) blasting time is at 10pm, when all the crew leaves the mine and no one can access the mine until the next morning.

The mine uses automated LHDs to haul the ore; the operator fill the bucket and unit is released for automated hauling. The system is flexible so that barriers can be repositioned to seal off the automated area and LHDs can move from one stope to another. Pyhäsalmi uses also automated drilling equipment with current capability for one-hole automation. The ore is dumped to ore passes, fed to jaw crusher and hoisted to the surface where it is send to the mill for floatation (Gleeson, 2010).

2.3 Rock mechanics and ground support

The Pyhäsalmi mine is characterized by high horizontal stress field, what has an influence on the mine planning. The average major principal stress measured at the -1125 level was 65Mpa dipping at 5º towards 310ºE. In order to avoid large stress failures stopes are designed to be parallel to this direction. Results of measured and estimated in-situ stresses can be found in table below.

Table 2-1. Primary stress field (Bergström, 2014).

Level	σ_V [MPa]	σ_H [MPa]	σ_h [MPa]
-1135 (measured)	33	65	41
-1400 (estimated)	41	75	45

The quality of rock is good. Values of uniaxial compressive strength and elastic modulus for intact rock are shown in Table 2-2.

Table 2-2. Primary rock properties (Bergström, 2014).

Rock type	UCS [MPa]	E [GPa]	ρ [kg/m^3]
Ore (massive sulfide)	90-120	90-140	4400
Waste rock (volcanites)	200-240	60-80	2700

Primarily, the rockmass is competent and stiff; rock is considered as prone to rockbursts. With advancing mining one fracture set (azimuth 47º and dip 70 º) in the massive pyrite

has become more apparent (Hakala, et al., 2013). The jointing in the waste rock is related to schistocity which is most prominent close to the ore. One of the major problems in the mine is detachment and slip of the contact zone wall rock. It was observed first in 2009 from damage in shotcrete. Observed block movement and slip along surfaces in yielded rockmass (along the schistocity surface in the ore contact area) has led to further fracturing of the orebody. Due to this, the stress field has changed and relaxation took place. The horizontal stress in remaining pillars inside the ore has been released, and the high stress is concentrated along the contact zone and around the orebody. After stress redistribution increased seismicity was observed outside the orebody.

The monitoring of rockmass conditions and stability consist of following elements:

- Microseismic monitoring system,
- Extensometers for local movement investigation and SMART cable bolts for determining actual support loads in critical areas (stope brows, active stopes vicinity, ore contact zone and ore passes),
- Fixed survey points,
- HI cells for measurements of 3D stress changes in time,
- Visual damage mapping in production levels,
- Stress modelling for stope scheduling (Bergström, 2014).

The Hollow Inclusion (HI) cell is an instrument to measure the absolute triaxial stress in rocks by overcoring and to monitor stress changes over time. It consists of an arrangement of strain gauges mounted in the wall of a hollow tube with known Elastic modulus. The cell is installed in a borehole and grouted.

There are few different types of rock mechanical reporting currently performed at the mine site. First of all, is daily seismic report for production personnel summarizing the seismic activity for last 24h and indicating if any area needs inspection by the shift supervisor. Second type is a weekly report summarizing seismic activity, extensometers reading and damage mapping results. Third type is a monthly report of seismic activity.

The ground support system in the mine consists of four elements:

- Rock bolts - fully grouted 2.2m length and 20mm diameter Kiruna bolts with wedge and 120mm washers; the minimum bolt density is 5 bolts per 1m of development,
- Mesh – welded mesh 125mm x 125mm, with 5.5mm wires,
- Shotcrete – 50-75mm layer thickness and 30kg/m^3 of steel fibers,

- Cable bolts – 5-9m cables, 15.2mm diameter (Bergström, 2014).

Depending on the local conditions and support requirements the set-up may vary from only bolting and shotcreting to a system with all four above-mentioned elements. For details please see Figure A-1 and Figure A-2 in Appendix A.

2.4 Seismic monitoring system

The seismic monitoring system was installed in 2001 by the Integrated Seismic System International Ltd. (ISS) and since then is focused on recording microseismic events. The latest system upgrade was completed in September 2013 by the Institute of Mine Seismology (IMS) who currently manages the system. Maintenance of the system and support service is also done by IMS. After upgrading, the system consists of:

- seismic server located at the surface for data processing and storage,
- 7 IMS station seismometers and IMS GS seismometers,
- 24 uniaxial (1G) and 10 triaxial (3G) geophones (see Table 2-3) with natural frequencies of 4.5Hz and 14Hz respectively (de Jongh, 2013).

The 4.5Hz geophones have operational frequency bandwidth between 3Hz and 2000Hz and are installed within 2 degrees of their pre-set orientation with respect to the vertical. The 14Hz geophones have operational frequency bandwidth between 8Hz and 2000Hz and can be installed at any angle. Geophones are fixed in 10m long, vertical boreholes with a 76mm diameter that were drilled in the roof of excavations (see Figure 2-4).

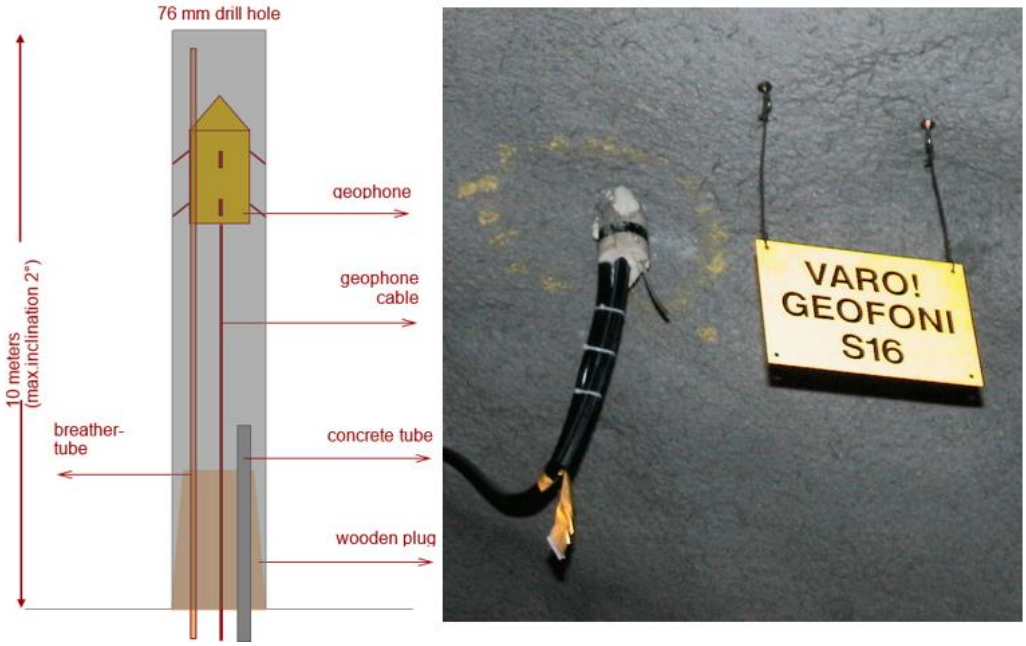

Figure 2-4. Schematic diagram (left) and picture of borehole geophone installed in the mine.

Table 2-3. List of active geophones in the seismic monitoring system (de Jongh, 2013).

Station	Geophones			
	X [m]	Y [m]	Z [m]	Type
IMS1 @ surface	2276	8307	-99	3G
	2159	8413	-107	1G
	2279	8307	-57	1G
	2313	8353	-108	1G
IMS2 @ -400 Level	2260	8431	-397	3G
	2301	8383	-396	3G
IMS3 @ -1075 Level	2383	8300	-1040	3G
	2247	8110	-1070	1G
	2232	8285	-1067	1G
	2192	8407	-1062	1G
	2446	8424	-1021	1G
IMS4 @ -1150 Level	2290	8273	-1133	3G
	2423	8346	-1111	1G
	2231	8476	-1130	3G
IMS5 @ -1200 Level	2409	8357	-1178	1G
IMS6 @ -1250 Level	2414	8439	-1250	1G
	2205	8500	-1239	1G
	2198	8310	-1264	1G
	2297	8219	-1242	1G
	2110	8300	-1228	1G
	2393	8236	-1156	1G
IMS7 @ -1325 Level	2209	8147	-1290	3G
	2216	8136	-1313	1G
	2099	8335	-1314	3G
	2305	8337	-1318	1G
IMS 8 @ -1350 Level	2403	8297	-1326	3G
	2282	8183	-1340	1G
	2269	8408	-1340	1G
	2185	8422	-1337	1G
	2441	8405	-1353	1G
IMS9 @ -1410 Level	2291	8203	-1402	3G
	2260	8279	-1390	1G
	2414	8392	-1398	1G
	2436	8243	-1399	1G

Six geophones are places above -400 level for backfill raise cave monitoring. Other seismic sensors are placed in production areas on levels -1075 to -1425. After the upgrade in 2013 more geophones were installed on the hanging wall side of the ore body resulting in better coverage. The total area monitored is equal to 524,500 m^2 and the average inter sensor spacing is equal to 124.2m.

Microseismic events are recorded 24h per day and are stored in the database. Special Info center was established providing real time access from any computer (including underground) in order to infer the time, location and magnitude of recorded events (Bergström, 2013).

Sensitivity of the system (as for January 2014) is described by:

- The minimal recordable magnitude varies from -2.1 to 1.3 (depending on the location; the best is achieved close to production areas, in the vicinity of installed geophones).
- 3D location error varies from 10m (close to the center of the mine) to 50m (see Figure 2-5).

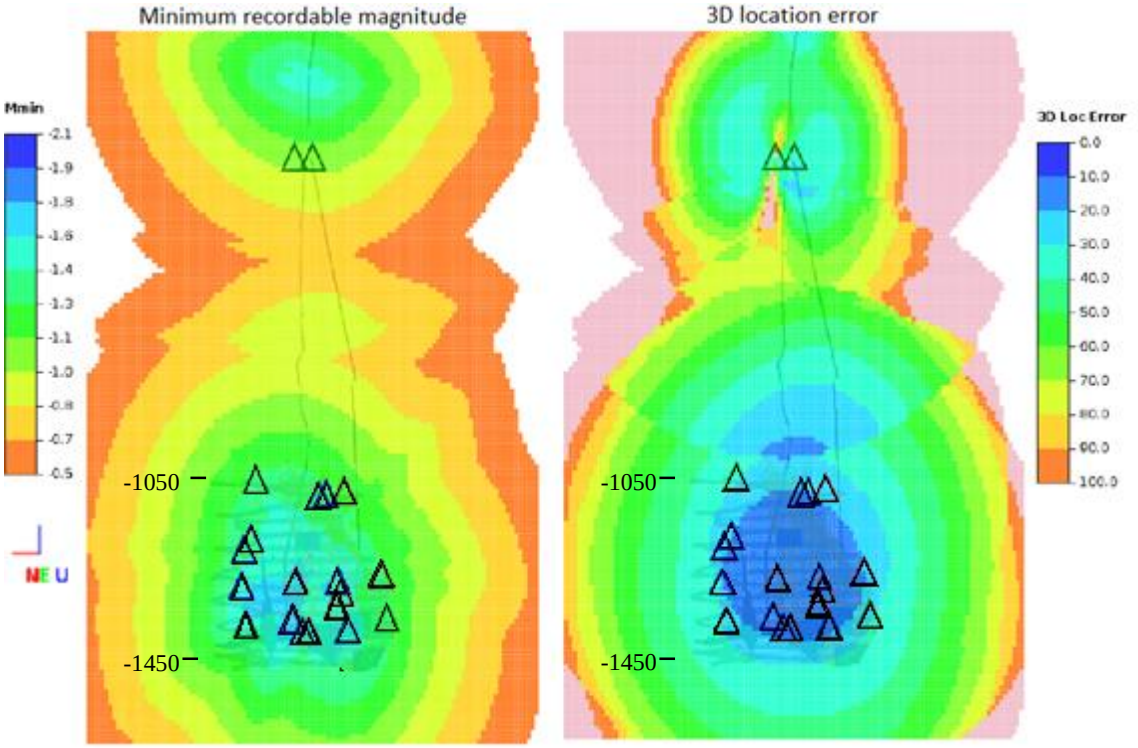

Figure 2-5. Seismic system sensitivity map – vertical section, view looking east, triangles illustrate installed geophones (Meyer, 2014).

3 Theoretical background

This chapter presents theoretical background for the thesis. It is divided into two parts. The first part describes the geotechnical risk assessment guideline for underground mines, proposed by Mishra (2012). The second part defines basic concepts related to seismicity in underground mines.

3.1 Geotechnical risk assessment guideline

The geotechnical risk assessment guideline is part of the I^2Mine project and aims to be used with geotechnical data from underground mines in order to identify and investigate geotechnical hazards that might pose risks. The goal is to evaluate the likelihood of geotechnical hazard to occur, and to assess its possible consequences. The geotechnical risk can be defined as:

$$Geotechnical\ risk = Likelihood\ of\ geotechnical\ hazard\ occurence \cdot Severity\ of\ geotechnical\ hazard$$

The guideline consists of two main parts: geotechnical hazard potential and geotechnical risk assessment. Next subsections present basic ideas of the guideline. For more details please consult Mishra (2012).

3.1.1 Geotechnical hazard potential

According to the guideline, the first step is identification of the Geotechnical Hazard Potential (GHP) by using proposed risk level classification method. The GHP aims to help in estimation of possible geotechnical hazards, and is meant to be used as a preliminary step for risk ranking and justification of the required Geotechnical Risk Assessment. GHP is based on following sub classification:

a) mining method
b) rockmass – based on stability number N_r (from Matthews stability graph method):

$$N_r = Q' \cdot A \cdot B \cdot C \quad (1)$$

Where:

Q' – the Barton's Q number with J_w (joint water parameter) taken as 1,

A – the influence of stress on the excavation and the rockmass – ignored at this stage; taken into account in SM parameter:

$$\text{Safety Margin (SM)} = \frac{rock\ mass\ strength}{major\ principal\ stress} - 1 \quad (2)$$

B – the influence of discontinuity and joint orientation to the excavation surface.

C – the impact of the orientation of the excavation plane itself and accounts for the influence of gravity.

$$C = 8 - 7 \cdot \text{Cos}\,\alpha \quad (3)$$

α is the angle of excavation plane inclination

After calculation of abovementioned parameters the results are used to assign the rockmass competency using Table 3-1 and Table 3-2. The classification code starting with 3 represents mining in operations stage.

Table 3-1. Rockmass classification for risk, based on safety margin (Mishra, 2012).

Range of SM	Classification code	Rock Competency
-1 to -0.8	3I	Very low
-0.8 to 0	3II	Low
0 to 0.5	3III	Fair
0.5 to 2	3IV	High
> 2	3V	Very high

Table 3-2. Rockmass classification for risk, based on modified stability number (Mishra, 2012).

Range of N_r	Classification code	Rock competency
0.0001 to 0.6	3I	Very low
0.6 to 7	3II	Low
7 to 30	3III	Fair
30 to 250	3IV	High
> 250	3V	Very high

The last step is to infer the GHP from Table 3-3 and to rank the areas under investigation, such as different sections of the mine. This can assist in a better allocation of resources to high risk areas in order to reduce it. Based on the results, formal geotechnical risk assessment is justified if the GHP is 3 or higher.

Table 3-3. Geotechnical Hazard Potential classification. Codes: O - open stoping, 1 – mine in pre-feasibility stage, 2 – mine in bankable feasibility stage, 3 – mine in planning and operations stage, I to V – hazard from very high to very low (Mishra, 2012).

GHP	Description	Code
Very Low (1)	Negligible chances of hazards arising from bulk rockmass property. Hazards can largely arise from random natural events, unforeseen discontinuity.	O1V
		O2V
		O3V
Low (2)	Minor chances of hazards arising from bulk rockmass property. This can be in terms of minor raveling and spalling. Hazards arising from random natural events, unforeseen discontinuity and human error. The extent of damage from such random event is noticeable but doesn't hamper routine mining activity.	O1IV
		O2IV
		O3IV
Fair (3)	Fair chances of hazards arising from bulk rockmass property. This can be routine if the rockmass is not supported/reinforced. Hazards arising from random natural events, unforeseen discontinuity and human error. The extent of damage from this can be higher than the routine visible failures. This can cause substantial damage to production.	O1III
		O2III
		O3III
High (4)	High frequency of hazards arising from bulk rockmass property. Accidents cause productivity loss recovered over weeks. An unsupported site may not be safe for onsite risk assessment itself. Hazards arising from random natural events, unforeseen discontinuities and human error. Such hazards cause major damage to production. May lead to closure of area.	O1II
		O2II
		O3II
Very High (5)	Very high frequency of hazards arising from bulk rockmass property. Accidents cause loss in productivity which may not be recovered over the year. Site for risk assessment must not be visited without reinforcement and couple of days of observation. Hazards arising from random natural events, unforeseen discontinuities and human error. Such hazard may cause permanent loss of raw material in the form of trapped ore.	O1I
		O2I
		O3I

3.1.2 Geotechnical risk assessment

The geotechnical risk assessment (GRA) procedure follows five main steps:

Step 1 – Outline the scope of risk assessment

The scope of GRA has to be defined in order to know what resources are needed and who will be performing the assessment. The requirements have to be specified accurately so that the available resources will be used in the best possible way. Furthermore, risk assessment parameters have to be selected based on the amount of available data: the more data is available the easier is to quantify risks, hence in operational stage

quantitative parameters are preferred to qualitative ones. However, current practice in many mines, including the Pyhäsalmi mine is to use qualitative parameters, even in operational stage. The reason is their simplicity of transferring knowledge and its comprehension by the workforce. In addition, outlining the scope of GRA involves selection of appropriate approach from deterministic, probabilistic or possibilistic. Mishra (2012) proposes a numerical tool for selection of abovementioned approaches (see chapter 4.2).

Step 2 – Identify hazards within the scope

Selection of identification tool depends on the scale and hazard scope of the assessment. For hazard specific GRA for large scale, Bow Tie Analysis (BTA) is considered as the best tool to identify all hazards that can result in a top event. Other tools for hazard identification are: Failure Mode & Effect Analysis (FMEA) for site specific GRA for large and small scale, Fault Tree Analysis (FTA) and Event Tree Analysis (ETA) for hazard specific GRA for small scale.

Step 3 – Evaluate the likelihood of hazard

The goal is to find the probability (likelihood) of an event to occur. Specific procedure depends on the approach selected within the scope. For deterministic approach, precise calculation is performed with measured parameters. This approach lies in line with modelling of hazardous situation. For probabilistic approach, the probability of hazard is evaluated by accounting for variability and uncertainty in data. If the approach is possibilistic, a correlation is established between influencing factors and failure by using indicative variables and utilizing empirical methods.

Step 4 – Assess the consequences

This step aims at an assessment of damages due to realization of hazards. It involves evaluation of the exposure of people and assets to a hazardous condition, and determination whether a hazard is tolerable or not. It is common to establish a common benchmark for evaluation of consequences to provide an easy way of classifying consequences. Ideally, severity is to be evaluated in terms of lost money, however it may be difficult to quantify all damage types as a financial loss.

Step 5 – Rank the risk to formulate a strategy of risk reduction

Final risk is a result of multiplication of likelihood and consequences. It can be represented in graphical format or using a matrix format. The first suits best when both the probability and consequences are evaluated quantitatively, hence the risk is quantitative. The latter is used when probability or consequences are not quantitative, and is the easiest format for risk representation and ranking.

3.2 Seismicity in mines

Seismic events in the mining environment represent the response of rockmass to mining activities that are inducing stress change and energy release. Seismic events are predominantly generated in the process of rockmass failure. Rockmass deformation can be associated with a series of small and large events over a period of time, where each event is a single element of a continuing failure process. Because of inhomogeneity in the rockmass, such as dykes, pillars or major discontinuities, some energy released during the mining process can be stored and ultimately lead to large scale rockmass failure (Hudyma, 2008).

A number of parameters have a direct influence on the occurrence of seismic events. Blake and Hedley (2001) mentioned four main parameters: rock properties, depth, aerial extent of mining and production rate. Hudyma (2004) lists some additional influencing factors: pre-mining stress and induced mining stress, stage of extraction and percentage of orebody extraction.

Seismic source is defined as an area within a rockmass where deformation or failure (resulting in seismic event) is caused by a combination of stress, geological structure and mining. Seismic source mechanism is referred as the type of deformation or failure that results in seismic stress wave creation (release of seismic energy). It indicates the maximum size of an event that can happen and is related to the timing of energy release (stress driven event happens directly after the mine blast; structurally driven are not related to mine blasting time) (Hudyma, 2008).

3.2.1 Seismic event size

Seismic event size or its intensity can be measured with a magnitude scale, with a most common example of Richter magnitude scale (also shortened as Richter magnitude) proposed by Richter (1935). It is a logarithmic scale of peak ground motion measured at a distance of 100km from seismic source. Although this scale is widely used for

measurement of earthquakes, the local scale of the seismic monitoring system installed in mines may differ from site to site. That is why bigger events, registered also by regional or national seismological networks, are used to calibrate the local magnitude scale to an approximate Richter magnitude scale. Table 3-4 presents a comparison of Richter magnitude scale and a qualitative description of subjective feeling of people in the mine, as a result of studies in Australian and Canadian mines.

Table 3-4. Richter magnitude of seismic events compared with qualitative description of how those events are felt in the mine (Hudyma & Potvin, 2004)

Approximate Richter Magnitude, M_L	**Qualitative description**
-3	• Small bumps felt nearby. Typically only heard relatively close to the source of the event. • Normally following development blasts. • Event may be audible but vibration likely too small to be felt. • Undetectable by seismic monitoring system.
-2	• Felt locally as thumps or bangs at a short distance from the event. • May be felt more remote from the source of the event (i.e. more than 100 meters away). • May be detectable by a microseismic monitoring system.
-1	• Often felt by many workers throughout the mine (i.e. hundreds of meters away). • Similar vibration to a distant underground secondary blast. • Will be detected by a microseismic monitoring system.
0	• Vibration felt and heard throughout the mine. • Bump commonly felt on surface (hundreds of meters away), but may not be audible. • Vibration felt on surface similar to those generated by a development round.
1	• Typically felt and heard very clearly on surface. • Vibrations felt on surface similar to a major production blast.
2	• Vibration felt on surface is greater than large production blasts. • Vibration detectable with regional earthquake monitoring systems.

Mining-induced seismic events of low magnitude (M_L from -4 to 0) are considered as microseismic events (Young, et al., 1992). Typically, they do not cause any observable, structural damage in mine openings, but are an indication of damage or inelastic deformation in a brittle rockmass (Falmagne, 2001). Microseismic events are the main portion of events recorded every day by seismic monitoring systems in mines (more than 95%), but they represent only a fraction of total seismic energy released due to mining

(Young, et al., 1992). Characteristic seismic source mechanisms of microseismic events are listed by Hudyma (2008):

- Intact brittle rock fracture,
- Coalescence of rockmass fractures (rock joints),
- Large stresses in stope abutments,
- Shearing, crushing and volumetric fracturing of mine pillars,
- Shear or rupture of lithological contacts.

Rockbursts are seismic events with a magnitude higher than 0 that are characterized by a sudden and violent release of stored energy that can result in dynamic failure of the rockmass. They can cause losses in production, human life, or in the worst case, a complete mine closure (Young, et al., 1992). In comparison to mining-induced seismicity, large seismic events can be triggered by fairly insignificant mining-related energy change that results in large failure of previously instable rockmass. Rockburst can be caused either by an implosional failure observed near mine openings, or by shear-related failure that outspread on greater distance from mine excavations (Hudyma, 2008). Ortlepp (1997) suggests five mechanisms of rockburst divided by their source mechanism, first motion recorded by seismic sensors and an approximate Richter magnitude (see Table 3-5).

Table 3-5. Mechanisms of damaging rockbursts (Ortlepp, 1997).

Seismic event	Postulated source mechanism	First motion from seismic source	Richter magnitude M_L
Strain-burst	Superficial spalling with violent ejection of fragments	Usually undetected, could be implosive	-0.2 to 0
Buckling	Outward explosion of large slabs pre-existing parallel to surface of opening	Implosive	0 to 1.5
Face crush/pillar burst	Violent explosion from stope face or pillar sides	Mostly implosive, complex	1.0 to 2.5
Shear rupture	Violent propagation of shear fracture through intact rockmass	Double-couple shear	2.0 to 3.5
Fault-slip	Violent renewed movement on existing fault or dyke contact	Double-couple shear	2.5 to 5.0

3.3 Seismic hazard

Seismic hazard is defined as “an estimation of the mean probability (over space and time) of the occurrence of a seismic event with a certain magnitude within a given time

interval." (Gibowicz & Kijko, 1994). Kaiser et al. (2005) separates seismic hazard into two types: rockmass degradation due to microseismic events, and dynamic loading due to seismic wave propagation.

Seismic hazard estimation is the key objective in seismic monitoring, however there is no unique and general measure to quantify it. It is commonly assessed as the largest possible event that can occur; event size is proportional to the level of ground movement induced, which creates the potential for rockmass damage. It is important to mention that it varies in space and time and is influenced by the location of maximum ore extraction and related stress concentration, as well as period of mine blasting. Seismic hazard can be evaluated as long, medium, and short-term. In contrast to earthquake seismology, thorough statistical seismic analysis is of limited importance for mine personnel. From this perspective, an analysis that can relate to rockmass failure mechanisms, hence coupling seismicity to mining activities, is more beneficial. (Hudyma, 2008).

One of the methods for quantification of seismic hazard is the so called Seismic Hazard Scale (SHS) developed by Hudyma (2004). The SHS uses three mine seismicity parameters: the rate of occurrence of events of a certain magnitude, the power law relation for mine seismicity (as it is shown in Equation (4) and the maximum observed event magnitude. The power law relation was developed by Gutenberg and Richter, and is recognized as a relation between the magnitude of seismic event and the frequency of occurrence:

$$log_{10}(N) = a - b \cdot M_L \tag{4}$$

Where:

N – number of events of at least magnitude M_L,

M_L – approximate Richter magnitude,

a – constant; measure of the level of seismicity,

b – slope of the power law relation; describes the relative number of small and large events in a certain time interval (Hudyma & Potvin, 2004).

The diagram illustrating the Gutenberg-Richter power law relation is called Gutenberg-Richter frequency-magnitude diagram (F-M diagram) and is presented on Figure 3-1.

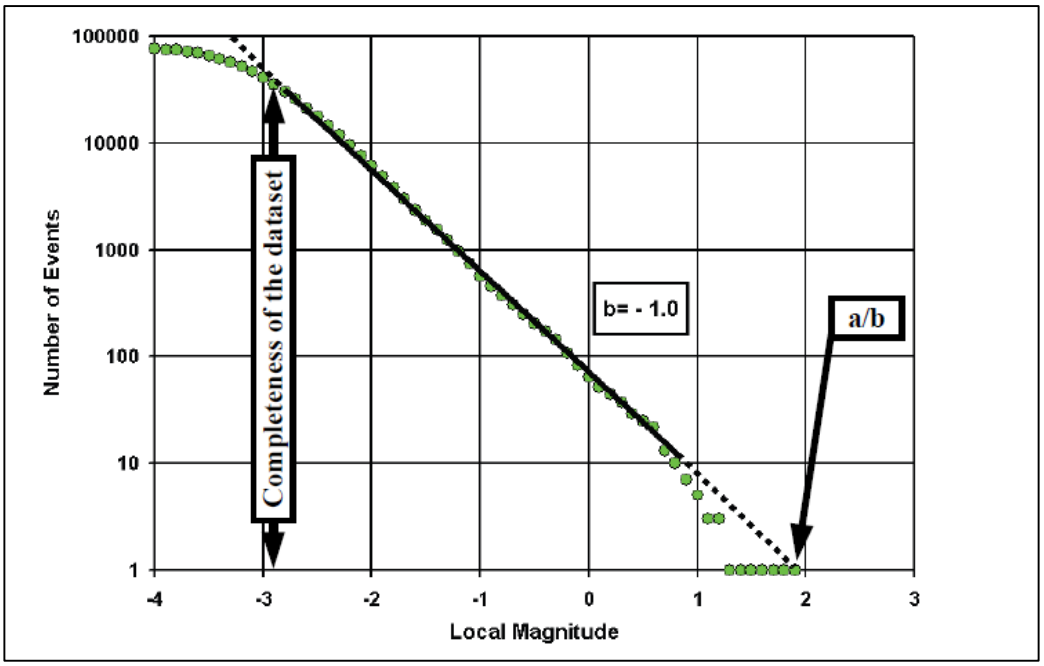

Figure 3-1. Gutenberg-Richter frequency-magnitude power law relation (F-M diagram, Eq. 4) for large population of seismic events. This is an example of good dataset with linear relationship that follows the power law (from Hudyma (2008): Figure 2.11)

The SHS is the x-axis intercept of the frequency magnitude relation, assuming b equal to 1:

$$SHS \approx log_{10}(N) + M_L \quad (5)$$

Table 3-6 presents a comparison of SHS with relative seismic hazard and the largest event that can occur. The SHS has been used to examine seismic hazard for events up to M_L of 3, because events of larger magnitudes may not follow the relation (b value less than 1).

Table 3-6. Comparison of SHS with relative seismic hazard and the largest event magnitude (Hudyma & Potvin, 2010; Mikula, et al., 2008).

SHS	Relative seismic hazard	Approximate magnitude of largest expected event, M_L
-2	Nil	-2
-1	Very low	-1
0	Low	0
1	Moderate	1
2	High	2
3	Very high	3

3.3.1 Quantitative Seismic Hazard and Risk Assessment Framework

As an example of current practice in seismic risk analysis that uses SHS for seismic hazard quantification, one can mention the Quantitative Seismic Hazard and Risk Assessment Framework (QSHRAF) approach applied in Mine Seismicity Risk

Assessment Program (MS-RAP), developed by the Australian Centre of Geomechanics (Mikula, et al., 2008). The risk assessment process is summarized on Figure 3-2.

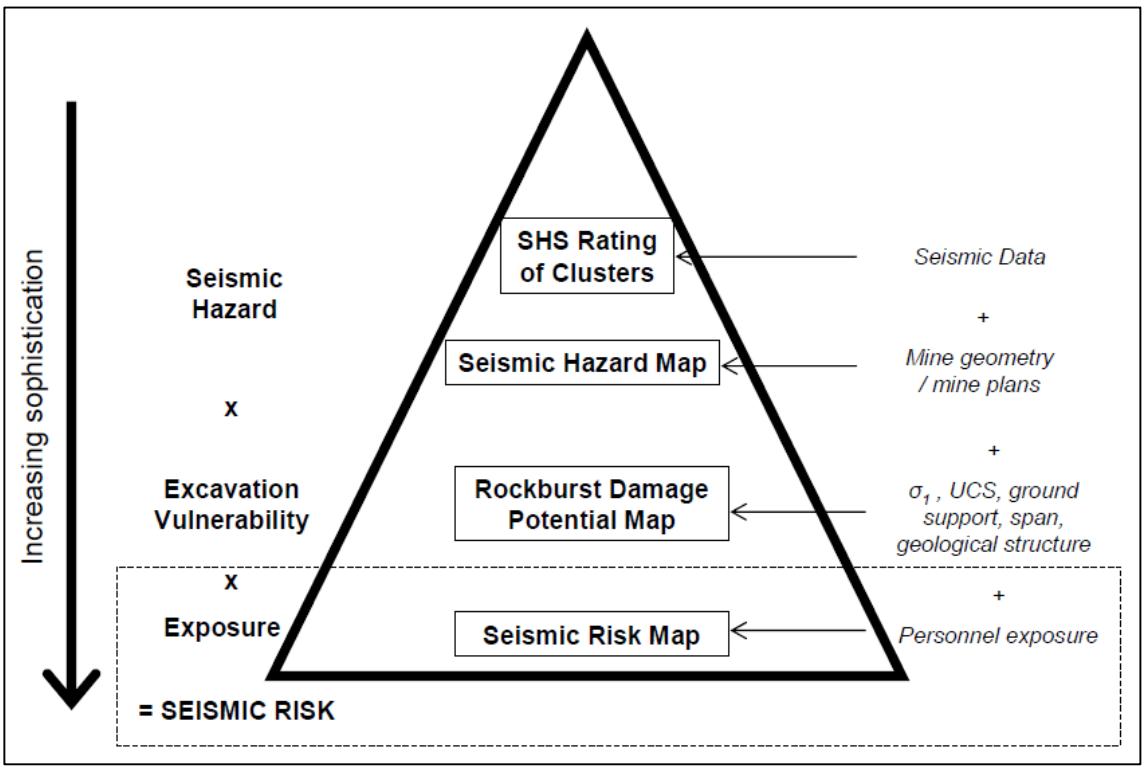

Figure 3-2. Risk assessment process applied within MS-RAP (from Mikula, et al., 2008: Figure 30).

First, the seismic data is grouped into clusters of events representing a single seismic source. The risk assessment starts from quantification of seismic hazard by calculating SHS for each cluster. Next, seismic hazard map is created using the mine geometry and mine plans, where SHS is assigned on each point on map.

Next, the Peak Particle Velocity (PPV) is calculated at each location under an assessment using the maximum local magnitude that is expected to occur. PPV is scaled for distance using following relation:

$$PPV = 1.4 \cdot \frac{10^{\frac{M_L}{2}}}{r} \tag{6}$$

PPV – Peak particle velocity at the location under assessment [m/s]:

M_L – local magnitude of the largest expected event,

r – distance from the cluster (seismic event location) to the location under assessment.

In the next step, excavation vulnerability potential for damages (EVP, see Equation (7) is assessed on the base of four parameters stress conditions (E_1), utilized ground support (E_2), excavation span (E_3) and geological structure (E_4). The EVP represents the increasing likelihood and severity of rockburst damage. It is calculated using following formula:

$$EVP = \frac{E_1}{E_2} \cdot \frac{E_3}{E_4} \tag{7}$$

Where:

E_1 – Stress condition factor as a ratio of static stress to rockmass strength in the vicinity of excavation, $E_1 = \frac{100 \cdot \sigma_{1M}}{UCS}$ [-],

σ_{1M} – the mining induced maximum stress at the place under assessment [MPa],

UCS – the intact unconfined compressive strength of the rock [MPa],

E_2 – Ground support capacity to withstand dynamic loading (see Table 3-7),

E_3 – Excavation span, taken as a diameter of a circle drawn within mine opening [m],

E_4 – Geological Structure (see Table 3-8) (Mikula, et al., 2008; Hudyma & Potvin, 2010).

Table 3-7. Ground support capacity scale – E_2 factor in Eq.7 (Potvin, 2009).

Classification	Surface support	Reinforcement	E_2 rating	Example
Low	None	Spot bolting (spacing > 1.5 m)	2	Spot bolting with split sets or solid bar bolts, minimal surface support
Moderate	Mesh or fibrecrete	Pattern bolting (spacing 1–1.5 m)	5	Pattern bolting with split sets or solid bar reinforcement, with mesh or 50mm fibrecrete
Extra bolting	Mesh or fibrecrete	Pattern bolting with a second bolting (overall spacing < 1m)	8	Pattern bolting with split sets or solid bar reinforcement, with mesh or 50mm fibrecrete. Plus an additional pass of pattern reinforcement, such as solid bar bolts
High static strength	Mesh or fibrecrete	Pattern bolting and pattern cable bolts	10	Pattern bolting with split sets or solid bar reinforcement, with mesh or 50mm fibrecrete. Plus pattern cable bolting
Very high dynamic capacity	Dynamic surface support	Pattern dynamic support	25	Pattern bolting with dynamic ground reinforcement such as cone bolts, with dynamic resistant surface support system

Table 3-8. Geological structure - E_4 factor in Eq.6 (Potvin, 2009).

E_4	Description
0.5	*Seismically active major structure* Major structural features such as faults, shears or discrete contacts intersect the location and act as a potential failure surface promoting rockmass failure. *Example:* The rock mass fails back or along a major fault, increasing the depth of failure considerably more than would otherwise occur in the rockmass.
1	*Unfavorable rock mass/no major structure.* The orientation of the rockmass discontinuity fabric may promote or enhance rockmass failure. Generally, this factor is applied when there are local cases in which the rock mass discontinuities promoted falls of ground much larger than would be expected. *Example:* A heavily jointed, blocky rock mass with kinematically unstable rockmass blocks. The rockmass is prone to deeper than normal gravity driven failure mechanisms.
1.5	*Massive rock mass/no major structure.* The rockmass is essentially massive, or non-persistent rock mass discontinuities may exist; including possible minor blast related fracturing. There are no major structures such as faults or shears, which may promote or enhance rockmass failure.

The rockburst damage potential (RDP) is found by multiplying EVP by PPV at a specific location (see Eq. 8).

$$RDP = EVP \cdot PPV \tag{8}$$

Mikula, et. al (2008) gives a scale of the extent of rockburst damage from R1 (no damage) to R5 (complete destruction of the support system) that was found empirically by investigating and back analyzing 254 cases of rockburst damage by Heal, et. al in 2006. The empirical chart relating the largest predicted ground movement (PPV) to the excavation susceptibility to damage (EVP) is presented on Figure 3-3. The rockburst damage potential increases with increasing EVP and PPV. The scale of projected damage determines the necessary dynamic capacity of installed ground support. Proper ground reinforcement that can withstand dynamic loading and large deformations is required in order to reduce the rockburst hazard and protect workers, mine infrastructure and sustain safe operation (Kaiser & Cai, 2012). By increasing the capacity of support, for example by installation of yielding support and elimination of the weakest link, the rockburst damage potential can be lowered (on Figure 3-3 point will move left, to lower rockburst damage scale zone).

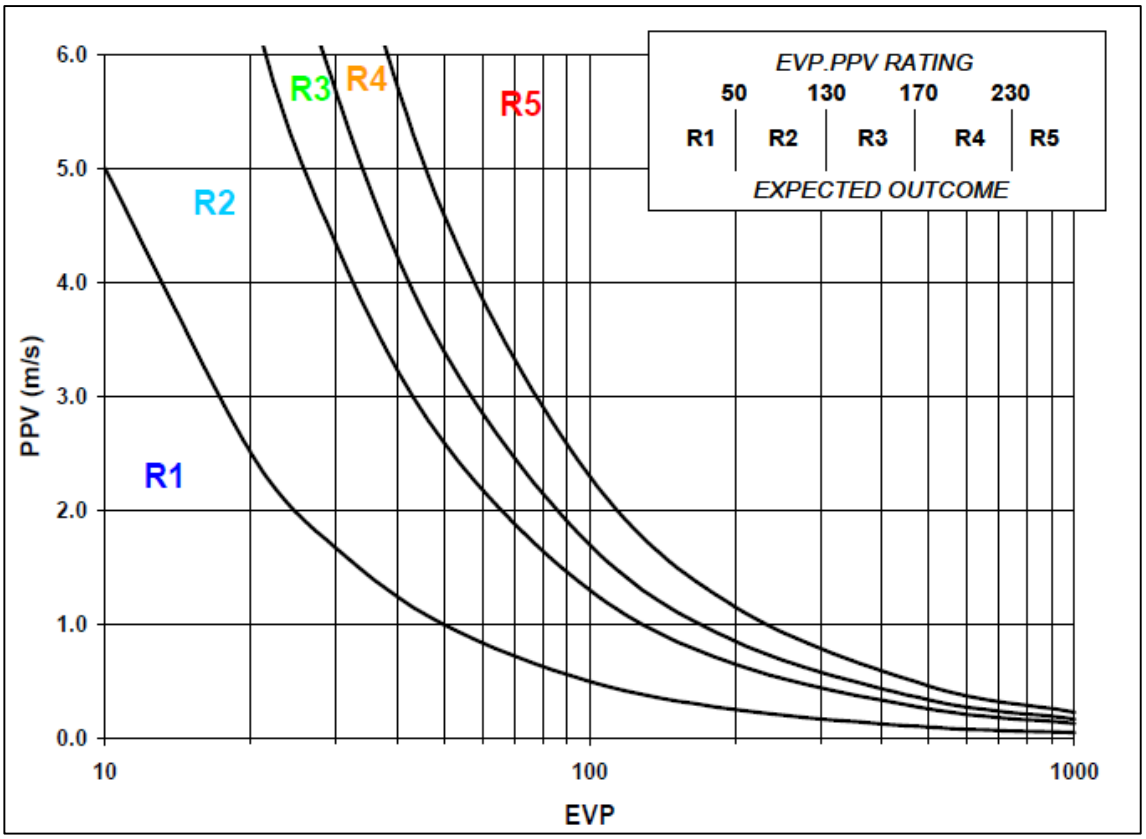

Figure 3-3. EVP vs PPV diagram showing zones with expected damage (from Mikula, et al., 2008: Figure 38).

Below, Table 3-9 presents the scale of RDP with qualitative description of expected rockmass and support damage.

Table 3-9. Rockburst damage potential scale showing expected rockmass and support damage (redrawn from Mikula, et al., 2008).

RDP	Rockburst Damage Scale	Expected rockmass damage	Expected support damage
0 to 25	R1	No damage / minor loose	No damage
25 to 50	R1	No damage / minor loose	No damage
50 to 130	R2	Minor damage / less than 1t displaced	Support system is loaded, loose mesh, plates deformed
130 to 170	R3	1 to 10t displaced	Some broken bolts
170 to 230	R4	10 to 100t displaced	Major damage to support system
230 to 280	R5	100+ t displaced	Complete failure of support system

The final seismic risk is calculated by taking into account exposure of personnel. Exposure is a function of the amount of time spent performing a number of tasks by mine personnel, the level of protection and the number of people involved. Areas are assigned with exposure ratings that were proposed by Owen (2004) after studies conducted at underground mines.

The seismic risk ratings (SRR) are qualitative: VL = Very Low, L = Low, M = Moderate, H = High, VH = Very High, E = Extreme, and depend on the type of mining activity (quantitative exposure rating) and the level of rockburst damage potential. Graphical representation of risk matrix is demonstrated in Table 3-10

Table 3-10. Seismic risk assessment matrix constructed from quantitative exposure rating (vertically) and rockburst damage potential (horizontally). The seismic risk ratings are qualitative: VL = Very Low, L = Low, M = Moderate, H = High, VH = Very High, E = Extreme (Mikula, et al., 2008).

	RDP=EVP x PPV	<25	25-65	65-115	115-170	170-225	225-280	>280
Excavation type/ activity	**Exposure rating**							
Restricted access (no entry)	100	VL	VL	L	M	M	H	H
Decline	1000	VL	L	M	M	H	VH	VH
Travelway - no active mining	1000	VL	L	M	M	H	VH	VH
Travelway - mining on the level	2000	VL	L	M	M	H	VH	VH
Production mucking area	3000	VL	L	M	M	H	VH	VH
Busy level / travelway drive / access	4000	VL	L	M	M	H	VH	VH
Development mining	7000	L	M	M	H	VH	VH	E
Production drilling	10000	M	H	H	H	VH	E	E
Production charge-up	10000	M	H	H	H	VH	E	E
Infrastructure areas / workshops	14000	M	H	VH	VH	E	E	E

3.3.2 Probabilistic Approach for Seismic Risk Assessment

The Probabilistic approach for Seismic Risk Assessment (PASRA) has been developed under the cooperation of Wen (2013). The first attempt to apply this approach was performed by Froehlich (2014). It is based on calculation of two factors. The first is the Released Energy Capacity (REC), as a relationship between the elevated energy due to seismic event and accumulated energy (induced stress) in the area of investigation. Second factor is the Absorbed Energy Capacity (AEC) based on the capacity of installed ground support. Seismic hazard can be evaluated by dividing REC by AEC factor. By applying it to sufficient data it is possible to estimate the likelihood of seismic hazard and to assign it to different areas.

The PASRA methodology uses the same concept as QSHRAF to cluster the data into logical groups representing a single seismic source in order to predict the maximum possible seismic event within a group. The F-M diagram is used to find the maximum

size of an event within a population as x-axis intercept. This event size is used then to calculate the maximum seismic energy of an event using following relationship:

$$log\ E_1 = a \cdot M_L + b \tag{9}$$

Where:

E_1 – predicted largest expected seismic event energy,

M_L - local magnitude,

a, b – constants.

The Released Energy Capacity (REC) formula links the largest predicted energy with the accumulated stress energy in the area under assessment:

$$REC = \frac{E_1}{E_2} = \frac{\Delta E + E_0}{E_0} \cdot \frac{\sigma_{uniaxial}}{\sigma_{max}} = \left(1 + \frac{\Delta E}{E_0}\right) \cdot k_\sigma = (1 + \frac{E_1 \cdot e^{-\varphi \cdot r}}{E_0}) \cdot k_\sigma \tag{10}$$

Where:

ΔE – Evaluated energy condition due to seismic events based on the seismic wave propagation at distance r from the seismic source in visco-elastic homogenous medium; after Sambuelli (2009),

E_0 – Accumulated energy in the investigated area representing the stress state in the area under investigation,

E_1 – Predicted largest expected seismic event energy calculated from the maximum magnitude within a cluster group using Equation (9),

φ – Attenuation coefficient,

k_σ – Relation $\frac{\sigma_{max}}{UCS}$,

r – Distance to seismic cluster.

The Absorbed Energy Capacity (AEC) reflects the ground support capacity to withstand and absorb the energy in the failure process following a significant seismic event. Originally, the AEC equation aims at quantification of the support load capacity per square meter in order to be comparable to REC. Here, due to the limitation of available data, AEC is represented by a rating scale dependent on installed support. The higher the capacity of the support to withstand dynamic damage, the larger the AEC. Seismic hazard is evaluated by dividing the REC by AEC:

$$Seismic\ hazard\ = 100 \cdot \frac{REC}{AEC} \tag{11}$$

3.4 Data clustering

Clustering is an unsupervised technique to classify data into groups (clusters) based on similarity. Data points contained within a valid cluster are more similar to each other, compared to data points outside the cluster (Jain, et al., 1999). Clusters are defined as connected regions of space containing large amount of points, opposed to regions with less dense data. The main goals of clustering are: to reduce the amount of data in order to allow for faster processing of information in representative groups of the entire data set, to generate hypothesis about the data and to predict some features of the data within specified clusters to extract useful knowledge. Clustering process can be divided into few steps: feature selection, algorithm selection, results validation and interpretation (see Figure 3-4).

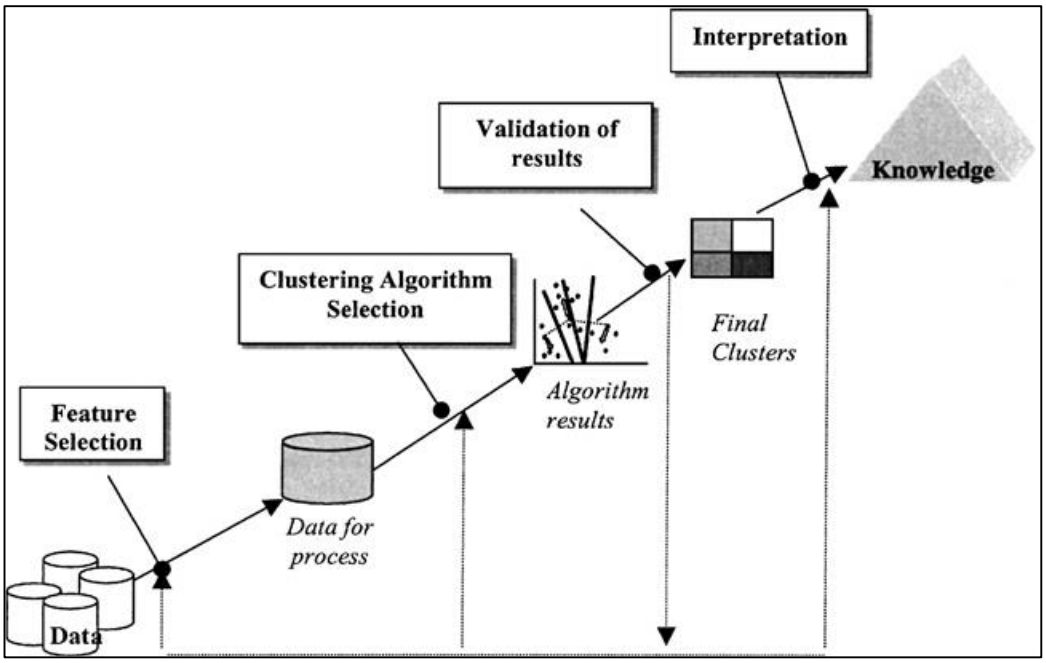

Figure 3-4. Steps of clustering process (from Halkidi et al. (2001): Figure 1).

The first step is to select the features on which we perform the clustering (for example spatial coordinates) depending on the type of data and the purpose of our analysis. The second step is to select an algorithm that will result in good cluster organization. Clustering algorithms are characterized by proximity measure and by clustering criterion. Proximity measure defines how similar are two data points. (Halkidi, et al., 2001). One of the most common proximity measures in data clustering is Euclidean distance that is used to calculate the dissimilarity between two data points. In three-dimensional space the Euclidean distance is defined as the length of the path between two points (x_1, y_1, z_1 and x_2, y_2, z_2) (Weisstein, 2012). It is calculated as follows:

$$d = \sqrt{(x_2 - x_1)^2 + (y_2 - y_1)^2 + (z_2 - z_1)^2} \quad (12)$$

Clustering criterion defines the type of function used for clustering and has an influence on the type of achieved clusters. It has to be selected in such a manner that will fit well the data set. The next step is to validate the results by utilizing suitable measures and criteria in order to investigate if the algorithm was appropriate. Last step is to interpret the results in order to draw conclusions about the data (Halkidi, et al., 2001).

3.4.1 Quality Threshold clustering algorithm

The Quality Threshold Clustering (QTCLUST) is a computationally efficient algorithm originally developed for gene clustering that groups data into cluster of high quality (Heyer, et al., 1999). Although it is a partitioning clustering method, it does not require to specify the number of clusters beforehand, what is the biggest advantage compared to other divisive methods (for example K-means clustering). The QTCLUST creates non-overlapping clusters with some points remaining outside of clusters considered as outliers. The distance from a point to a group of points is calculated as the maximum length from any point from the group to the point (complete linkage using the Euclidean distance – as in Equation (12). The QTCLUST algorithm has two parametrical constraints: the minimum number of data points to be considered as a cluster (minimum cluster size), and the maximum allowable radius of a cluster (measured from the centroid). This ensures that the diameter does not exceed user-defined threshold and provides high quality and compactness of created clusters (Bednarik & Kovacs, 2012). The procedure of QTCLUST algorithm can be summarized with following steps:

- Create a potential cluster for random point by iteratively inserting the closest points to the already existing group.
- Repeat step one until the size of cluster is larger than the threshold.
- Save the most populated potential cluster as the first true cluster.
- Remove the already clustered points from the data and repeat the procedure with the reduced set of points.

The QTCLUST can be used in grouping of seismic events to break the data into compact clusters. This can speed up (in terms of significant compression of data) and improve the efficiency of analysis. (Kaiser, et al., 2005).

3.4.2 Single linkage hierarchical clustering algorithm

The Single linkage hierarchical clustering algorithm (SLINK), also referred as nearest neighbor algorithm, is an agglomerative hierarchical algorithm that groups data by joining similar clusters. At first, each data point is allocated to its own cluster. Then the two most similar clusters are joined iteratively until there is only a single cluster. The distance between two clusters is the minimum of all distances between cluster pairs. The SLINK algorithm produces relatively few, elongated and chain-like clusters. The algorithm yields a dendrogram that represent different levels of cluster grouping, that can be cut at different heights to find the final clustering result (Jain, et al., 1999).

One of the advantages of SLINK algorithm is its simplicity and versatility. Hudyma (2008) illustrated a successful application of SLINK algorithm in grouping of smaller clusters of seismic data in order to distinguish single seismic sources from large data sets of seismic events.

4 Geotechnical risk assessment in the Pyhäsalmi mine

The current practice of risk assessment regarding geotechnical hazards in the Pyhäsalmi mine focuses mainly on two aspects. One is an evaluation of risks related to stoping. Mine personnel keeps record of all the stopes in a special log summarizing data prior, during and after mining. The data includes: area of the mine, development condition, mining phase, past seismicity record, geological structures and important features, risk from adjacent backfilling, and presence of orebody contact. The risk assessment approach is based on a point-based ranking with a scale from small risk (rank I) to very high risk (rank V). The stope log also contains information about expected stope performance and procedures in case of higher risk. After mining each stope is evaluated and used for back analysis (Pyhäsalmi Mine Oy, 2013). The second geotechnical assessment is a valuation of risks and effects of ore subsidence and movements along the northern contact zone. The mine utilizes monitoring instrumentation consisting of multi-point borehole extensometers to monitor displacements around contact zone and smart cables to monitor draw points brows near contact zones. Identified risks are: fall of ground in development headings adjacent to contact zone, increased cost of ground support rehabilitation, increased damage along the contact zone, large failures in stopes and increased monitoring costs. (Bergström, 2012)

Due to recent increase of seismic activity, as an evidence deterioration of rockmass, seismic risk is considered as high and large events can be expected. Monitoring of rockmass condition principally relies on seismic system installed at the mine. Mine personnel has a goal for further understanding of seismic data that requires performing seismic analysis (Bergström, 2014). This analysis can help in estimating the seismic hazard, especially to evaluate if larger events can have a negative influence, and how they can be managed. This proofs a necessity for development and implementation of seismic risk assessment approach. It also confirms that geotechnical risk assessment focusing on seismic risk clearly fits into the Pyhäsalmi mine strategy to extend the knowledge of this phenomenon.

Chapter 4.1 presents and attempt to evaluate the GHP using data from the Pyhäsalmi mine. Chapter 4.2 describes the selection process of risk assessment approach. Chapter 4.3 presents hazard identification for seismic risk by the use of bow-tie analysis.

4.1 Geotechnical hazard potential evaluation

The assessment of the GHP has been performed according to the procedure described in chapter 3.1.1. Evaluation was executed for the massive sulfide (ore) and volcanites (waste rock). Following assumptions were taken into account:

- Open stoping is selected as mining method.
- Q' value has been used in design modelling in the past (not up to date).
- Ore has one dominant fracture set with dip equal to 70°.
- Waste rock has foliation parallel to the ore contact, dip varies from 0º to 90º, here 20º is taken as a worst case scenario, because it is kinematically worst and gives the lowest B factor (equal to 0.3) in calculation of stability number N_r from Equation (1).
- Excavation planes have an inclination of 0° and 90° for roof and wall respectively.
- Rockmass strength is taken from the inputs of the stress model; Hoek-Brown failure criterion.
- Major principal stress is taken as an estimate for the -1400 level (see chapter 2.3).

First, the modified stability number was evaluated based on Equation (1) from chapter 3.1.1. The results can be found in Table 4-1.

Table 4-1. Results of the modified stability number for massive sulfide and volcanites.

	ore		waste rock	
Parameter	roof	wall	roof	wall
Q'	100	100	35	35
B	0.8	0.3	0.3	0.3
C	1	8	1	8
N_r	80	240	10.5	84

Second, the safety margin was calculated using Equation (2) from chapter 3.1.1. The results can be found in Table 4-2.

Table 4-2. Results of the safety margin for massive sulfide and volcanites.

Parameter	Massive sulfide	Volcanites
In-situ rock strength [MPa]	71	76
Major principal stress [MPa]	30	75
Safety Margin (SM)	1.4	0

As can be seen in Table 4-1 and Table 4-2, the lowest values of both the stability number and safety margin are found for volcanites. The summarized results for massive sulfide and for volcanites are presented in tables below. Based on those results, the rockmass competency has been assigned according to Table 3-1 and Table 3-2 (see chapter 3.1.1).

Table 4-3. Results of rockmass classification for massive sulfide; risk in operation stage.

Parameter	Value	Rockmass competency	Code
N_r	80	High	3IV
SM	1.4	High	3IV

Table 4-4. Results of rockmass classification for volcanites; risk in operation stage.

Parameter	Value	Rockmass competency	Code
N_r	10.5	Fair	3III
SM	0	Low	3II

The results given in Table 4-4 and Table 4-3 indicate that the rock competency is high (3IV category) and low (3II category) for massive sulfide and volcanites respectively. Taking into account the mining method (open stoping) and rockmass competency (high competency – code O3IV; low competency – code O3II) the classification presented in Table 3-3 (see chapter 3.1.1) indicates that the Geotechnical Hazard Potential is low (2) for massive sulfide and high (4) for volcanites. When the GHP is high, hazards related to the rockmass properties are expected to arise from random natural events and to be of high frequency. Such hazards may cause major damage leading to loss of production and financial damage. This confirms the conditions and challenges that are currently

confronted in the mine. Given results indicate that the formal risk assessment is justified for the volcanites, and not for the massive sulfide.

4.2 Risk assessment tool selection

The approach for geotechnical risk assessment is selected based on the methodology proposed by Mishra (2012). In the selection process, a tool presented on Figure 4-1 is used to find the most appropriate assessment approach. It is based on several GRA scope categories, each of which has an assigned amount of points for three approaches: deterministic, possibilistic and probabilistic. The amount of points for each category has been proposed by Mishra and is not changed here. At the end, all the points are summarized and the approach which scores the most is selected for further analysis. Available alternatives of the GRA categories, as well as selected ones are described below.

Type – the three possible types of GRA are: proactive, reactive and change implementation. The proactive GRA is performed in advance of a planned operation and is mostly done in the planning stage, when physical access to assess hazard is not possible. The reactive GRA assesses a site with possible physical access, mostly after an event has already occurred and when monitoring of the site is being carried out. Reactive GRA is further subdivided into: routine reactive GRA concerning confirmation of risks expected to happen and identification of new unexpected risks, and symptom based reactive GRA that is commenced when a failure symptom has already occurred. The change implementation GRA is performed when a change in existing mine design or operation takes place and alternatives of different risk scenarios have to be assessed. In this study GRA is aimed for quantification of expected seismic hazard, based on the analysis of data from seismic monitoring system, so it can be considered as reactive – routine.

Area scale – the risk assessment can be performed on small (local) scale by investigation of local geology, excavation geometry and reinforcement pattern, or on large scale, where GRA focuses on rock mechanics of the entire area of a mine, applied mining method and sequence and other large scale operations. In this study the risk will be assessed on large scale, because large area of the mine (most hazard prone mining levels) will be evaluated (see chapter 5.2).

Hazard scope – GRA can be: hazard specific when carried out to evaluate a single major hazard in a mine, or site specific when assessing the entire area, where all potential hazard

are taken into account. Main focus of this study will be put on evaluation of risks related with seismic hazard, therefore scope is considered as hazard specific.

Reporting requirements – GRA can be performed as part of internal reporting within a company, or as part of external reporting to confirm that the operational risks are handled according to legal standards. Although this study aims to investigate the applicability of the proposed geotechnical guideline as a part of the I^2Mine project, the results of GRA will be used within the company (Pyhäsalmi mine), hence GRA can be considered as internal.

Resources availability (data, equipment and personnel) – GRA can be performed with resources availability considered as: high, when sufficient personnel, equipment (such as monitoring system) and data is available to assess the likelihood of hazard, average when not sufficient geotechnical data is available, but historical data of geotechnical hazards exists, and finally low when data and personnel are limited and on-site instrumentation is not available. In this study, despite the fact that only one person is carrying out the investigation (externally) with a limited access and within limited time frame, there is a sufficient amount of geotechnical monitoring data available in the mine (especially largely abundant seismic monitoring data), hence the available resources are selected as high.

Results of the selection, together with assigned points has been displayed on Figure 4-1. The steps involved in using the tool are as follows:

Step 1 – Fill the checklist for the boxes on the right for each of the five GRA scope categories. For example in the completed form below, the GRA is identified to be "routine" (shaded in green). The amount of points for deterministic (De), probabilistic (Pr) and possibilistic (Po) is transferred to the "GRA Type" box (following red arrows).

Step 2 – Repeat step 1 for the remaining four categories on the left.

Step 3 – Sum up the De, Pr and Po values for the boxes on the left and input them in the "Total" box. The approach with the highest sum of points is the preferred risk assessment approach.

The results of tool selection suggest the probabilistic approach (with a score of 9) to be implemented in the geotechnical risk assessment procedure.

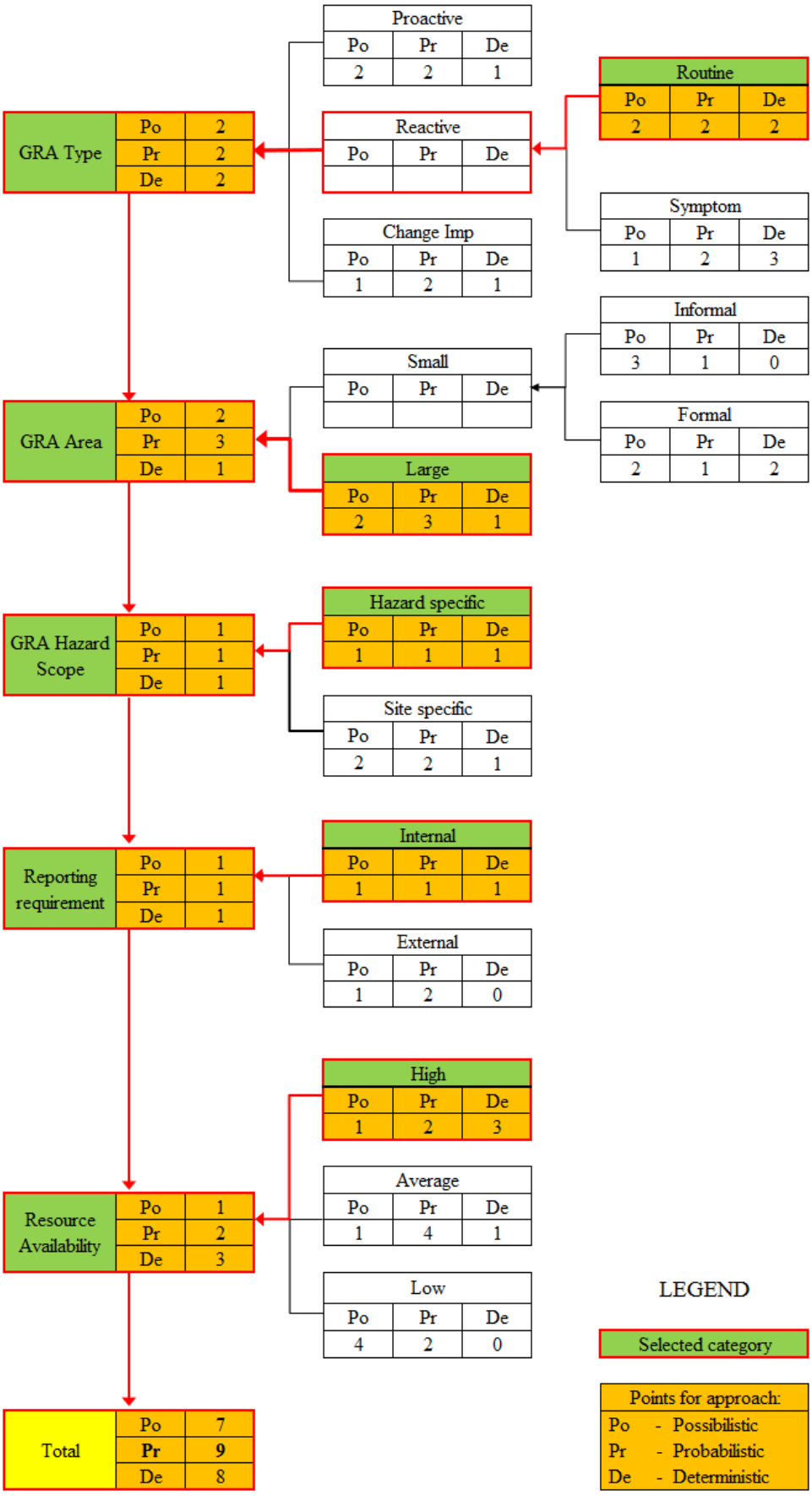

Figure 4-1. Results of the geotechnical risk assessment approach selection.

4.3 Hazard identification

The selection of hazard identification tool depends on the Geotechnical Risk Assessment scale and hazard scope. If the risk assessment is to be performed on large area and with hazard specific scope, the most appropriate hazard identification tool is the bow tie analysis (BTA) (Mishra, 2012). BTA offers a simple approach to identify hazards and potential threats that can result in an undesirable event with several adverse consequences. BTA analysis consists of identification of hazards, threats and consequences related to the top event. Hazards are considered as unsafe situations that can potentially result in the top event by realization of specific mechanisms (threats). Table 4-5 present BTA for large seismic event as a top event (major hazard) leading to damage of mine openings.

Table 4-5. Bow Tie Analysis for large seismic event.

Hazards	Threats	Top event	Consequences
Inadequate ground support	Support load exceeds capacity	**Large seismic event leading to damage of mine openings**	Fatalities and injuries of workforce
Inadequate mine design			Damage of infrastructure and machinery
Active geological structure (fault)	Violent release of accumulated energy		Production interruption
Accumulation of energy in rockmass			Increased cost
Large extent of ore extraction	Stress exceeds rockmass strength		Ore loss
High stress concentration			Reputation damage & community concern

To prevent or reduce consequences of the top event two types of control measures can be utilized: pre-accident and post-accident. The first type of measures is used to prevent the top event from happening. The latter is used to minimize the impact of an event after it has already occurred. The goal of the GRA is to find the most appropriate control measure that can result in effective risk reduction. For example if the ground support type or capacity is not sufficient to withstand large movement of rock, changes in design have to be made to prevent any damages to the tunnel profile. On the other hand, special emergency chambers can be installed in case the damage happens to facilitate rescue of mine personnel.

It is important to mention that hazards presented here should not be confused with seismic hazard definition presented in chapter 3.3. The approach presented in this study evaluates seismic hazard by taking into account multiple hazardous situations and threats (presented in Table 4-5) as the influencing parameters.

5 Seismic Risk Assessment

This chapter presents an attempt to assess seismic risk in the Pyhäsalmi mine using the two approaches described in chapters 3.3.1 and 3.3.2. The first subsection gives an overview of the seismic data retrieved from the database in the mine. The data is first analyzed statistically and quantified with methods used as current worldwide practice of seismic risk assessment in underground mines. Data is also clustered in order to reduce the amount of data, and allow for faster analysis. The second subparagraph describes the selection of mining levels for further analysis. The third subsection presents the results of seismic hazard assessment using Probabilistic Approach for Seismic Risk Assessment (PASRA) method and the fourth subsection demonstrates calculation of seismic risk using The Quantitative Seismic Hazard and Risk Assessment Framework (QSHRAF) approach. The last subsection presents the final representation of seismic risk.

5.1 Seismic data analysis

Seismic events have been retrieved from the seismic database in the Pyhäsalmi mine. This study examines events recorded in the period from 02-11-2002 to 27-02-2014. The total number of events amounts to 206 157. Each record in the database is characterized by several parameters: date, time, location in local coordinates system, location error, seismic moment and seismic energy (for P- and S-wave), static and dynamic stress drop, source size radius, and local magnitude.

The quality of data depends primarily on the process of waveform transformation and used parameters. Investigation of the data quality is not part of this thesis and the data is accepted as given. However, one abnormality has been detected in the location of seismic events, so that 141 events were located above the ground surface. This might suggest mistakes in data processing and using wrong parameters. To avoid any further biases those events were deleted.

5.1.1 Events statistics

This subsection presents statistics of seismic events. Table 5-1 contains mean, median, minimum and maximum of some seismic event parameters. As can be seen the minimum local magnitude recorded by the seismic system amounted to -4.1 and the maximum to 2.2, with an average of -1.6.

The apparent stress is a measure of stress change at the seismic source. Depending on the type of seismic source it can vary considerably; regions of high stress typically are a source of high energy and high apparent stress. On contrary, low apparent stress events take place in low-stress or highly fractured regions (Hudyma, 2008; Gibowicz & Kijko, 1994). The energy of seismic events varies from very low value of $6.82 \cdot 10^{-5}$ J to as high as $1.99 \cdot 10^{7}$ J, with a mean of $9.71 \cdot 10^{2}$ J.

Table 5-1. Basic statistics of seismic event parameters.

	X [m]	Y [m]	Z [m]	Location error [m]	Seismic Energy [J]	Apparent Stress [bar]	Local magnitude M_L
Mean	8312	2280	-1245	5.0	9.71E+02	2.85E+00	-1.6
Median	8323	2297	-1268	5.0	5.29E+00	1.00E-01	-1.6
Min	8000	2000	-1499	0.0	6.82E-05	0.00E+00	-4.1
Max	8600	2599	0	253.0	1.99E+07	1.63E+04	2.2

As can be seen on Figure 5-1, the prevailing local magnitude range is from -2 to -1. Most of the events have a magnitude between -3 and 0. Only 1% of events have a local magnitude larger or equal than 0.

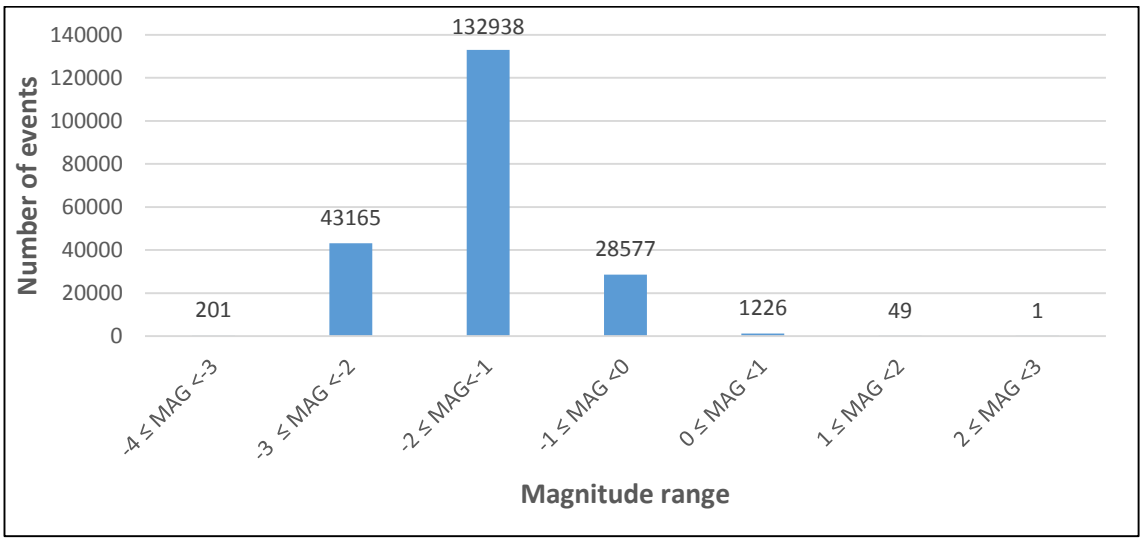

Figure 5-1. Number of seismic events subdivided by the magnitude.

Seismic events with local magnitude higher than or equal to 0 have been plotted on Figure 5-2. It can be seen that the number of larger events increased since the beginning of recording seismic activity, however in 2013 we can see a drop in large events. Number for the year 2014 is projected based on first months, but the increase is visible.

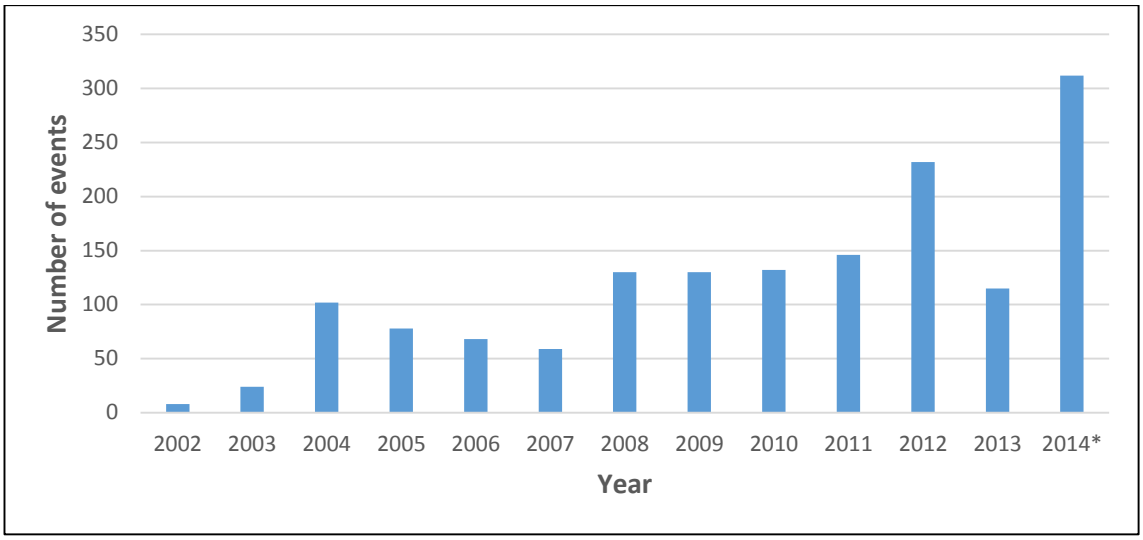

*Figure 5-2. Number of seismic events per year greater than or equal to magnitude 0; *projected based on first two months.*

Figure 5-3 shows daily histogram of seismic events. It is clearly visible that the number of events per day increased. Moreover, in the past two years more extreme values start to appear, with the largest number (2071 events per day) on 11-01-2014, and the second largest frequency (1461 events per day) on 16-02-2014. One of the explanations of increasing seismic activity is an intensification of movement of the northern ore contact zone and an increase in subsidence rate. As it has been observed by Bergstrom (2012), displacement increases were correlated with increased seismicity. Important fact to mention is that the seismic system upgrade in September 2013 provided additional geophones, and this results in higher sensitivity of the system, hence more events can be recorded.

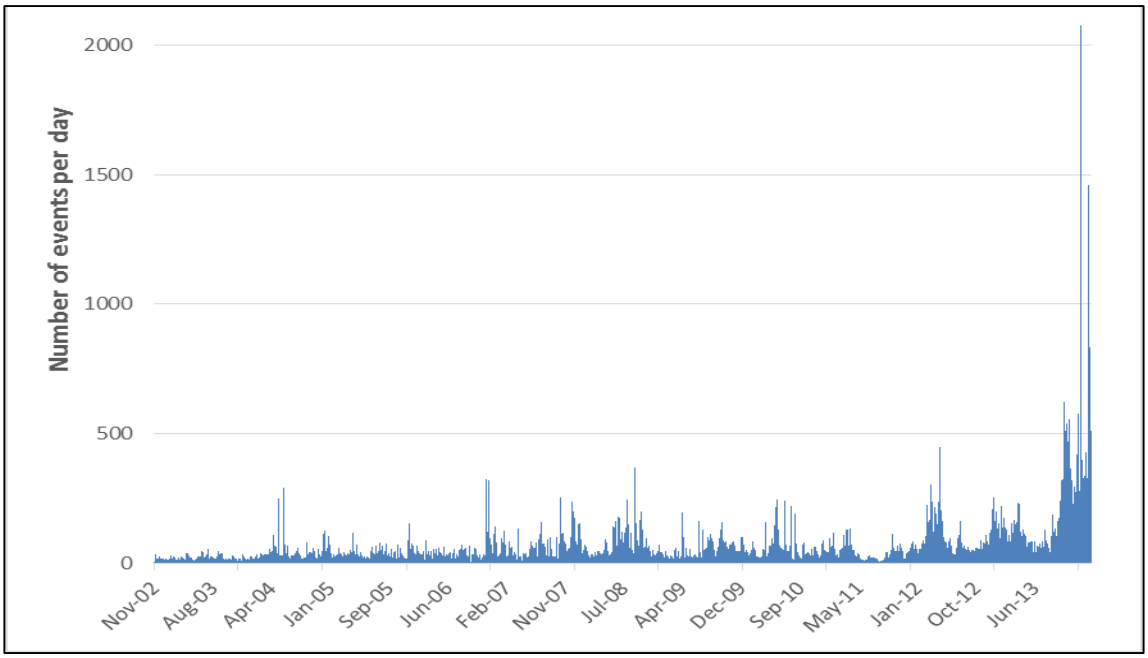

Figure 5-3. Daily histogram of seismic events for the period from 25-11-2002 to 27-02-2014.

To investigate if there is a significant link between the time of day and occurrence of seismic events, all events were grouped by the hour of day in which they took place. Resulting diurnal chart is plotted on Figure 5-4.

As can be seen, considerable amount of seismic events occurred in the 22nd hour of day, in comparison to other hours. It is an indication that there is a direct relation with blasting time in the mine (at 22:00). This means that large portion of events can be considered as stress driven.

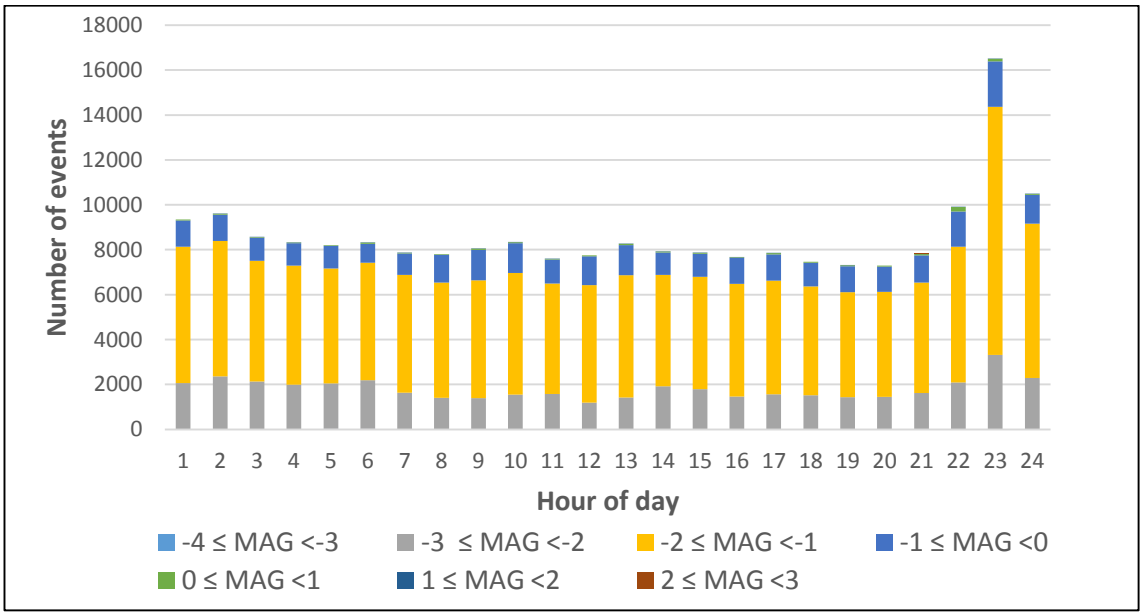

Figure 5-4. Diurnal chart showing the distribution of seismic events by the hour of day; subdivided by the magnitude.

5.1.2 Seismic events clustering

The main idea behind clustering of seismic events is to compress the amount of thousands event into smaller groups to increase the efficiency of investigation. The assumption used is that a single cluster (or cluster group) represents a single seismic source. Resulting clusters (or cluster groups) can be used for the evaluation of maximum possible event that can occur as a measure of seismic hazard.

The process of seismic events clustering is divided into three stages (see Figure 5-5).

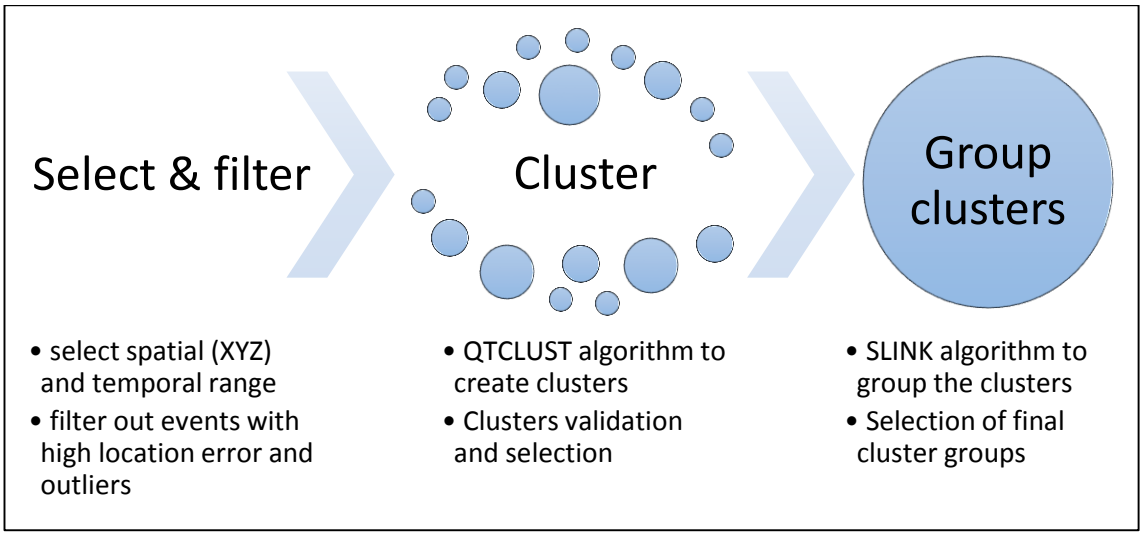

Figure 5-5. Flowchart presenting three stages of clustering process.

In the first stage, the amount of seismic monitoring data is reduced using spatial and temporal constraints in order to allow for trouble-free and faster analysis:

- Data is selected from the last 3 years of monitoring (from 01.01.2011 to 27.02.2014) – to limit the amount of data for processing, mainly because of high computational demand of the clustering process. Analyzing more than 200000 events can be very slow, problematic and almost certainly unnecessary (Hudyma, 2014).
- Data is selected from inside the range for Y: from 2000 to 2600, for X: from 8000 to 8600, for Z: from -1500 to -900) – as events located close to the production areas that have influence on the risk assessment process.

Next, data is filtered to select only good quality data:

- Reject events with high location error (above 95% percentile; ≥ 8m) to eliminate the events that could bias the results.

- Reject outliers using density based approach (using isolation distance) – events that do not have at least one neighbor within a sphere of a 20m radius around them are rejected.

In the second stage, the Quality Threshold Clustering algorithm (QTCLUST) is used to create compact clusters of seismic events. The main reason to use QTCLUST in this stage is its computational efficiency compared to hierarchical clustering methods (like SLINK) that are impossible to use with given amount of data.

Clustering routine was performed using an open source programming language and environment for statistical computation – R, which is available as a free software. The software has integrated collection of statistical analysis tools including the two clustering algorithms applied in this study.

In order to find optimal values for two parameters of the QTCLUST algorithm a sensitivity analysis has been performed. The goal is to maximize the number of seismic event and the amount of seismic energy within the clusters, and at the same time keep a reasonable number of created clusters. The cluster radius should be set up to be as low as possible and at maximum equal to the sub-level spacing of production levels (25m in the Pyhäsalmi mine). Small radius tends to ensure that seismic events within a cluster are from a single seismic source, but can drastically increase computation time and the total number of clusters. By decreasing the cluster radius and increasing the minimum number of events (required to be classified as a cluster), the total number of events, as well as the sum of the seismic energy being clustered is decreasing. A good clustering routine should include at least 90% of total seismic energy and more than 75% of total number of seismic events (Hudyma, 2008).

During the sensitivity analysis the cluster radius was differentiated between 20, 25 and 30m. The minimum number of events was varied from 10 to 40. Results are presented in Table 5-2.

It can be seen that for a cluster radius of 20m results are rather poor in terms of the total seismic energy within the clusters. For the minimum cluster size of 10 events the sum of energy is only 82% of the total, what is below the minimum 90% required for good clustering. Moreover, the number of QT clusters (901) is large and can be problematic to handle in the next stage. The most efficient is cluster radius of 30m, but as it was stated

before, it exceeds the sublevel distance in the mine, and hence it is not appropriate to use it. Ultimately, cluster radius of 25m is selected together with the minimum size of 15 events (highlighted in red) that gives good results in both the total number of events clustered (96% of total) and seismic energy (90% of total).

Table 5-2. Sensitivity analysis of QTCLUST algorithm parameters.

Cluster radius [m]	Min. events	Nr of events clustered		Sum of energy [J]		Number of clusters
20	10	98450	95%	3.90E+07	82%	901
	15	97340	94%	3.80E+07	80%	861
	20	94908	91%	3.37E+07	71%	720
	25	92304	89%	3.01E+07	64%	630
	30	90872	87%	2.88E+07	61%	522
	35	89379	86%	2.89E+07	61%	495
	40	87429	84%	2.60E+07	55%	430
25	10	101826	98%	4.30E+07	91%	791
	15	100071	96%	4.27E+07	90%	646
	20	98289	95%	3.95E+07	84%	541
	25	96926	93%	3.84E+07	81%	479
	30	95757	92%	3.47E+07	73%	436
	35	94577	91%	3.36E+07	71%	399
	40	93030	90%	3.16E+07	67%	352
30	10	101541	98%	4.34E+07	92%	488
	15	101572	98%	4.43E+07	94%	492
	20	100405	97%	4.24E+07	90%	425
	25	99471	96%	4.31E+07	91%	380
	30	98707	95%	4.06E+07	86%	351
	35	97675	94%	3.82E+07	81%	320
	40	96819	93%	3.81E+07	81%	297

The results of QTCLUST are 646 QT clusters created from 100071 seismic events. Figure 5-6 and Figure 5-7 illustrate all seismic events that were clustered, omitting the outliers, with different coloring for different QT clusters. It can be seen that it is rather difficult to analyze the results based on spatial distribution of clusters and further grouping of cluster is inevitable.

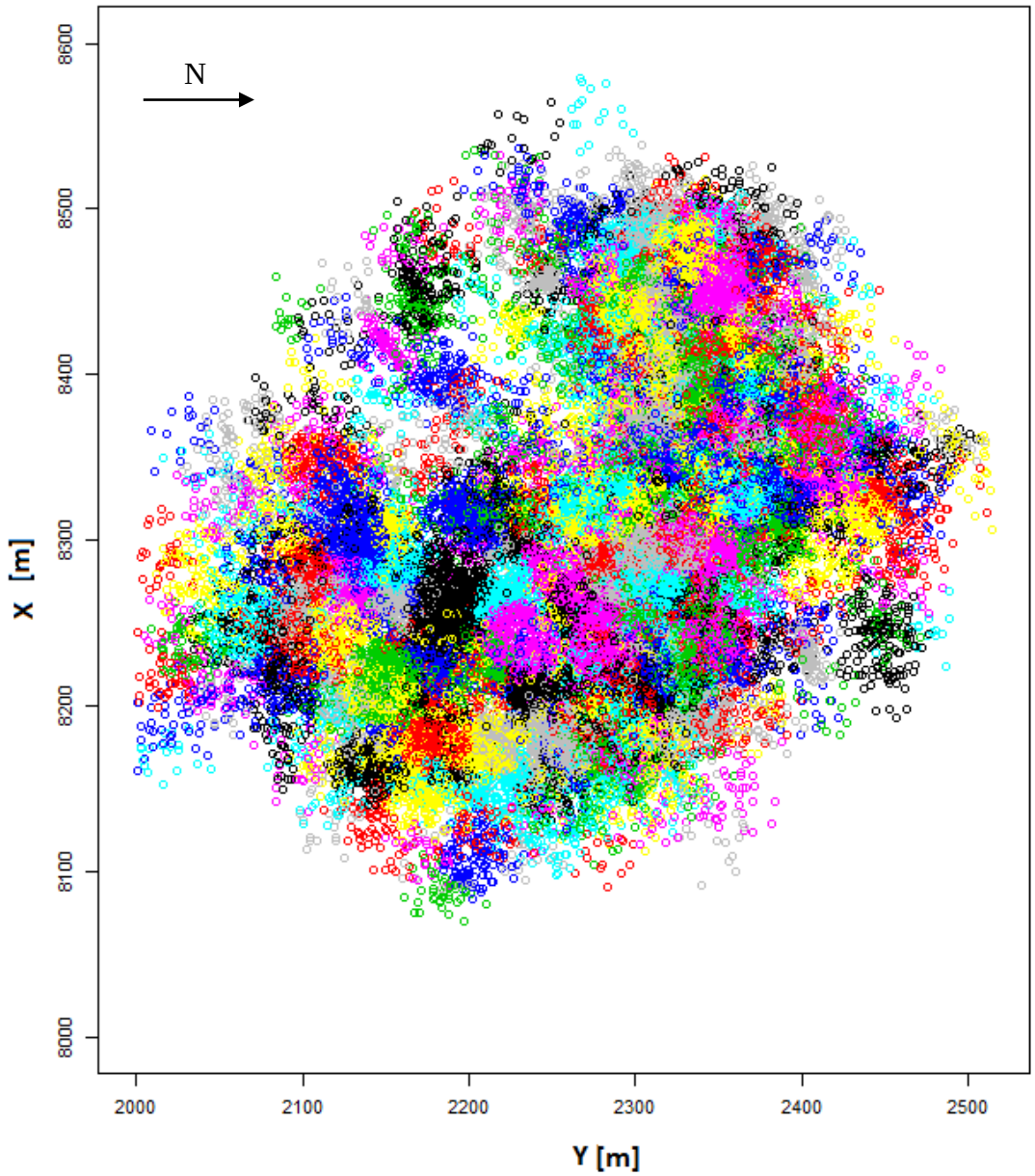

Figure 5-6. Plot of 646 QT clusters created in the second stage of clustering using QTCLUST algorithm; plotted in the X-Y space. Colors illustrate different QT clusters.

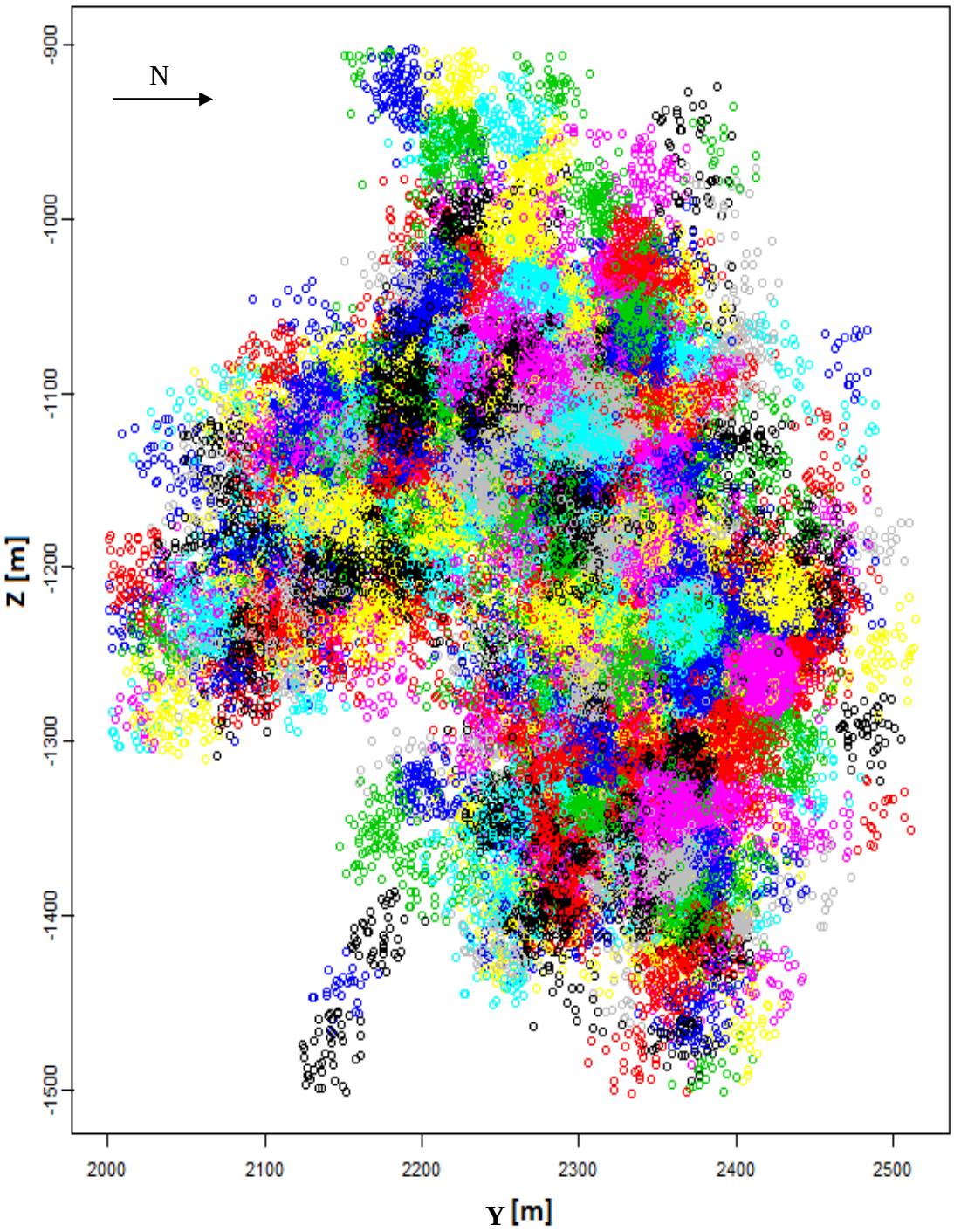

Figure 5-7. Plot of 646 QT clusters created in the second stage of clustering using QTCLUST algorithm; plotted in the Y-Z space, view looking east. Colors illustrate different QT clusters.

The QT clusters were checked for validity using the F-M diagram drawn from the population of seismic events within clusters. Graphs were plotted using range of local magnitudes. The a and b parameters (from Equation (4) for each cluster were found using linear regression (the least squares method). Ideally, the dataset would be expected to follow linear relation for 2 or more orders of magnitude and have a slope of about -1 (Hudyma, 2008).

Figure 5-8 illustrates F-M diagram for cluster QT121. As can be seen, the linear relation is preserved for magnitudes between -2 and -0.25, what is close to ideal. The slope of the curve is -1, what represents the power law relation. Not all clusters showed such a good fitting of F-M diagram and both the slope and the range of linear relation is not ideal. Figure 5-9 illustrates F-M diagram of cluster QT84 which linear relation is only followed for one order of magnitude and slope is -1.9. One of the reasons may be rather low magnitude range of the dataset from Pyhäsalmi that results in faster flattening of the curve and do not allow for larger magnitude range to be approximated with linear relation. Other possibilities are: poor filtering of mine blasts, erroneous parameters of seismic events, waveform corruption due to proximity of electrical noise, or even poor calibration of local magnitude.

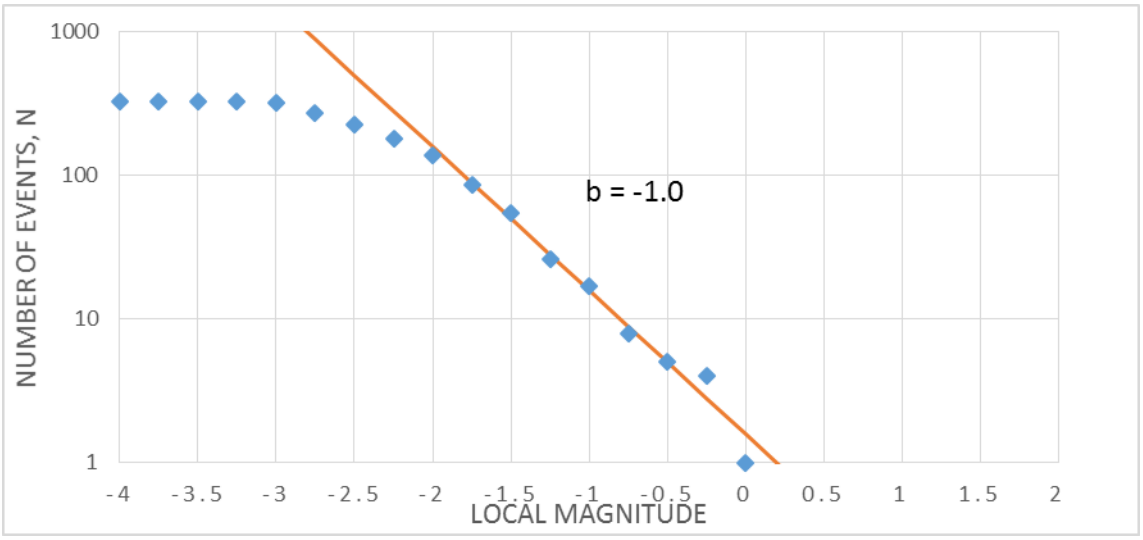

Figure 5-8. Frequency-Magnitude relation of the cluster QT121.

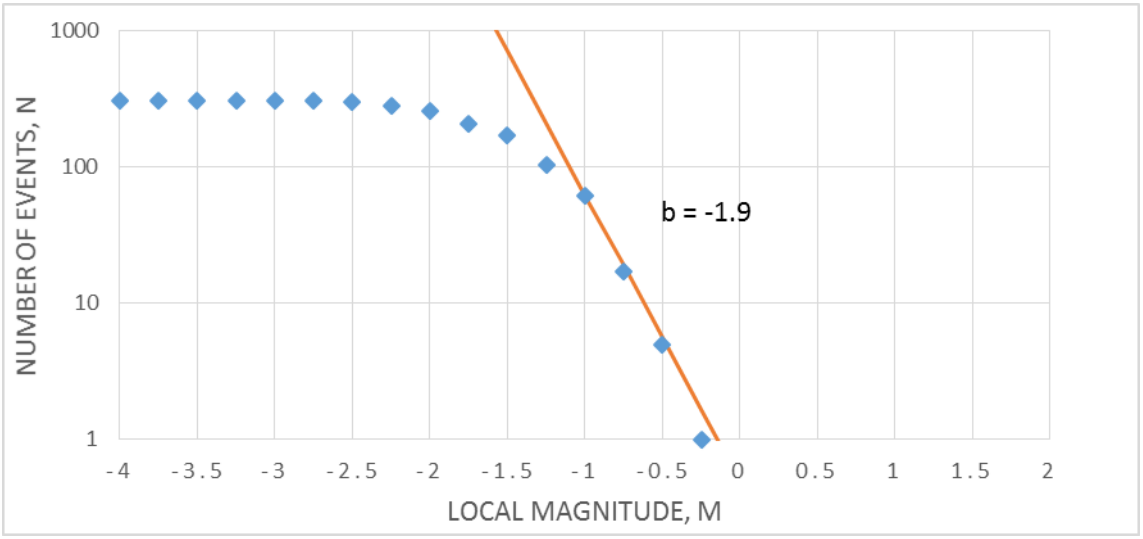

Figure 5-9. Frequency-Magnitude relation of the cluster QT84.

After validation of QT clusters, several parameters were calculated for each of them to investigate their significance as a single seismic source, and to create a basis for further analysis. The parameters were as follows:

- number of significant (MAG > 0) and large (MAG > 1) events,
- b value and a/b value (x-axis intercept) of the Frequency-magnitude relation (see Equation (4),
- median of the S-wave to P-wave energy ratio,
- the sum of seismic energy,
- the sum of apparent stress.

The QT clusters created in the second stage of clustering were evaluated in order to limit the number of clusters by rejecting marginal clusters that represent minor failure of rockmass. In order to be categorized as marginal a cluster needs to meet at least two of the following criteria:

- The number of events in a cluster is low (< 20-50).
- All events are small (MAG < -1).
- The total amount of Apparent Stress is low (< 30 bar).
- The total amount of seismic energy is low (< $1 \cdot 10^3$ J).

After rejection of marginal clusters the resulting number of clusters was 366. Those clusters were selected for the next stage. Five most populous QT clusters with calculated parameters can be viewed in Table B-1 in Appendix B.

In the third stage of clustering, the Single linkage clustering algorithm (SLINK) was used to link similar QT clusters into groups representing one seismic source. Euclidean distance between cluster centroids was used as a distance metrics. Next, the similarity of neighboring clusters was evaluated using following parameters:

- b-value of the Frequency-magnitude relation,
- median of the S-wave to P-wave energy ratio,
- top 5 maximum magnitudes recorded (values and dates),
- top 5 Apparent Stress peaks (values and dates),
- number of significant and large events,
- top 5 daily event histogram peaks (values and dates).

When the clusters showed similarities in those parameters (with a special emphasis on first four) they were linked together into logical groups. It was possible to create 82 cluster groups, where:

- 72 groups contain at least two QT cluster and maximum 12 QT cluster (group S20).
- 10 groups contain 10 single QT clusters with maximum number of events.
- 2 groups contain 2 single QT clusters with the highest sum of seismic energy.

Table 5-3 presents five most populous clusters groups with centroids calculated as the average of centroids from all the QT clusters within a group (for results of all 82 groups please see Table B-2, Figure B-1and Figure B-2 in Appendix B). The maximum expected magnitude is found by combining all seismic events from QT cluster contained within a single group and producing an F-M diagram from resulting data set to find the x-axis intercept. In the last step, each point within a single cluster group was assigned with maximum predicted magnitude, with an assumption that seismic event of predicted size can occur everywhere within a cluster group.

Table 5-3. Five most populous cluster groups created in the third stage of clustering using SLINK algorithm.

Cluster group	X [m]	Y [m]	Z [m]	Max. predicted M_L	Nr of events	∑ Seismic Energy [J]	∑ App. Stress [bar]
S20	8337.8	2373.8	-1257.6	0.9	11097	3.60E+06	1.65E+04
S02	8268.7	2320.7	-1129.4	1.0	6564	1.16E+06	2.90E+03
S03	8366.2	2355.5	-1361.4	0.1	5581	2.30E+05	2.40E+03
S12	8379.3	2309.1	-1276.8	0.2	5579	1.89E+06	6.37E+03
S39	8352.9	2351.9	-1203.8	1.1	4464	1.16E+06	3.35E+03

Summary of the clustering process is presented in Figure 5-10. As can be seen, 82 Cluster groups created from 297 QT cluster in the third stage contain 84% of total number of seismic events (87 462 from 103 933 events). Furthermore, they represent 88% of the total seismic energy ($4.18 \cdot 10^7$ J from $4.73 \cdot 10^7$ J) and can be considered as a good representation of the total population of seismic events.

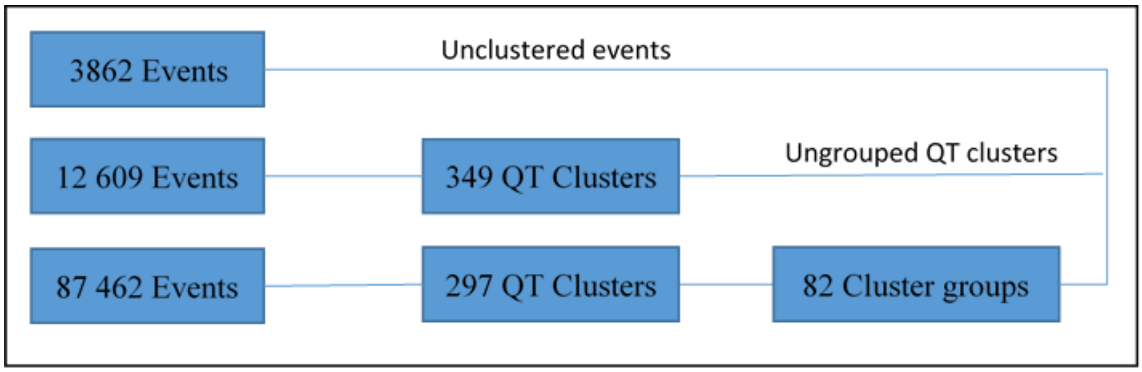

Figure 5-10. A schematic summary of the clustering process

It has to be noted that due to the large amount of data, not all the results of the clustering process are presented in this study in tabular format. Tables with all the results can be presented on a request.

5.2 Selection of the investigation area

An analysis and interpretation of damages in production levels has been performed to find the most unsafe levels, and to narrow down the area under investigation. It has been assumed that high level of damage can be linked to high seismicity level, hence giving an indication of high deterioration of the rockmass.

Damage data has been mapped by the mine personnel. Each damage record stored in the database is described by several parameters:

- date of inspection,
- damage severity (subdivided into seven classes: very minor, minor, moderate, major, serious, very serious, collapse),
- damage depth,
- support type used and condition its condition,
- location and surface extent,
- description,
- photograph (if the damage is more serious).

All the damages are also stored as a DTM surface file in Surpac software that allows to localize each damage on the mining level map. The type of damage varies from superficial cracks and fallouts of the shotcrete layer only in part of the excavation (very minor damage), to more severe collapses of the all the tunnel profile, mainly under faulting conditions (very serious to collapse type of severity). An example of more severe damage can be found on Figure 5-11.

Figure 5-11. An example of rockburst damage that occurred 24.12.2001 on mining level 1200, at the upper level of stope GBL21.

During the analysis, all damages (according to the severity type) were summed for each mining level. Results are plotted on Figure 5-12 together with the number of seismic events with a local magnitude of 0 or higher.

As seen from Figure 5-12, the highest number of damages was mapped on the 1300 level. However, many of them are only of very minor or minor severity. To select levels with the highest level of deterioration, further investigation has been performed by ranking the levels by number of damages in each class of moderate and higher severity. Next, damages on levels ranked on the top in each category were summed up to find the ones with highest number. Three mining levels which scored the maximum number are: 1225, 1250 and 1275. These are selected for further investigation of seismic risk.

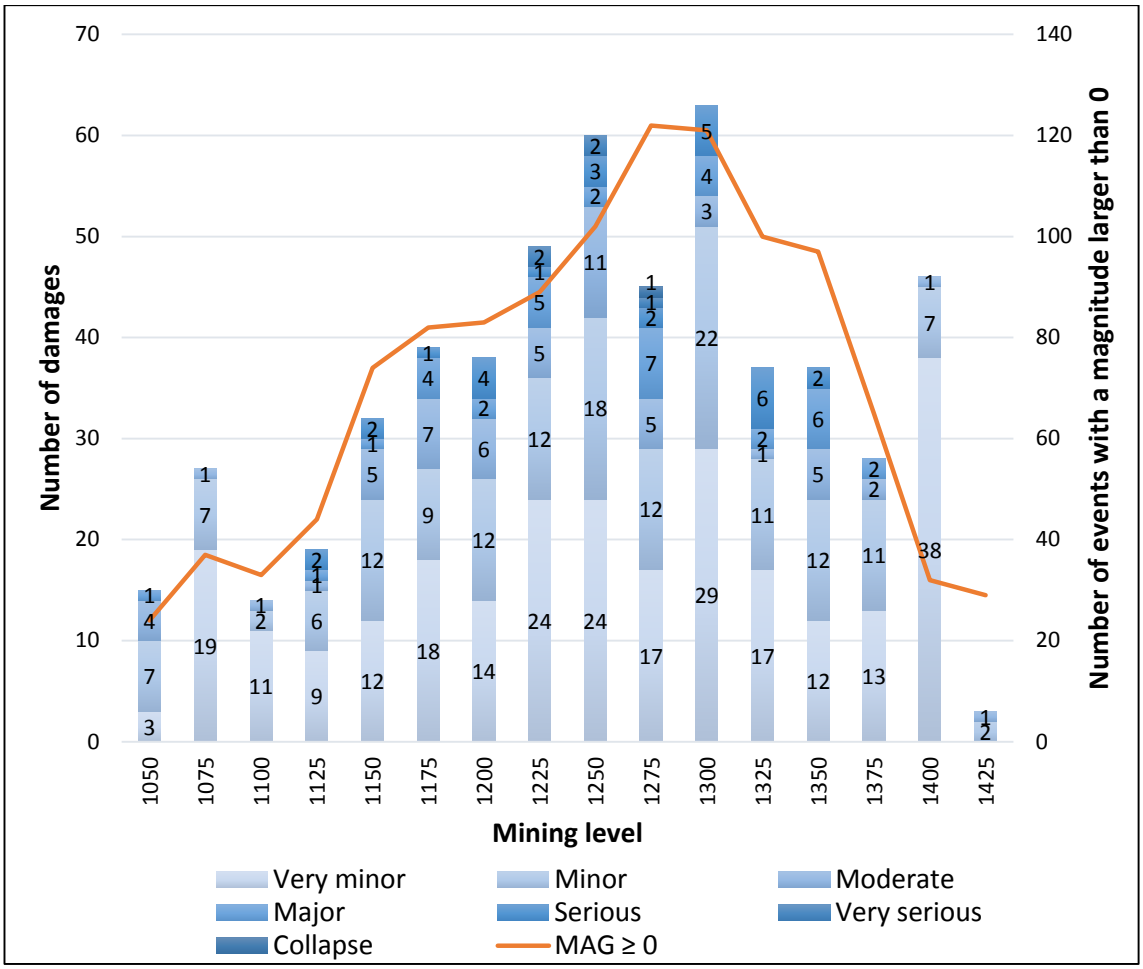

Figure 5-12. All damages mapped on the mining levels in 2013, subdivided into severity classes. Number of seismic events with a local magnitude 0 or higher.

It is possible that large amount of damages on these levels is related to higher ore extraction. During the time period from September 2013 to January 2014 the largest number of stopes were extracted on the level 1275. Furthermore, as it is shown on the Figure 5-12, the number of seismic events with a magnitude larger than 0 (significant events) correlates well with the damages observed on selected mining levels.

5.2.1 Division of selected mining levels

Selected mining levels were divided using a square grid consisting of 20m by 20m squares indexed vertically with a capital letter from A to U and horizontally with a number from 1 to 19 (see Figure 5-13, Figure 5-14 and Figure 5-15). Each square in the grid (assessment zone) was assigned with four characteristics:

- ground support type,
- maximum compression stress,
- intact rock strength (UCS)

- X, Y, Z coordinates of the excavation centroid point.

The support type was assigned based on the ground support map from the mine. Additionally, each support type was indexed with a number (support index), according to following rules:

- No bolts - 1
- Rock bolts - 2
- Cable bolts - 3
- Rock bolts and cable bolts – 4
- Mesh - 5
- Rock bolts and mesh - 25
- Rock bolts, cable bolts and mesh - 45

If there were mine openings with two different support types in one zone, then the name of this zone also included the support index, for example on mining level 1275 zones G16:2 and G16:25 for excavation supported with rock bolts and rock bolts with mesh, respectively.

The maximum compression stress was assigned based on the rock mechanics numerical model that was sectioned at the elevation of selected mining levels (Hakala, et al., 2013). Intact rock strength was taken from the input parameters of the rock mechanics numerical model as follows:

- Ore – 105 MPa
- Waste rock – foliation (on the ore-waste contact zone) – 110 MPa
- Waste rock– residual strength in zones were rockmass has yielded– 75 MPa
- Waste rock – 180 MPa

The resulting allocation of abovementioned parameters for assessment zones in all levels can be found in Appendix C.

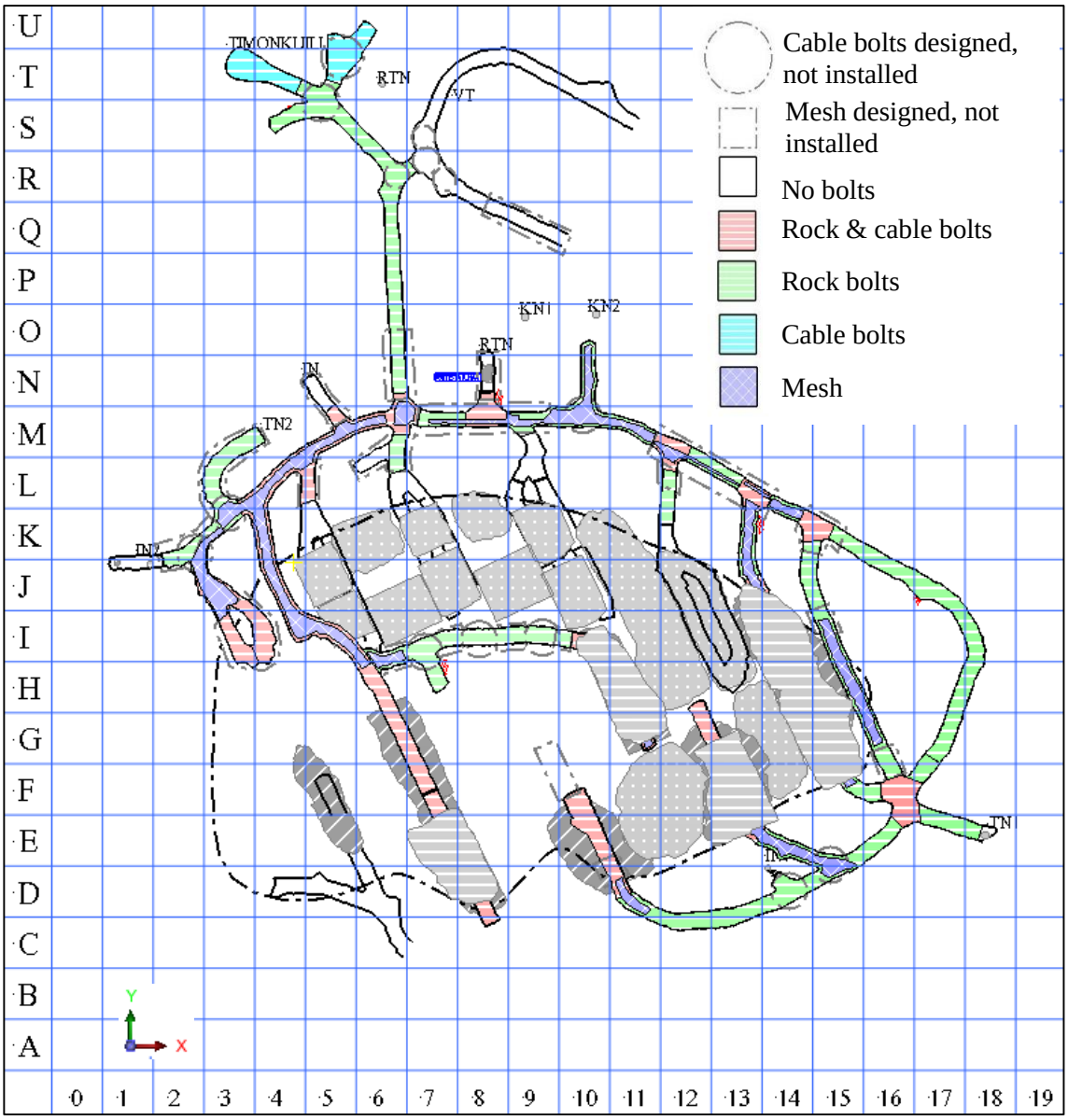

Figure 5-13. Mining level -1225 with assessment zones. Colors represent different support type.

Figures above and below show selected mining levels with assessment zones. Different colors illustrate the ground support type, according to the legend. Dashed line in black represents the ore-waste rock contact zone. Mining stopes are filled with gray color. The alphabetical symbols represent mine infrastructure elements: KN - orepass, TN – backfill raise, RTN, RTNP and IN – ventilation raises, VT – access ramp, TIMONKULU – shaft.

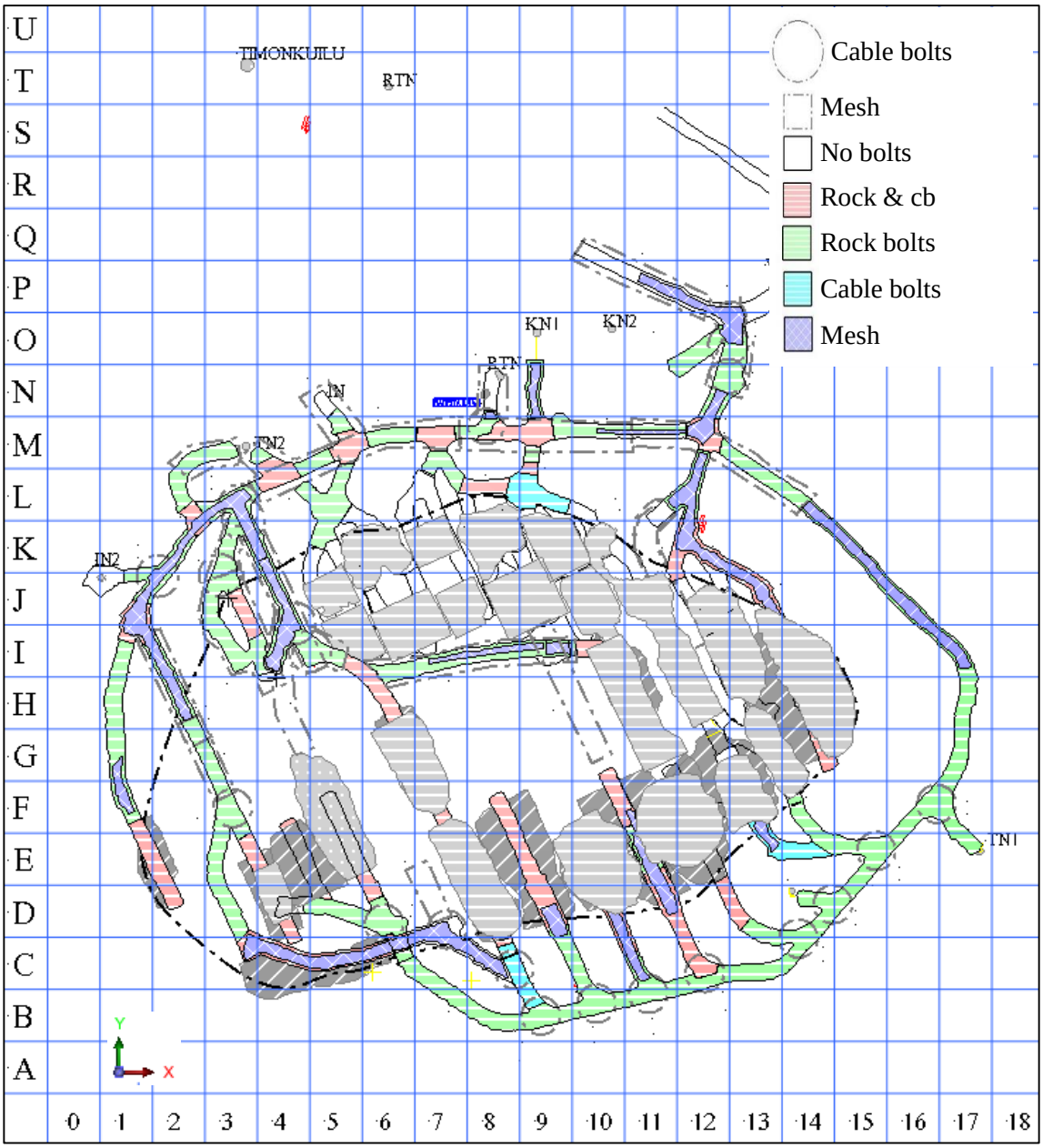

Figure 5-14. Mining level -1250 with assessment zones. Colors represent different support type.

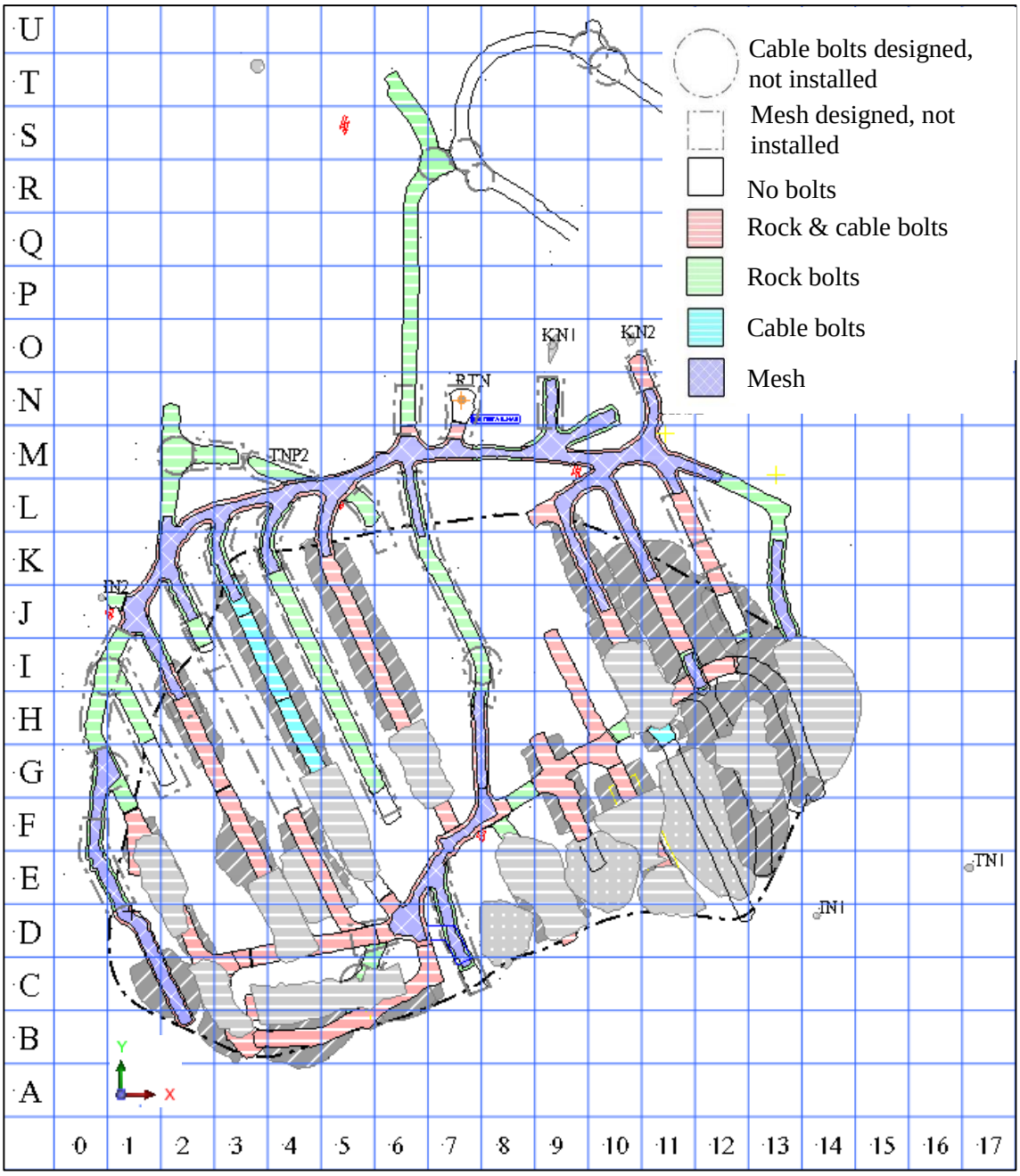

Figure 5-15. Mining level -1275 with assessment zones. Colors represent different support type.

5.3 Seismic hazard assessment

The assessment of seismic hazard has been performed using the two methodologies described in chapters 3.3.1 and 3.3.2. The reason to select two approaches was that the Probabilistic Approach for Seismic Risk Assessment (PASRA) methodology lacks a possibility to compare the results with a rockburst damage scale developed from real cases. It is difficult to assess the hazard as low or high, and only relative comparison within a mine is possible. On the other hand, the Quantitative Seismic Hazard and Risk

Assessment Framework (QSHRAF) method gives the opportunity to quantify the hazard using empirically developed scale.

As it was stated in chapter 2.3, due to fracturing of the orebody the stresses inside has been redistributed and concentrated along the ore-waste contact zone and around the orebody. This also resulted in an increase in seismicity. Taking this into account, hazard assessment has been performed only on assessment zones located outside of the orebody and on the contact zone.

5.3.1 PASRA

The seismic hazard was evaluated using the Probabilistic Approach for Seismic Risk Assessment (PASRA) methodology described in chapter 3.3.2. First, the energy of maximum possible event was calculated within each cluster group. To find the relationship between local magnitude and seismic energy (as in Equation (9), a plot was created from events database using magnitude and corresponding seismic energy. The relationship was found using least squares regression. Results are plotted on Figure 5-16. It is important to note that the data was selected from years 2011 to 2013. When seismic events from 2014 were included, the linear relationship was not as good. This may be an indication of poor system calibration after the upgrade at the end of 2013.

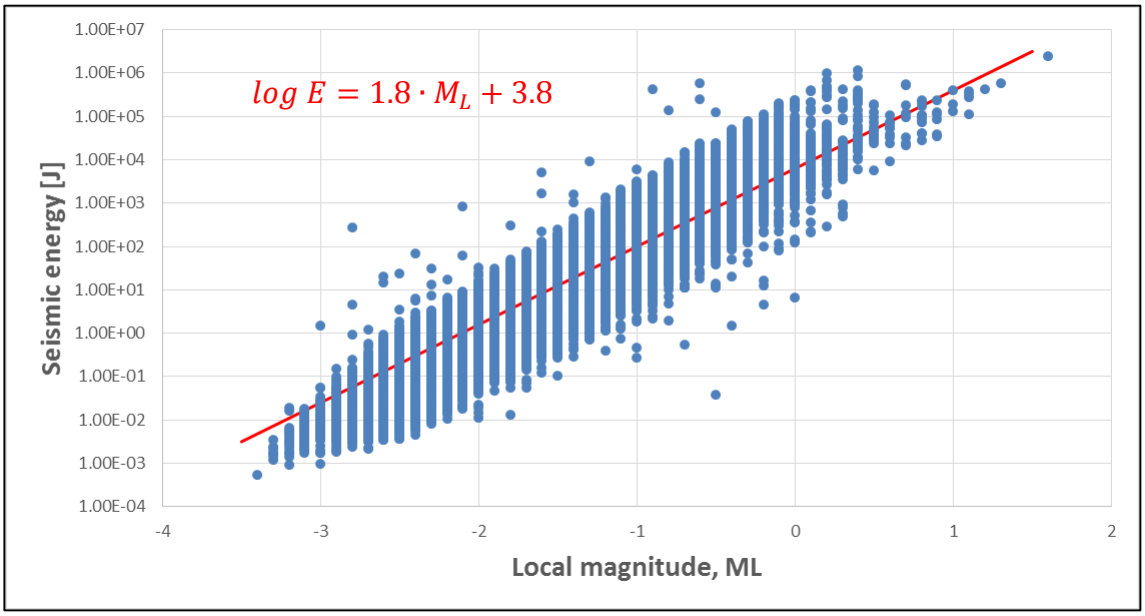

Figure 5-16. Local magnitude and seismic energy relation plotted from monitoring data from years 2011-2013. Equation from linear regression (in red) used to calculate seismic energy based on local magnitude.

Next, the Euclidean distance (Equation (12) was used to create a distance matrix with length between all seismic events within cluster groups (seismic sources) and centroids

of mine opening within grids. The reason for calculating distance matrix for all points within cluster groups (seismic sources) is a conservative assumption that the maximum predicted event can occur at every point within a cluster group with equal probability. The Released Energy Capacity (REC) was calculated for each cell in the distance matrix according to Equation (10), with the energy of maximum predicted seismic event scaled for distance. The attenuation coefficient was selected to be equal to 0.0001. Next, the maximum value of REC was found for each centroid of mine opening.

The maximum intensities of REC were found for assessment zones: E14, I18 and L9 on mining level 1225; I2, L7 and O13 on mining level 1250; K2, L3 and L2 on mining level 1275. From the results of REC it was observed that the distance from the centroid of assessment zones to cluster groups did not have influence on REC result. For all assessment zones on all levels the maximum predicted energy was related to only one cluster group (S39 with the highest predicted local magnitude of 1.1). Even when the distance from the source to assessment zone was as large as 313m (from zone E17 to group S39) the highest REC was still related to this group. This is an indication that the distance scaling factor in REC formula (as in Equation (10) is inappropriate.

The Absorbed Energy Capacity (AEC) was evaluated using qualitative scale of ground support capacity present in Table 5-4.

*Table 5-4. Absorbed Energy Capacity scale for ground support (*including fibrecrete when mesh is not used and shotcrete when mesh is used).*

Support type*	AEC rating
No bolts	1
Rock bolts	2
Cable bolts	3
Rock bolts and cable bolts	4
Rock bolts and mesh	5
Rock bolts, cable bolts and mesh	6

Seismic hazard was calculated as the REC/AEC factor according to Equation(11). On the mining level 1225 the top scores of REC/AEC were found for assessment zones: L9, L7, L6 and R7 (see Figure 5-17). The average REC/AEC is 12.4. On the mining level 1250 the top scores of REC/AEC were found for assessment zones: P10, N8, N5 (see Figure 5-18). The average REC/AEC is 8.7. On the mining level 1275 the top scores of REC/AEC were found for assessment zones: N7, R7:1, S7 and R8 (see Figure 5-19). The average REC/AEC is 9.7. Detailed results of PASRA can be found in Table C-1, Table C-2 and Table C-3 in Appendix C.

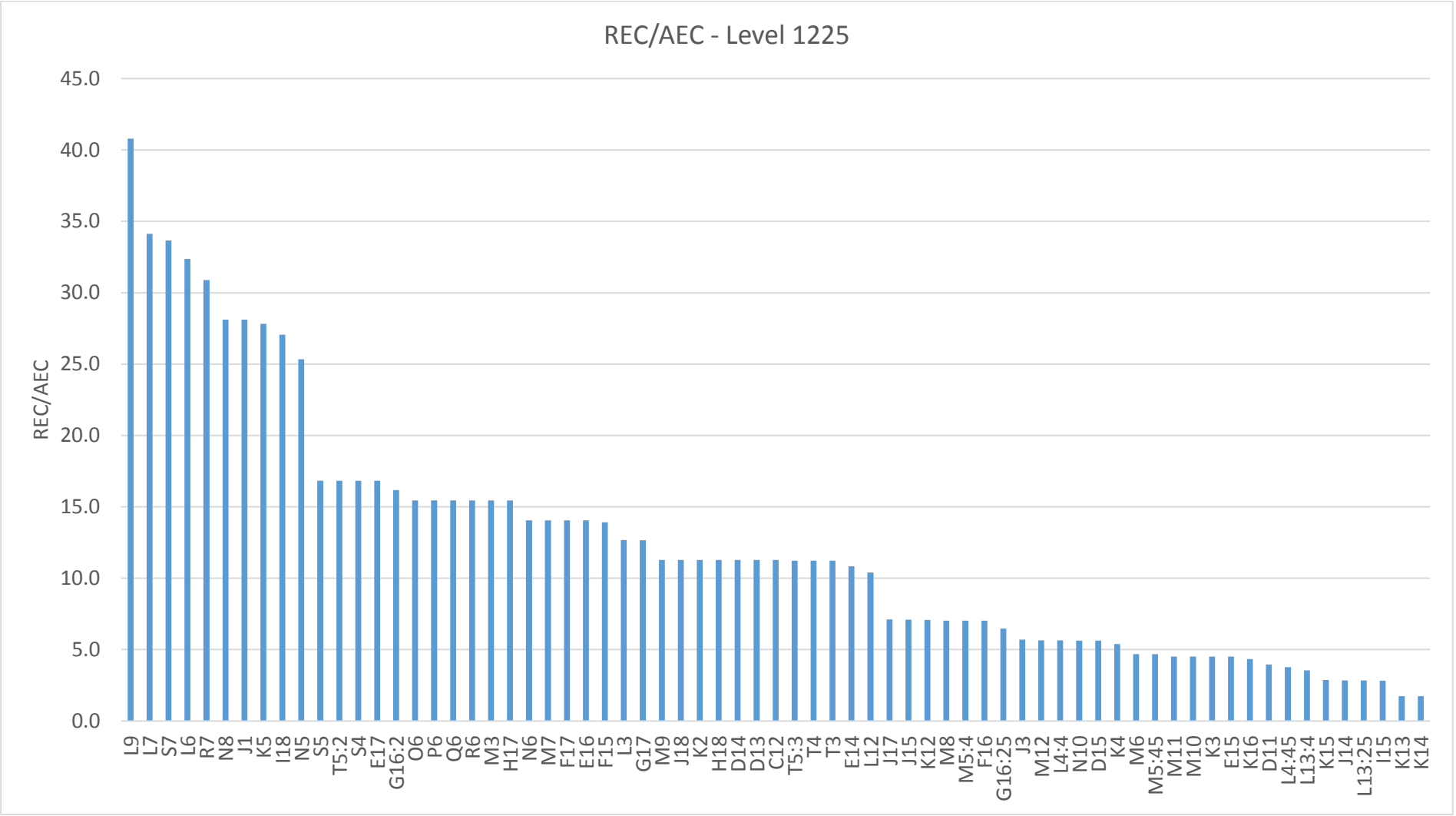

Figure 5-17. Results of REC/AEC for mining level 1225.

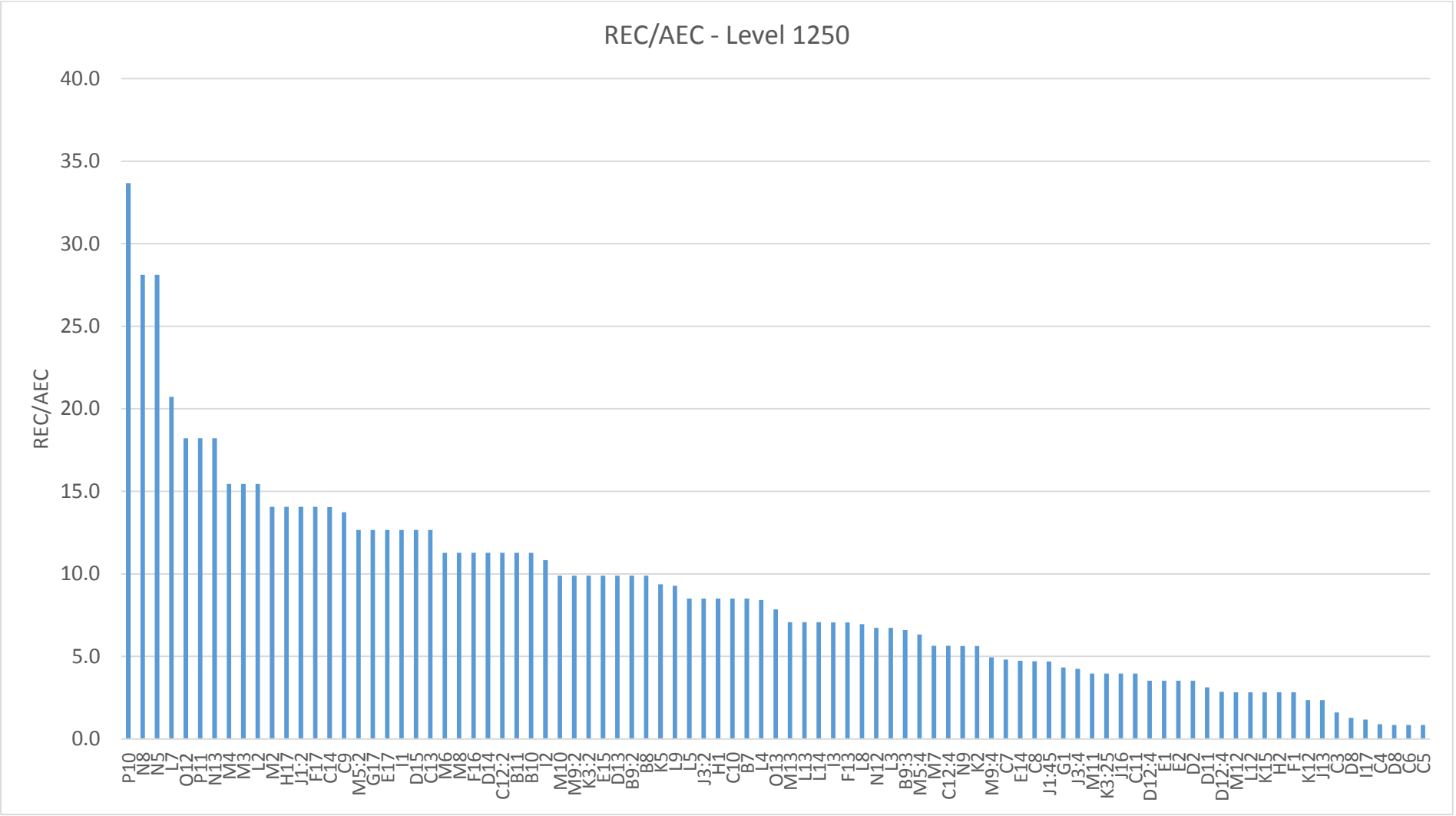

Figure 5-18. Results of REC/AEC for mining level 1250.

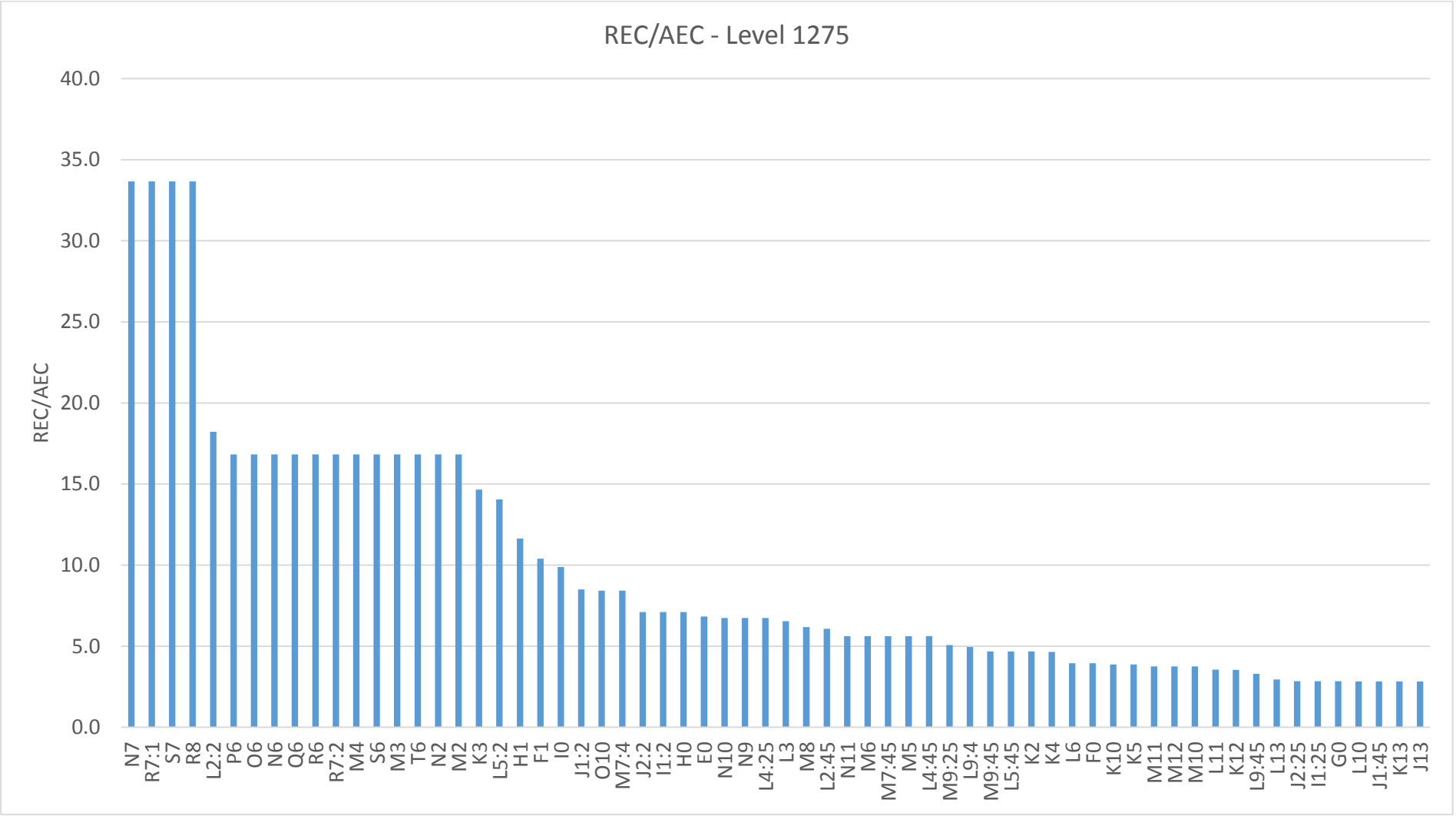

Figure 5-19. Results of REC/AEC for mining level 1275.

5.3.2 QSHRAF

The Quantitative Seismic Hazard and Risk Assessment Framework (QSHRAF) approach (described in chapter 3.3.1) has been used to evaluate seismic hazard. It is based on evaluation of the maximum ground motion using Peak Particle Velocity (PPV) as in Equation (6). Calculation of PPV was done for every centroid of assessment zones is similar to calculation of REC in PASRA. Euclidean distance formula was used to create a distance matrix with distances between all seismic events (grouped into cluster groups - seismic sources) and assessment zones centroids. Then PPV was calculated using the maximum predicted magnitude assigned to each seismic event, for each distance value, to scale the PPV for length. Then, the largest expected PPV was found for each zone. Results of PPV for each level can be found in Appendix D.

Next step was to calculate Excavation Vulnerability Potential (EVP) according to Equation (7), stress condition factor (E_1) was calculated as a ratio of static stress to rockmass strength (UCS) in the vicinity of excavation. The values for stress were taken from the rock mechanics numerical model and rock strength was assigned as described in chapter 5.2.1. Ground support capacity (E_2) has been assigned to assessment zones using the support scale presented in Table 3-7, however slight changes has been made in order to include the different support classes used in the mine. Meshing and shotcreting is used in every excavation in the mine, therefore the rating for 'No bolts' support type has been lowered from 5 (minimal surface support without rock bolts) to 4 (surface support without rock bolts). On the other hand, if an additional mesh was used, the E_2 rating was increased to 6 (to account for increased capacity of additional surface support). Table 5-5 gives a summary of support types and allotted E_2 factor.

Table 5-5. Ground support capacity (E_2) scale for ground support.

Support type	E_2
No bolts	4
Mesh	4
Rock bolts	5
Cable bolts	5
Rock bolts and cable bolts	10
Rock bolts and mesh	6

Excavation span (E_3) was calculated as a diameter of a circle drawn within excavations in assessment zones. Geological structure factor (E_4) has been assigned with a value of 0.5 to assessment zones along the ore-waste contact zone as a potential failure surface promoting rockmass failure. Other zones were assigned with E_4 factor equal to 1.5.

The Rockburst Damage Potential (RDP) was calculated as a product of PPV and EVP (as in Equation (8) and evaluated using the EVP vs PPV diagram (as in Figure 3-3) and rockburst damage scale (as in Table 3-9). Results of the largest RDP for assessment zones on three mining levels were plotted on Figure 5-20.

As can be seen on EVP vs PPV chart, four assessment zones on mining level 1225 are within the R2 rockburst damage zone (minor damage/less than 1t of rock displaced): M9 (RDP = 121.3), N5 (RDP = 76.9), N8 (RDP = 57.9), K5 (RDP = 54.5). It is important to note that N5 zone has surface support only (shotcrete and mesh) and no rock bolt, so the E_2 rating is 4. Other zones are within the R1 zone (no damage/minor loose), however two zones: K2 (RDP = 49.8) and L9 (RDP = 46.5) are very close to the R2 zone and only slight increase in PPV may result in damage. The average RDP on this level is 15.8.

On mining level 1250 are within the R3 rockburst damage zone (1 to 10t rock displaced): N8 (RDP = 157.6), L7 (RDP = 147.8), N5 (RDP = 147.3). One assessment zone – M9:2 (RDP = 61.3) is in the R2 rockburst damage zone. Other zones are within the R1 zone (no damage/minor loose), however two zones: M4 (RDP = 45.8) and L5 (RDP = 45.4) are very close to the R2 zone and only minor intensification of PPV may result in damage. The average RDP on level is 15.9.

Five assessment zones on mining level 1275 are within the R2 rockburst damage zone (minor damage/less than 1t of rock displaced): M3 (RDP = 77.3), N7 (RDP = 75.2), K3 (RDP = 64.8), M2 (RDP = 59.5) and L3 (RDP = 53.6. Other zones are within the R1 zone (no damage/minor loose), yet zone N10 (RDP = 47.5) is very close to the R2 zone and only slight increase in PPV may result in higher hazard and damage. The average RDP on this level is 16.5.

Detailed results of EVP, PPV and RDP calculation, as well as EVP vs PPV diagrams for all assessment zones can be consulted in Appendix D.

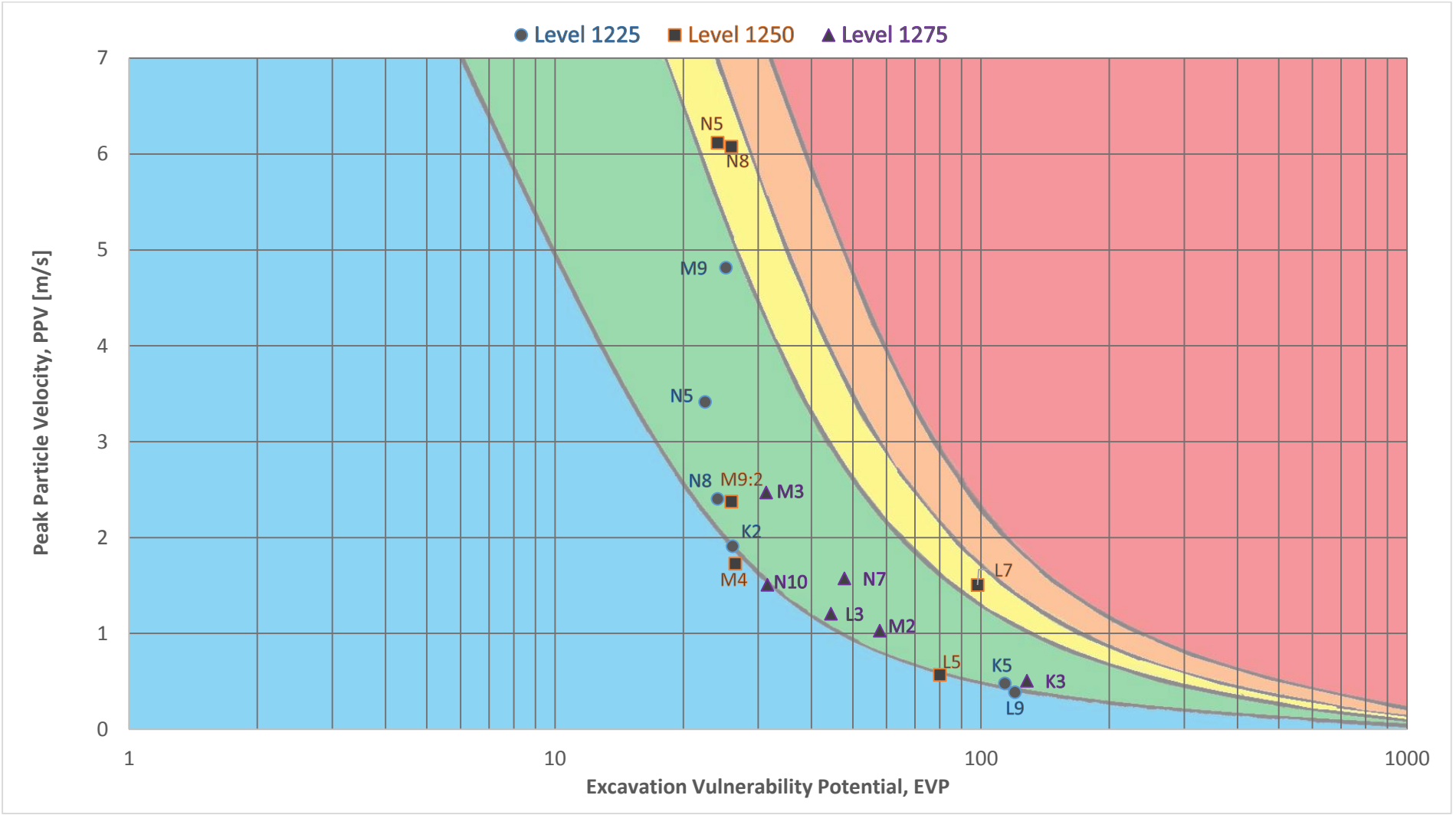

Figure 5-20. EVP vs. PPV diagram illustrating assessment zones with the largest rockburst damage potential (Mikula, et al., 2008).

5.4 Seismic risk evaluation and representation

Final seismic risk is calculated using the Quantitative Seismic Hazard and Risk Assessment Framework (QSHRAF) approach as a product of seismic hazard express in RDP parameter and exposure to hazard of mine personnel that has been assigned using the scale presented Table 3-10.

Table 3-10 illustrates as well the risk matrix with different Seismic Risk Ratings (SRR) that are assigned to each assessment zone. Below, Figure 5-21 illustrates the number of assessment zones with assigned SRR on each mining level. The SRR varies from 'Very Low' (VL) to 'Extreme' (E). As can be seen, the majority of assessment zones have very low seismic risk. On mining level 1225: 60 zones (87.0% of total) have very low SRR, 8 zones (11.6% of total) have low SRR and 1 zone (M9, 1.4% of total) has moderate SRR. On mining level 1250: 70 zones (76.0% of total) have very low SRR, 18 zones (18.7% of total) have low SRR and 3 zones (N8, L7, N5; 3.3% of total) have moderate SRR. On mining level 1275: 54 zones (84.4% of total) have very low SRR, 9 zones (14.1% of total) have low SRR and 1 zone (M3; 1.6% of total) has moderate SRR. Detailed results showing SRR for all assessment zones can be consulted in Appendix D.

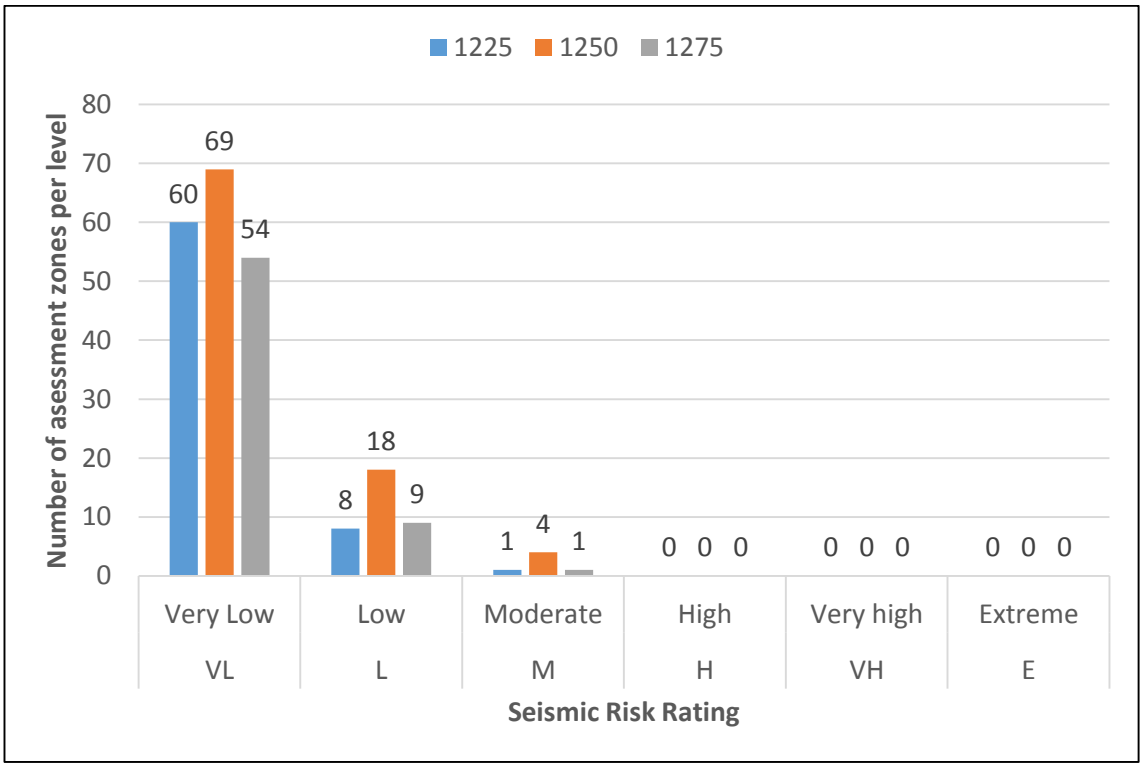

Figure 5-21. The number of assessment zones on each mining level assigned with Seismic Risk Ratings.

5.5 Seismic hazard and risk mitigation

The degree of damage due to seismic events (seismic hazard) can be lowered using following strategies:

- Install additional support to decrease Excavation Vulnerability Potential (EVP), hence reducing Rockburst Damage Potential (RDP) and risk
- Reduce span of excavation in newly designed areas

Risk mitigation can only be commenced when the acceptable level of risk is known. It has to be specified by mine management beforehand, as a realistic target that will be used to evaluate different mitigation scenarios. Here, mitigation measures are only considered as initial recommendations, because the tolerable level of risk is not known. Furthermore, measures are presented merely in existing mine openings, therefore only the first strategy is evaluated.

Risk can be lowered through an increase of support capacity, therefore reducing the damage potential. On mining level 1225 all assessment zones have maximum RDP within the damage zone R2 (damage expected to be contained by support), therefore only installation of surface support which is sufficiently to transfer load to individual reinforcing elements is required. Following upgrades of the support system are recommended for zones:

- M9 – installation of rock bolts, cable bolts and additional meshing, (reduction of RDP from 121.3 to 60.6 and risk from moderate to low), further reduction is possible only through installation of dynamic support system, such as cone bolts with dynamic surface support.
- N5 - installation of rock bolts, cable bolts and additional meshing, (reduction of RDP from 76.9 to 51.2 and risk from low to very low).
- N8, K5 and L9 – installation of rock bolts and mesh.
- K2 – additional mesh (reduction of RDP from 49.8 to 41.5 and risk from low to very low).

On mining level 1250, RDP can be lowered in zones:

- N8 and N5 - installation of rock bolts, cable bolts and additional meshing (reduction of risk from moderate to very low).

- L7 - installation of dynamic support system, such as cone bolts with dynamic surface support (reduction of RDP from 147.8 to 29.6 and risk from moderate to low).
- M4 and L5 – installation of additional mesh.

On mining level 1275, RDP can be lowered in zones:

- M3 - installation of cable bolts and additional meshing (reduction of RDP from 77.3 to 38.8 and risk from moderate to low).
- N7 - installation of rock bolts and mesh (reduction of RDP from 75.2 to 50.2 and risk from low to very low).
- M2 - installation of additional mesh.

Results of RDP reduction can be seen on EVP vs PPV diagrams in Appendix E.

6 Discussion

This chapter is divided into two parts. First, it discusses the results and main aspects of seismic risk assessment in the Pyhäsalmi mine and compares two assessment methods. Second, it articulates strengths and weaknesses of the Geotechnical Risk Assessment guideline as a result of experience gained in the process of risk assessment.

6.1 Seismic hazard and risk assessment

The process of seismic risk assessment has several limitations. First of all, data clustering is very cumbersome and time-consuming procedure; automation through software would be beneficial. Secondly, applied procedure has to be updated constantly in order to include new events, so that risks can be monitored with advancing mining rate. Thirdly, successful assessment depends highly on correctness of local magnitude scale and other seismic parameters, especially seismic event location. Next, from the results of Released Energy Capacity (REC, see chapter 5.3.1) it can be observed that the distance from the centroid of assessment zones to cluster groups does not have influence on REC result. For all assessment zones on all levels the maximum predicted energy is related to only one cluster group (S39 with the highest predicted local magnitude of 1.1). Even when the distance from the source to assessment zone is as large as 313m (from zone E17 to group S39) the highest REC is still related to this group. This is an indication that the distance scaling factor in REC formula (as in Equation (10) is inappropriate.

The results from two approaches used in the process of seismic hazard assessment, namely the Probabilistic Approach for Seismic Risk Assessment (PASRA) results and the Quantitative Seismic Hazard and Risk Assessment Framework (QSHRAF) are compared here. The highest seismic hazard using PASRA method is found in following assessment zones:

- on mining level 1225: L9,L7,L6,R7
- on mining level 1250: P10,N8, N5
- on mining level 1275: N7, R7:1, S7, R8.

Mining level 1225 has the highest average seismic hazard (average REC/AEC of 12.4).

On the other hand, the highest level of seismic hazard using QSHRAF method was found on level 1275 (average RDP of 16.5). Most hazardous assessment zones are:

- on mining level 1225: M9, N5, N8, K5

- on mining level 1250: N8, L7, N5, M9:2
- on mining level 1275: M3, N7, M2, L3

Although there are some assessment zones that have high seismic hazard for both methods (for example zones N8 and N5 on mining level 1250, and zone N7 on mining level 1275), it can be seen that the results of two methods are different. The dissimilarity can be explained by discrepancies in calculation of seismic hazard using those methods, for example:

- PASRA is based on seismic energy and QSHRAF on local magnitude.
- Ground support factors are different for both methods.
- There is no geological structure factor in PASRA.

It has to be stated that QSHRAF method is more trustworthy, since it is implemented in the Mine Seismicity Risk Assessment Program (MS-RAP) software that is currently used in many mines all over the world.

6.2 Geotechnical risk assessment guideline

The geotechnical risk assessment guideline supports in successful selection of an appropriate assessment approach. It gives a selection of tool to identify hazards and then to assess the risks related to those hazards. It provides examples of hazard and required steps to assess risk, however the list is not complete. During the application of guideline it was found out that it is not perfectly suited for assessment of seismic risk.

The Geotechnical Hazard Potential evaluation method aids in fast description of the general hazard level in the mine, however it has some limitations. First, is uses Barton's Q system that is not used in the mine on regular basis. It would be beneficial to implement other geotechnical parameters to evaluate hazard potential. Second, only few mining method are available in the guideline. More detailed selection of mining method could bring more benefit to be more specific.

The Geotechnical Risk Assessment (GRA) approach selection tool (see chapter 4.2) helps in fast and reliable selection of appropriate methodology of risk assessment. However some remarks have to be made regarding the number of point assigned to each GRA category. The final results (selected approach) highly depends on amount of points for each category where each category can score from 0 to 4 points. Particularly the category 'available resources', as the only category with a maximum score of 4 points, has a very

big influence on the final score and have to be carefully chosen in order not to introduce any bias. Furthermore, the deterministic approach is unlikely to score the highest amount of points to be selected as the most appropriate one, what is questionable.

Last issue discussed here relates to the amount of required geotechnical data available for analysis. In this study, seismic activity has been selected as the geotechnical hazard for the assessment, primarily because the amount of data and measurements results easily available for analysis. This emphasizes the importance of geotechnical monitoring carried out on regular basis in order to provide sufficient data density.

7 Conclusions

In conclusion, seismic risk in the Pyhäsalmi mine can be considered as low. In majority of assessment zones the level of seismic risk is found to be very low or low and only in six assessment zones is moderate. The biggest risk is found in mine openings located at the northern ore-waste contact zone, near mine infrastructure such as ore passes, fresh air rescue chamber and access drive. Those areas require special attention and installation of additional ground support in order to prevent damages in case a severe seismic event takes place. This result confirms the necessity for further development and implementation of seismic risk monitoring and risk assessment as an important element of safe mining operations.

The Geotechnical Risk Assessment guideline that was a basis for the risk assessment process in this study supports in successful selection of appropriate assessment approach and aids in selection of tools to assess geotechnical risks. Its applicability can be considered as high, however some elements could be improved to use its full potential. Focus should be put on reevaluation of the risk assessment approach selection tool, as well as to creation of a geotechnical hazards database with recommended assessment approaches with required geotechnical data and hazard descriptions. This could provide a basis for fast selection of required data, calculation methods and resources that are needed in the risk assessment process.

8 Recommendations for future work

This chapter gives recommendations for future work and is divided into two sections: seismic risk assessment and risk mitigation measures, and further development of the Geotechnical Risk Assessment guideline.

8.1 Seismic risk assessment and mitigation

In order to further develop the seismic risk assessment process in the Pyhäsalmi mine following steps are recommended:

- Develop a scale of personnel exposure that is well-suited for operating conditions in the mine. This can be done through detailed measurement of time spent by workers in each location and measurements of personal protection.
- Put emphasis on keeping a good record of all damages related to seismic events, so that they could be easier evaluated in the future. This could help to tune the damage scale to a particular seismic event size.
- Install additional ground support in areas where seismic risk is the highest in order to prevent damages.

8.2 Geotechnical risk assessment guideline improvement

In order to further upgrade the Geotechnical Risk Assessment guideline following recommendations are given:

- Include the description of seismic risk assessment approach as part of development of a systematic collection of assessment approaches with required geotechnical data and hazard descriptions. This could help to simplify the selection process of appropriate assessment approach that is well-suited for specific hazard conditions.
- Apply the guideline internally within a company by mine personnel to test how the guideline can be included as a systematic duty of mine personnel responsible for geotechnical risk assessment and how successfully it could help to perform the assessment. This will result in larger resources allocation.
- Use the guideline to investigate other geotechnical hazards and other risk assessment approaches. Particularly risk assessment for small scale area, as well as site specific risk assessment will bring more information on applicability of the guideline.

References

Bednarik, L. i Kovacs, L., 2012. Efficiency analysis of quality threshold clustering algorithms. *Production Systems and Information Enegineering,* 6(2013), pp. 15-26.

Bergström, P., 2012. *Ground Control Audit - Subsidence,* Pyhäsalmi Mine: Internal company presentation.

Bergström, P., 2013. *Ground Control Audit - Seismicity,* Pyhäsalmi Mine: Internal company presentation.

Bergström, P., 2014. *Rock mechanics at the Pyhäsalmi Mine,* Pyhäsalmi Mine: Internal company presentation.

Blake, W. & Hedley, D., 2001. *Rockburst case histories for north american hardrock mines,* Sudbury: Canadian Mining Research Organization.

de Jongh, R., 2013. *Installation report: Pyhäsalmi Mine Oy,* Pyhäsalmi: Not published.

Falmagne, V., 2001. *Quantification of rock mass degradation using microseismic monitoring and applications for mine design,* Ph.D. thesis: Queen's University, Ontario, Canada.

First Quantum Minerals, 2013. *Pyhasalmi Production Stats.* [Online] Available at: http://www.first-quantum.com/Our-Business/operating-mines/Pyhasalmi/Production-Stats/default.aspx [Accessed 3 March 2014].

Froehlich, T., 2014. *Guideline for geotechnical risk assessment: Geotechnical risk assessment in the Garpenberg mine, Sweden,* Helsinki: Unpublished.

Gibowicz, S. & Kijko, A., 1994. *An introduction to mine seismology.* 1st ed. San Diego: Academic Press.

Gleeson, D., 2010. Innovation at depth. *International Mining,* Volume April, pp. 12-18.

Hakala, M., Lamberg, M. & Kuula, H., 2013. *Life of Mine Rock Mechanical Simulation,* s.l.: Unpublished.

Halkidi, M., Batistakis, Y. & Vazirgiannis, M., 2001. On Clustering Validation Techniques. *Journal of Intelligent Information Systems,* 17(2-3), pp. 107-145.

Heyer, L., Kruglyak, S. & Yooseph, S., 1999. Exploring expression data: identification and analysis of coexpressed genes. *Genome Res,* 9(11), pp. 1106-15.

Hudyma, M., 2004. *Mining-Induced Seismicity in Underground, Mechanised, Hardrock Mines—Results of a World Wide Survey,* Nedlands: Australian Centre for Geomechanics.

Hudyma, M. & Potvin, Y., 2004. Seismic hazard in Western Australian mines. *The Journal of The South African Institute of Mining and Metallurgy,* 104(5), pp. 265-276.

Hudyma, M. & Potvin, Y. H., 2010. An Engineering Approach to Seismic Risk Management in Hardrock Mines. *Rock Mechanics and Rock Engineering,* 43(6), pp. 891-906.

Hudyma, M. R., 2008. *Analysis and Interpretation of Clusters of Seismic Events in Mines,* PhD thesis: The University of Western Australia.

Hudyma, M. R., 2014. *Personal correspondation.* s.l.:s.n.

Jain, A., Murty, M. & Flynn, P., 1999. Data Clustering: A Review. *ACM Computing Surveys,* 31(3), pp. 264-323.

Kaiser, P. K. & Cai, M., 2012. Design of rock support system under rockburst condition. *Journal of Rock Mechanics and Geotechnical Engineering,* 4(3), pp. 215-227.

Kaiser, P., Vasak, P. & Suorineni, F., 2005. *Hazard Assessment In Burst-prone Mines - Seismic Data Interpretation With 3D Virtual Reality Visualization.* London, International Society for Rock Mechanics.

Meyer, S., 2014. *Monthly Seismic Report: 01 Jan 2014, 00:00 - 01 Feb 2014, 00:00,* Pyhasalmi: Unpublished.

Mikula, P., Heal, D. & Hudyma, M., 2008. *Generic Seismic Risk Management Plan for Underground Hardrock Mines,* Nedlands: Australian Centre for Geomechanics.

Mishra, R. K., 2012. *Guidelines for getechnical risk assessment in underground mines,* MSc thesis: Aalto University.

Numminen, M., 2012. *Pyhasalmi mine geology - presenation.* s.l.:s.n.

Ortlepp, W. D., 1997. *Rock fracture and rockbursts: an illustrative study.* Johannesburg: South African Institute of Mining and Metallurgy.

Owen, M., 2004. *Exposure model – Detailed profiling and quantification of the exposure of personnel to geotechnical hazards in underground mines,* PhD Thesis: The University of Western Australia.

Oye, V. & Roth, M., 2005. *Source parameters of microearthquakes from the 1.5km deep Pyhasalmi ore mine, Finland.* Stanford, California, Stanford University.

Potvin, Y., 2009. Strategies and tactics to control seismic risk in mines. *The Journal of The Southern African Institute of Mining and Metallurgy,* 109(3), pp. 177-186.

Puustjärvi, H., 2006. *Pyhäsalmi Modeling Project,* Unpublished: Geological Survey of Finland.

Pyhäsalmi Mine Oy, 2013. *Life of mine,* Pyhajarvi: Internal company presentation.

Richter, C., 1935. An instrumental earthquake magnitude scale. *Bulletin of the Seismological Society of America,* 25(1), pp. 1-32.

Sambuelli, L., 2009. Theoretical derivation of a peak particle velocity-distance law for the predictian of virbrations from blasting. *Rock Mechanics and Rock Engineering*, 42(3), pp. 547-556.

Trzaska, W. et al., 2010. Laguna in Pyhäsalmi. *Acta Physica Polonica B*, 41(7), pp. 1779-1787.

Weisstein, E. W., 2012. *"Distance" From Mathworld-A Wolfram Web Resource.* [Online] Available at: http://mathworld.wolfram.com/Distance.html [Accessed 21 03 2014].

Wen, Z., 2013. *Probabilistic approach for seismic risk assessment.* Helsinki: s.n.

Young, R., Maxwel, S., Urbanic, T. & Feignier, B., 1992. Mining-induced microseismicity: Monitoring and applications of imaging and source mechanism techniques. *Pure and applied geophysics*, 139(3-4), pp. 697-719.

Appendices

A Ground support system standard

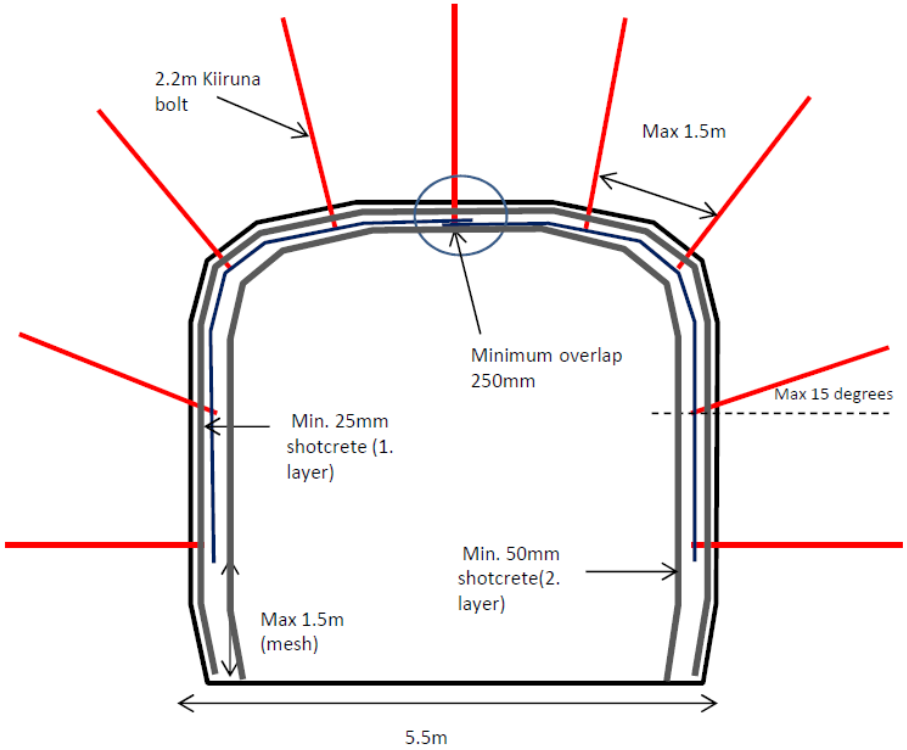

Figure A-1. Minimum standard for 5.5m wide meshed heading – for wider headings additional support to be installed (Bergström, 2014).

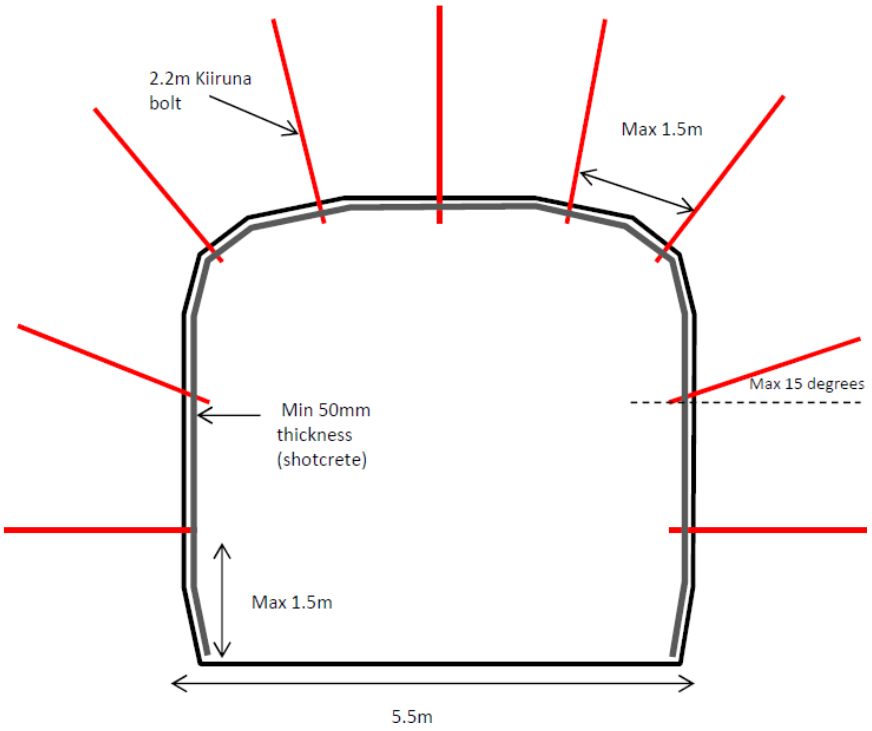

Figure A-2. Minimum standard for 5.5m wide heading without mesh – for wider headings additional support to be installed (Bergström, 2014).

B Seismic events clustering

Table B-1. Five most populous clusters created using the QTCLUST algorithm with parameters used for evaluation and comparison in the third stage of clustering procedure.

Cluster ID	QT 5	QT 21	QT 4	QT 14	QT 8
X [m]	8332.5	8270.6	8337.4	8366.6	8372.4
Y [m]	2366.3	2312.2	2373.0	2354.3	2314.8
Z [m]	-1232.2	-1124.1	-1260.8	-1337.1	-1265.5
Nr of events	3908	3664	3047	2098	1848
Nr of significant events	27	2	6	1	7
Number of large events	1	0	0	0	0
b-value	-1.1	-1.0	-1.3	-1.9	-1.1
a/b	1.2	1.4	0.7	0.1	1.1
Median S:P Energy	17.9	16.9	13.7	11.0	8.3
Histogram peak 1	2013-11-21	2014-02-17	2012-05-04	2013-11-02	2012-12-27
Histogram peak 2	2012-05-04	2014-02-16	2013-10-31	2013-11-07	2013-11-10
Histogram peak 3	2013-11-22	2014-02-20	2013-04-12	2012-12-28	2014-02-15
Histogram peak 4	2013-12-02	2013-10-31	2012-12-20	2013-01-31	2011-01-09
Histogram peak 5	2013-11-28	2013-11-02	2013-09-08	2013-10-26	2013-01-29
ASTH peak 1	314.1	29.1	228.8	88.4	85.7
ASTH peak 2	228.3	26.1	106.2	46.9	82.0
ASTH peak 3	202.2	20.8	80.5	29.2	80.0
ASTH peak 4	112.7	20.6	77.4	14.3	76.1
ASTH peak 5	95.4	20.2	75.3	14.0	45.4
ASTH peak date 1	2012-05-25	2012-11-16	2013-03-26	2011-11-03	2011-01-16
ASTH peak date 2	2012-08-13	2012-12-05	2011-01-01	2012-12-06	2011-01-09
ASTH peak date 3	2011-03-24	2012-12-05	2012-10-29	2011-01-17	2011-02-08
ASTH peak date 4	2011-02-15	2012-12-05	2011-03-14	2011-12-10	2011-02-08
ASTH peak date 5	2011-07-20	2012-11-21	2011-06-22	2012-05-07	2011-01-09
Max magnitude 1	1.0	0.4	0.6	0.0	0.4
Max magnitude 2	0.5	0.2	0.1	-0.1	0.2
Max magnitude 3	0.5	-0.1	0.1	-0.4	0.2
Max magnitude 4	0.5	-0.1	0.1	-0.5	0.1
Max magnitude 5	0.5	-0.2	0.0	-0.5	0.1
Max magnitude date 1	2011-01-28	2012-11-19	2012-05-13	2012-10-11	2013-09-23
Max magnitude date 2	2012-05-04	2014-01-21	2012-03-04	2011-01-30	2013-09-12
Max magnitude date 3	2012-12-19	2013-08-23	2012-03-15	2013-07-16	2014-02-15
Max magnitude date 4	2013-03-16	2014-02-20	2013-09-07	2012-06-15	2011-04-02
Max magnitude date 5	2013-09-12	2012-11-16	2013-02-05	2012-10-13	2011-11-14
∑ E [J]	2.17E+06	4.60E+05	4.99E+05	6.46E+04	2.82E+05
∑ App stress [bar]	5933.2	1203.2	4509.9	883.8	1651.8

Table B-2. Cluster groups created in the third stage of clustering using SLINK clustering algorithm.

Cluster group	X [m]	Y [m]	Z [m]	Max. predicted M_L	Nr of events	∑ Energy [J]	∑ App stress [bar]
S01	8375.4	2353.2	-1124.6	0.6	1927	3.44E+05	8.47E+02
S02	8268.7	2320.7	-1129.4	1.0	6564	1.16E+06	2.90E+03
S03	8366.2	2355.5	-1361.4	0.1	5581	2.30E+05	2.40E+03
S04	8164.9	2159.8	-1175.3	0.3	1052	1.06E+06	6.81E+03
S05	8445.7	2306.2	-1204.6	0.3	1249	2.30E+05	1.97E+03
S06	8319.0	2311.7	-1072.6	0.5	2171	4.17E+05	9.60E+02
S07	8442.2	2330.8	-1084.7	0.8	3818	3.40E+05	1.69E+03
S08	8298.0	2290.2	-1357.2	0.9	1786	7.84E+05	2.60E+03
S09	8307.9	2318.2	-1150.6	0.2	1409	3.87E+05	3.54E+02
S10	8217.5	2304.8	-1315.8	0.6	2489	9.52E+04	5.22E+02
S11	8242.6	2350.6	-1135.5	0.8	333	2.86E+05	4.14E+02
S12	8379.3	2309.1	-1276.8	0.2	5579	1.89E+06	6.37E+03
S13	8426.5	2370.3	-1096.7	0.7	280	1.32E+05	2.93E+02
S14	8465.1	2296.4	-1069.2	0.5	843	5.24E+05	6.55E+01
S15	8367.4	2294.5	-1347.0	0.7	1397	1.00E+06	2.77E+03
S16	8452.7	2253.6	-1252.0	-0.2	58	4.69E+05	3.66E+02
S17	8218.5	2183.9	-1168.7	-0.2	184	4.77E+04	6.45E+02
S18	8311.0	2365.4	-1168.3	0.7	120	1.05E+05	6.05E+01
S19	8329.2	2333.7	-1325.4	0.3	2024	1.46E+05	1.17E+03
S20	8337.8	2373.8	-1257.6	0.9	11097	3.60E+06	1.65E+04
S21	8409.1	2333.8	-1169.7	0.4	1142	1.88E+05	9.14E+02
S22	8241.4	2271.5	-1231.5	-0.3	70	4.52E+04	3.57E+02
S23	8249.6	2326.1	-1207.2	0.5	2856	7.73E+05	2.64E+03
S24	8219.7	2314.9	-1246.2	0.5	3052	5.66E+05	2.81E+03
S25	8468.7	2286.6	-1155.2	-0.1	438	1.07E+05	4.83E+02
S26	8322.2	2218.9	-1021.4	0.0	713	2.72E+05	2.28E+03
S27	8252.4	2326.4	-1302.0	-0.1	874	4.79E+04	3.32E+02
S28	8223.5	2105.5	-1199.5	0.0	736	1.06E+06	5.46E+03
S29	8284.2	2149.1	-1115.5	0.1	1095	3.02E+05	2.86E+03
S30	8212.4	2297.5	-1363.8	0.2	545	3.29E+05	9.27E+02
S31	8262.9	2293.1	-1074.9	0.7	1504	1.09E+06	1.88E+03
S32	8467.9	2186.0	-1165.1	0.0	48	4.07E+05	1.46E+02
S33	8281.8	2103.1	-1252.9	0.1	294	1.63E+06	3.11E+03
S34	8265.2	2258.9	-1417.0	-0.1	60	6.27E+04	1.85E+02
S35	8320.8	2220.1	-938.3	-0.1	277	2.55E+05	2.07E+03
S36	8311.9	2098.0	-1136.7	0.2	465	6.06E+05	3.52E+03
S37	8389.3	2334.5	-1069.9	0.3	1034	1.31E+05	4.78E+02
S38	8450.7	2363.2	-1064.0	0.0	78	2.62E+04	9.56E+01
S39	8352.9	2351.9	-1203.8	1.1	4464	1.16E+06	3.35E+03
S40	8209.6	2269.9	-1403.2	-0.1	381	4.59E+04	4.77E+02
S41	8177.5	2295.6	-1294.7	0.1	871	2.63E+05	1.14E+03

Cluster group	X [m]	Y [m]	Z [m]	Max. predicted M_L	Nr of events	∑ Energy [J]	∑ App stress [bar]
S42	8244.4	2207.7	-1114.1	0.5	2067	8.02E+05	4.22E+03
S43	8211.4	2149.6	-1131.8	-0.1	534	2.93E+05	2.77E+03
S44	8323.1	2271.9	-993.4	0.3	862	3.64E+05	1.82E+03
S45	8452.6	2337.5	-1151.0	0.3	2004	1.06E+05	1.71E+03
S46	8243.1	2049.2	-1233.5	0.1	255	2.07E+05	1.37E+03
S47	8398.8	2295.5	-1164.5	0.0	209	1.65E+04	9.87E+01
S48	8379.2	2393.6	-1292.9	0.4	316	3.30E+05	2.80E+02
S49	8252.8	2122.2	-1118.1	0.1	232	3.02E+05	1.25E+03
S50	8170.6	2228.0	-1174.6	0.1	1409	4.84E+05	5.73E+03
S51	8201.7	2260.3	-1104.9	0.0	1279	1.12E+05	3.02E+03
S52	8208.3	2313.1	-1159.7	0.1	942	3.03E+05	2.23E+03
S53	8217.0	2306.9	-1081.2	-0.1	105	2.42E+04	1.60E+02
S54	8364.1	2327.3	-1030.8	0.1	526	1.29E+05	8.43E+02
S55	8417.6	2248.9	-1334.1	0.2	181	1.37E+05	7.77E+02
S56	8357.7	2329.2	-989.2	0.0	137	4.25E+04	2.46E+02
S57	8223.1	2040.2	-1201.8	0.2	133	1.92E+05	1.17E+03
S58	8495.1	2317.3	-1091.3	0.0	229	1.92E+04	1.18E+02
S59	8261.9	2034.6	-1279.6	0.0	113	1.60E+05	8.06E+02
S60	8269.2	2087.7	-1101.2	0.1	153	5.55E+05	1.13E+03
S61	8488.3	2235.1	-1233.2	0.1	63	2.05E+05	3.49E+02
S62	8348.6	2097.7	-1218.0	0.3	234	5.02E+06	1.22E+04
S63	8461.2	2179.9	-1098.0	0.3	142	7.27E+05	4.48E+02
S64	8303.6	2052.4	-1219.3	0.2	133	6.65E+05	1.47E+03
S65	8210.3	2363.3	-1094.3	0.3	40	8.68E+04	1.15E+02
S66	8162.4	2279.9	-1328.0	0.3	237	5.60E+04	3.88E+02
S67	8479.9	2370.2	-1104.6	0.1	279	5.16E+04	2.93E+02
S68	8478.8	2173.4	-1222.9	0.2	61	5.45E+05	4.56E+02
S69	8478.3	2284.7	-1324.8	0.1	175	1.05E+05	9.62E+02
S70	8370.8	2092.1	-1154.1	0.1	67	1.97E+05	9.00E+02
S71	8365.0	2208.6	-1028.4	-0.2	102	5.25E+04	4.57E+02
S72	8253.7	2305.4	-1332.6	0.9	1016	2.83E+05	2.41E+02
S73	8365.4	2365.5	-1305.8	0.4	767	8.07E+04	5.49E+02
S74	8321.2	2432.8	-1213.4	0.2	327	2.73E+04	1.60E+02
S75	8230.3	2303.3	-1125.6	0.0	245	2.11E+04	3.13E+02
S76	8328.3	2303.4	-1280.8	0.0	182	1.18E+04	4.81E+01
S77	8394.1	2359.9	-1082.0	0.3	175	1.78E+04	2.15E+02
S78	8301.1	2229.6	-1076.5	0.0	147	9.81E+03	2.06E+02
S79	8415.3	2352.1	-1041.1	0.3	139	1.87E+04	8.56E+01
S80	8220.9	2262.6	-1135.6	-0.6	111	1.66E+04	3.33E+02
S81	8264.6	2150.6	-1087.5	-0.1	110	6.91E+04	4.23E+02
S82	8246.2	2087.5	-1176.5	0.1	66	1.82E+05	7.63E+02

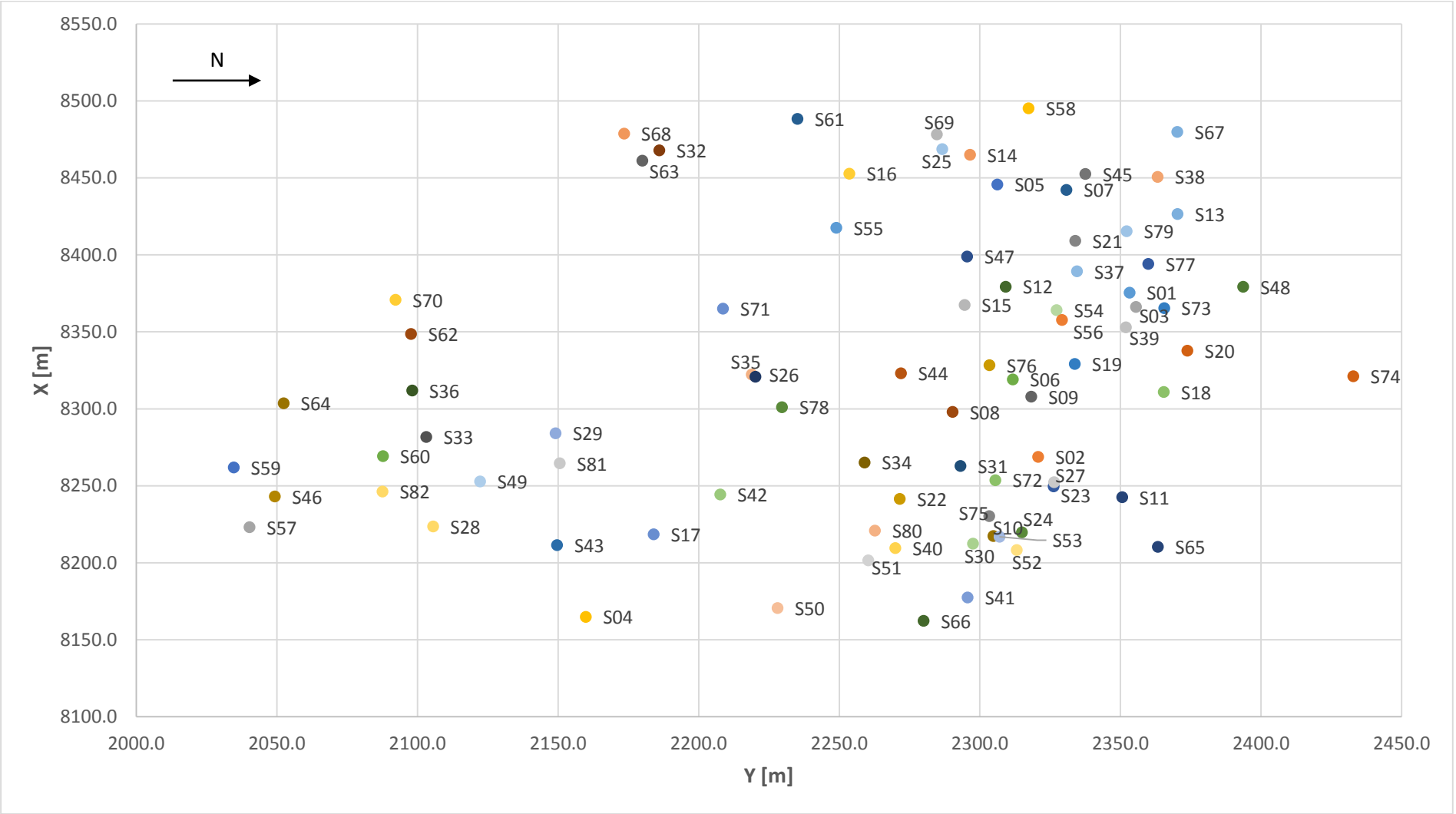

Figure B-1. Cluster groups created in the third stage of clustering using SLINK clustering algorithm, plan view.

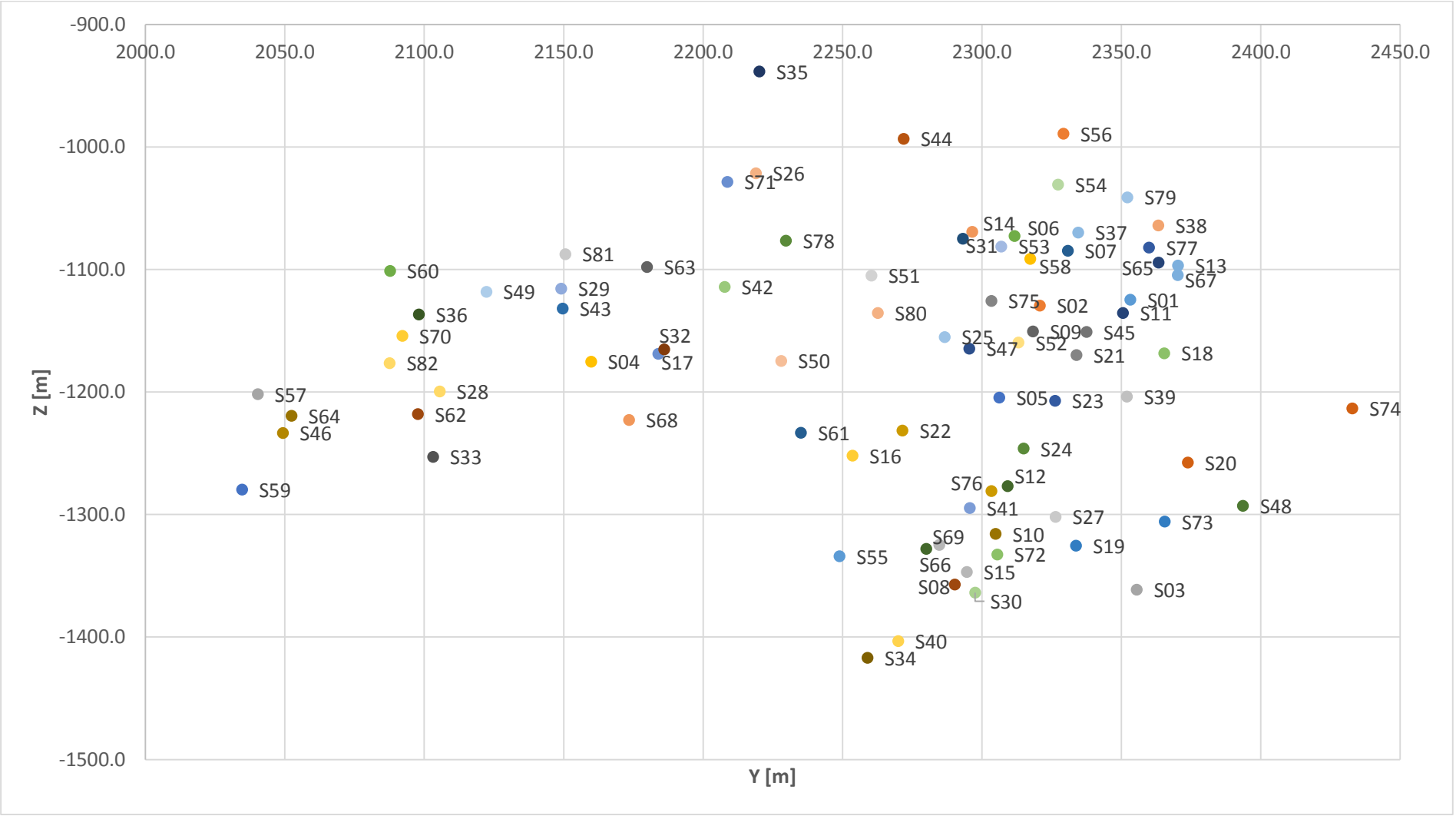

Figure B-2. Cluster groups created in the third stage of clustering using SLINK clustering algorithm, view looking east.

C Seismic Risk Assessment – PASRA

a. Level 1225

Table C-1. Results of the seismic risk assessment using PASRA for mining level 1225.

GRID	MAX σ [Mpa]	UCS [Mpa]	MAX REC	MAX M_L	Closest group with max REC	AEC	REC/AEC
C12	40	180	0.09	1.1	S39	2	4.3
D11	35	180	0.31	1.1	S39	5	6.2
D13	40	180	0.11	1.1	S39	2	5.7
D14	40	180	0.09	1.1	S39	2	4.3
D15	50	180	0.23	1.1	S39	5	4.5
E14	40	75	0.34	1.1	S39	5	6.8
E15	40	180	0.31	1.1	S39	5	6.2
E16	50	180	0.28	1.1	S39	2	14.1
E17	60	180	0.32	1.1	S39	2	16.2
F15	30	110	0.23	1.1	S39	2	11.3
F16	50	180	0.31	1.1	S39	4	7.7
F17	50	180	0.23	1.1	S39	2	11.3
G16:2	35	110	0.25	1.1	S39	2	12.7
G16:25	35	110	0.28	1.1	S39	5	5.6
G17	45	180	0.32	1.1	S39	2	16.2
H17	55	180	0.14	1.1	S39	2	7.1
H18	40	180	0.25	1.1	S39	2	12.7
I15	10	75	0.34	1.1	S39	5	6.7
I18	40	75	0.34	1.1	S39	2	16.8
J1	50	180	0.23	1.1	S39	1	22.6
J14	15	110	0.34	1.1	S39	5	6.7
J15	15	110	0.28	1.1	S39	2	14.1
J17	25	180	0.21	1.1	S39	2	10.4
J18	40	180	0.09	1.1	S39	2	4.3
J3	25	75	0.28	1.1	S39	6	4.7
K12	10	75	0.28	1.1	S39	2	14.1
K13	15	180	0.34	1.1	S39	5	6.7
K14	15	180	0.34	1.1	S39	5	6.7
K15	20	180	0.34	1.1	S39	4	8.4
K16	15	180	0.31	1.1	S39	2	15.4
K2	40	180	0.14	1.1	S39	2	7.1
K3	40	180	0.28	1.1	S39	5	5.6
K4	35	110	0.23	1.1	S39	6	3.8
K5	30	110	0.28	1.1	S39	1	28.1
L12	15	75	0.41	1.1	S39	2	20.4
L13:25	10	75	0.34	1.1	S39	5	6.7
L13:4	10	75	0.34	1.1	S39	4	8.4
L3	45	180	0.23	1.1	S39	2	11.3
L4	40	180	0.28	1.1	S39	4	7.0
L4	40	180	0.31	1.1	S39	6	5.1

GRID	MAX σ [Mpa]	UCS [Mpa]	MAX REC	MAX M_L	Closest group with max REC	AEC	REC/AEC
L6	35	110	0.23	1.1	S39	1	22.6
L7	25	75	0.20	1.1	S39	1	19.8
L9	30	75	0.23	1.1	S39	1	22.6
M10	40	180	0.28	1.1	S39	5	5.6
M11	40	180	0.31	1.1	S39	5	6.2
M12	40	180	0.23	1.1	S39	4	5.6
M3	55	180	0.23	1.1	S39	2	11.3
M5:4	50	180	0.14	1.1	S39	4	3.5
M5:45	50	180	0.28	1.1	S39	6	4.7
M6	50	180	0.25	1.1	S39	6	4.2
M7	50	180	0.14	1.1	S39	2	7.1
M8	50	180	0.14	1.1	S39	4	3.5
M9	40	180	0.28	1.1	S39	2	13.9
N10	50	180	0.23	1.1	S39	5	4.5
N5	45	180	0.28	1.1	S39	1	27.8
N6	50	180	0.14	1.1	S39	2	7.1
N8	50	180	0.54	1.1	S39	1	54.1
O6	55	180	0.31	1.1	S39	2	15.4
P6	55	180	0.14	1.1	S39	2	7.1
Q6	55	180	0.54	1.1	S39	2	27.1
R6	55	180	0.34	1.1	S39	2	17.1
R7	55	180	0.28	1.1	S39	1	28.1
S4	60	180	0.28	1.1	S39	2	14.1
S5	60	180	0.28	1.1	S39	2	14.1
S7	60	180	0.23	1.1	S39	1	22.6
T3	60	180	0.32	1.1	S39	3	10.8
T4	60	180	0.23	1.1	S39	3	7.5
T5:2	60	180	0.32	1.1	S39	2	16.2
T5:3	60	180	0.23	1.1	S39	3	7.5

b. Level 1250

Table C-2. Results of the seismic risk assessment using PASRA for the mining level 1250.

GRID	MAX σ [Mpa]	UCS [Mpa]	MAX REC	MAX M_L	Closest group with max REC	AEC	REC/AEC
B10	40	180	0.23	1.1	S39	2	11.3
B11	40	180	0.23	1.1	S39	2	11.3
B7	30	180	0.17	1.1	S39	2	8.5
B8	35	180	0.20	1.1	S39	2	9.9
B9:2	35	180	0.20	1.1	S39	2	9.9
B9:3	35	180	0.20	1.1	S39	3	6.6
C10	30	180	0.17	1.1	S39	2	8.5
C11	35	180	0.20	1.1	S39	5	4.0
C12:2	40	180	0.23	1.1	S39	2	11.3
C12:4	40	180	0.23	1.1	S39	4	5.6
C13	45	180	0.25	1.1	S39	2	12.7
C14	50	180	0.28	1.1	S39	2	14.1
C3	10	110	0.10	1.1	S39	6	1.6
C4	5	105	0.05	1.1	S39	6	0.9
C5	5	110	0.05	1.1	S39	6	0.8
C6	5	110	0.05	1.1	S39	6	0.8
C7	10	110	0.10	1.1	S39	2	4.8
C8	10	75	0.14	1.1	S39	3	4.7
C9	20	75	0.27	1.1	S39	2	13.7
D11	20	110	0.19	1.1	S39	6	3.1
D12:4	10	75	0.14	1.1	S39	4	3.5
D12:4	20	180	0.11	1.1	S39	4	2.9
D13	35	180	0.20	1.1	S39	2	9.9
D14	40	180	0.23	1.1	S39	2	11.3
D15	45	180	0.25	1.1	S39	2	12.7
D2	10	75	0.14	1.1	S39	4	3.5
D8	5	110	0.05	1.1	S39	4	1.3
D8	5	110	0.05	1.1	S39	6	0.8
E1	10	75	0.14	1.1	S39	4	3.5
E14	25	180	0.14	1.1	S39	3	4.7
E15	35	180	0.20	1.1	S39	2	9.9
E17	45	180	0.25	1.1	S39	2	12.7
E2	10	75	0.14	1.1	S39	4	3.5
F1	10	75	0.14	1.1	S39	5	2.8
F13	10	75	0.14	1.1	S39	2	7.1
F16	40	180	0.23	1.1	S39	2	11.3
F17	50	180	0.28	1.1	S39	2	14.1
G1	15	180	0.09	1.1	S39	2	4.3
G17	45	180	0.25	1.1	S39	2	12.7
H1	30	180	0.17	1.1	S39	2	8.5
H17	50	180	0.28	1.1	S39	2	14.1

GRID	MAX σ [Mpa]	UCS [Mpa]	MAX REC	MAX M_L	Closest group with max REC	AEC	REC/AEC
H2	10	75	0.14	1.1	S39	5	2.8
I1	45	180	0.25	1.1	S39	2	12.7
I17	10	180	0.06	1.1	S39	5	1.2
I2	40	75	0.54	1.1	S39	5	10.8
I3	10	75	0.14	1.1	S39	2	7.1
J1:2	50	180	0.28	1.1	S39	2	14.1
J1:45	50	180	0.28	1.1	S39	6	4.7
J13	10	75	0.14	1.1	S39	6	2.4
J16	35	180	0.20	1.1	S39	5	4.0
J3:2	30	180	0.17	1.1	S39	2	8.5
J3:4	30	180	0.17	1.1	S39	4	4.2
K12	10	75	0.14	1.1	S39	6	2.4
K15	10	75	0.14	1.1	S39	5	2.8
K2	50	180	0.28	1.1	S39	5	5.6
K3:2	35	180	0.20	1.1	S39	2	9.9
K3:25	35	180	0.20	1.1	S39	5	4.0
K5	20	110	0.19	1.1	S39	2	9.4
L12	10	75	0.14	1.1	S39	5	2.8
L13	10	75	0.14	1.1	S39	2	7.1
L14	10	75	0.14	1.1	S39	2	7.1
L2	55	180	0.31	1.1	S39	2	15.4
L3	60	180	0.34	1.1	S39	5	6.7
L4	60	180	0.34	1.1	S39	4	8.4
L5	30	180	0.17	1.1	S39	2	8.5
L7	45	110	0.41	1.1	S39	2	20.7
L8	30	110	0.28	1.1	S39	4	7.0
L9	30	110	0.28	1.1	S39	3	9.3
M10	35	180	0.20	1.1	S39	2	9.9
M11	35	180	0.20	1.1	S39	5	4.0
M12	30	180	0.17	1.1	S39	6	2.8
M13	10	75	0.14	1.1	S39	2	7.1
M2	50	180	0.28	1.1	S39	2	14.1
M3	55	180	0.31	1.1	S39	2	15.4
M4	55	180	0.31	1.1	S39	2	15.4
M5:2	45	180	0.25	1.1	S39	2	12.7
M5:4	45	180	0.25	1.1	S39	4	6.3
M6	40	180	0.23	1.1	S39	2	11.3
M7	40	180	0.23	1.1	S39	4	5.6
M8	40	180	0.23	1.1	S39	2	11.3
M9:2	35	180	0.20	1.1	S39	2	9.9
M9:4	35	180	0.20	1.1	S39	4	4.9
N12	60	180	0.34	1.1	S39	5	6.7
N13	65	180	0.36	1.1	S39	2	18.2
N5	50	180	0.28	1.1	S39	1	28.1
N8	50	180	0.28	1.1	S39	1	28.1

GRID	MAX σ [Mpa]	UCS [Mpa]	MAX REC	MAX M_L	Closest group with max REC	AEC	REC/AEC
N9	50	180	0.28	1.1	S39	5	5.6
O12	65	180	0.36	1.1	S39	2	18.2
O13	70	180	0.39	1.1	S39	5	7.8
P10	60	180	0.34	1.1	S39	1	33.7
P11	65	180	0.36	1.1	S39	2	18.2

c. Level 1275

Table C-3. Results of seismic risk assessment using PASRA for mining level 1275.

GRID	MAX σ [Mpa]	UCS [Mpa]	MAX REC	MAX M_L	Closest group with max REC	AEC	REC/AEC
E0	25	75	0.34	1.1	S39	5	6.8
F0	35	180	0.20	1.1	S39	5	4.0
F1	15	75	0.21	1.1	S39	2	10.4
G0	25	180	0.14	1.1	S39	5	2.8
H0	25	180	0.14	1.1	S39	2	7.1
H1	25	110	0.23	1.1	S39	2	11.6
I0	35	180	0.20	1.1	S39	2	9.9
I1:2	25	180	0.14	1.1	S39	2	7.1
I1:25	25	180	0.14	1.1	S39	5	2.8
J1:2	30	180	0.17	1.1	S39	2	8.5
J1:45	30	180	0.17	1.1	S39	6	2.8
J2:25	25	180	0.14	1.1	S39	5	2.8
J2:2	25	180	0.14	1.1	S39	2	7.1
J13	10	75	0.14	1.1	S39	5	2.8
K2	50	180	0.28	1.1	S39	6	4.7
K3	80	110	0.73	1.1	S39	5	14.7
K4	25	110	0.23	1.1	S39	5	4.7
K5	25	110	0.23	1.1	S39	6	3.9
K10	25	110	0.23	1.1	S39	6	3.9
K12	10	75	0.14	1.1	S39	4	3.5
K13	10	75	0.14	1.1	S39	5	2.8
L2:2	65	180	0.36	1.1	S39	2	18.2
L2:45	65	180	0.36	1.1	S39	6	6.1
L3	70	180	0.39	1.1	S39	6	6.5
L4:45	60	180	0.34	1.1	S39	6	5.6
L4:25	60	180	0.34	1.1	S39	5	6.7
L5:45	50	180	0.28	1.1	S39	6	4.7
L5:2	50	180	0.28	1.1	S39	2	14.1
L6	35	180	0.20	1.1	S39	5	4.0
L9:4	35	180	0.20	1.1	S39	4	4.9
L9:45	35	180	0.20	1.1	S39	6	3.3
L10	30	180	0.17	1.1	S39	6	2.8
L11	25	180	0.14	1.1	S39	4	3.6
L13	10	180	0.06	1.1	S39	2	2.9
M2	60	180	0.34	1.1	S39	2	16.8
M3	60	180	0.34	1.1	S39	2	16.8
M4	60	180	0.34	1.1	S39	2	16.8
M5	60	180	0.34	1.1	S39	6	5.6
M6	60	180	0.34	1.1	S39	6	5.6
M7:45	60	180	0.34	1.1	S39	6	5.6

GRID	MAX σ [Mpa]	UCS [Mpa]	MAX REC	MAX M_L	Closest group with max REC	AEC	REC/AEC
M7:4	60	180	0.34	1.1	S39	4	8.4
M8	55	180	0.31	1.1	S39	5	6.2
M9:45	50	180	0.28	1.1	S39	6	4.7
M9:25	45	180	0.25	1.1	S39	5	5.1
M10	40	180	0.23	1.1	S39	6	3.8
M11	40	180	0.23	1.1	S39	6	3.8
M12	40	180	0.23	1.1	S39	6	3.8
N2	60	180	0.34	1.1	S39	2	16.8
N6	60	180	0.34	1.1	S39	2	16.8
N7	60	180	0.34	1.1	S39	1	33.7
N9	60	180	0.34	1.1	S39	5	6.7
N10	60	180	0.34	1.1	S39	5	6.7
N11	60	180	0.34	1.1	S39	6	5.6
O6	60	180	0.34	1.1	S39	2	16.8
O10	60	180	0.34	1.1	S39	4	8.4
P6	60	180	0.34	1.1	S39	2	16.8
Q6	60	180	0.34	1.1	S39	2	16.8
R6	60	180	0.34	1.1	S39	2	16.8
R7:2	60	180	0.34	1.1	S39	2	16.8
R7:1	60	180	0.34	1.1	S39	1	33.7
R8	60	180	0.34	1.1	S39	1	33.7
S6	60	180	0.34	1.1	S39	2	16.8
S7	60	180	0.34	1.1	S39	1	33.7
T6	60	180	0.34	1.1	S39	2	16.8

D Seismic Risk Assessment – QSHRAF

a. Level 1225

Table D-1. Results of seismic risk assessment using QSHRAF for mining level 1225.

GRID	MAX σ [Mpa]	UCS [Mpa]	MAX PPV	MAX M_L	Closest cluster group	E_1	E_2	E_3	E_4	EVP	RDP	Exposure	SEISMIC RISK RATING
C12	40	180	0.05	0.3	S62	22	5	6	1.5	17.8	0.9	1000	VL
D11	35	180	0.09	0.3	S62	19	6	6	0.5	38.9	3.3	1000	VL
D13	40	180	0.07	0.2	S68	22	5	6.3	1.5	18.7	1.2	1000	VL
D14	40	180	0.18	0.2	S68	22	5	9	1.5	26.7	4.7	1000	VL
D15	50	180	0.18	0.2	S68	28	6	6	1.5	18.5	3.3	1000	VL
E14	30	75	0.11	0.2	S68	40	6	7.2	1	48.0	5.1	1000	VL
E15	30	180	0.14	0.2	S68	17	6	9.6	1.5	17.8	2.5	1000	VL
E16	50	180	0.25	0.2	S68	28	5	6	1.5	22.2	5.5	1000	VL
E17	60	180	0.18	0.2	S68	33	5	6	1.5	26.7	4.9	3000	VL
F15	30	110	0.32	0.2	S68	27	5	6	0.5	65.5	21.0	1000	VL
F16	50	180	0.30	0.2	S68	28	10	11.8	1.5	21.9	6.5	1000	VL
F17	60	180	0.31	0.2	S68	33	5	6.5	1.5	28.9	9.0	1000	VL
G16:2	35	110	0.39	0.2	S68	32	5	6.6	1	42.0	16.2	1000	VL
G16:25	35	110	0.26	0.2	S68	32	6	6.6	0.5	70.0	18.0	1000	VL
G17	45	180	0.14	0.2	S68	25	5	6.6	1.5	22.0	3.2	1000	VL
H17	55	180	0.09	0.1	S61	31	5	6.2	1.5	25.3	2.3	1000	VL
H18	60	180	0.14	0.1	S61	33	5	6	1.5	26.7	3.8	1000	VL
I15	10	75	0.11	0.1	S61	13	6	6.2	0.5	27.6	3.1	1000	VL
I18	30	75	0.15	0.1	S61	40	5	6.5	1.5	34.7	5.1	1000	VL
J3	25	75	0.31	0.5	S24	33	10	11.2	0.5	74.7	23.0	1000	VL

GRID	MAX σ [Mpa]	UCS [Mpa]	MAX PPV	MAX M_L	Closest cluster group	E_1	E_2	E_3	E_4	EVP	RDP	Exposure	SEISMIC RISK RATING
J14	10	110	0.12	1.1	S39	9	6	7	1	10.6	1.3	1000	VL
J15	10	110	0.13	0.3	S05	9	5	6.2	1.5	7.5	1.0	1000	VL
J17	25	180	0.13	0.1	S61	14	5	6.2	1.5	11.5	1.5	1000	VL
J18	40	180	0.23	0.1	S61	22	5	8.6	1.5	25.5	5.8	1000	VL
J1	50	180	0.51	0.5	S24	28	4	5	1.5	23.1	11.8	100	VL
K2	40	180	1.91	0.5	S24	22	5	8.8	1.5	26.1	49.8	2000	L
K3	30	180	1.05	0.5	S24	17	6	10	1.5	18.5	19.5	2000	VL
K4	25	110	0.34	-0.3	S22	23	10	6.6	0.5	30.0	10.3	3000	VL
K5	25	110	0.48	0.5	S23	23	4	10	0.5	113.6	54.4	100	VL
K12	10	75	0.34	1.1	S39	13	5	6	0.5	32.0	10.8	1000	VL
K13	15	180	0.47	0.3	S05	8	6	6	1	8.3	3.9	1000	VL
K14	15	180	2.26	0.3	S05	8	6	5.6	1.5	5.2	11.7	1000	VL
K15	15	180	1.34	0.3	S05	8	10	9.6	1.5	5.3	7.1	1000	VL
K16	15	180	0.20	0.3	S05	8	5	6.3	1.5	7.0	1.4	1000	VL
L3	45	180	0.54	0.5	S23	25	5	6.8	1.5	22.7	12.3	3000	VL
L4:45	40	180	1.02	0.5	S23	22	10	9.4	1.5	13.9	14.2	3000	VL
L4:4	40	180	0.60	0.5	S23	22	10	5.4	1	12.0	7.2	1000	VL
L6	25	110	0.31	0.5	S24	23	4	5.2	1	29.5	9.1	1000	VL
L7	20	75	0.28	0.5	S24	27	4	9.9	0.5	132.0	36.7	100	VL
L9	20	75	0.39	0.9	S20	27	4	9	0.5	120.0	46.5	1000	L
L12	10	75	0.81	1.1	S39	13	5	5.2	1.5	9.2	7.5	1000	VL
L13:25	10	75	0.87	0.3	S05	13	6	5.5	1.5	8.1	7.1	1000	VL
L13:4	10	75	0.55	0.3	S05	13	10	9.2	1.5	8.2	4.5	1000	VL
M3	60	180	0.49	0.5	S23	33	5	6.6	1.5	29.3	14.5	3000	VL
M5:45	50	180	1.11	0.5	S23	28	10	8	1.5	14.8	16.4	2000	VL
M5:4	50	180	1.85	0.5	S23	28	10	5.2	1.5	9.6	17.8	2000	VL

GRID	MAX σ [Mpa]	UCS [Mpa]	MAX PPV	MAX M_L	Closest cluster group	E_1	E_2	E_3	E_4	EVP	RDP	Exposure	SEISMIC RISK RATING
M6	45	180	1.23	0.5	S23	25	10	10.5	1.5	17.5	21.4	4000	VL
M7	45	180	0.88	0.9	S20	25	5	5.5	1.5	18.3	16.2	4000	VL
M8	50	180	1.31	0.9	S20	28	10	10.6	1.5	19.6	25.7	4000	L
M9	40	180	4.82	0.9	S20	22	5	8.5	1.5	25.2	121.3	3000	M
M10	40	180	1.28	1.1	S39	22	6	10.5	1.5	25.9	33.2	3000	L
M11	40	180	1.31	1.1	S39	22	6	5.5	1.5	13.6	17.8	1000	VL
M12	40	180	1.57	1.1	S39	22	10	9.5	1.5	14.1	22.2	1000	VL
N5	45	180	3.42	0.5	S23	25	4	5.4	1.5	22.5	76.9	100	L
N6	50	180	1.01	0.5	S23	28	5	5.5	1.5	20.4	20.5	4000	VL
N8	50	180	2.40	0.9	S20	28	4	5.2	1.5	24.1	57.9	100	VL
N10	50	180	2.02	1.1	S39	28	6	6.1	1.5	18.8	38.1	3000	L
O6	60	180	1.34	1.1	S39	33	5	5.4	1.5	24.0	32.2	4000	L
P6	60	180	1.00	1.1	S39	33	5	6.2	1.5	27.6	27.4	4000	L
Q6	60	180	0.39	1.1	S39	33	5	6	1.5	26.7	10.5	4000	VL
R6	60	180	0.17	1.1	S39	33	5	9.5	1.5	42.2	7.3	4000	VL
R7	60	180	0.08	1.1	S39	33	4	10.6	1.5	58.9	4.6	4000	VL
S4	60	180	0.07	1.1	S39	33	5	6	1.5	26.7	1.9	1000	VL
S5	60	180	0.08	1.1	S39	33	5	11.4	1.5	50.7	4.0	1000	VL
S7	60	180	0.21	0.9	S20	33	4	9.3	1.5	51.7	10.9	4000	VL
T3	60	180	0.05	1.1	S39	33	5	10.6	1.5	47.1	2.4	100	VL
T4	60	180	0.06	1.1	S39	33	5	6	1.5	26.7	1.6	100	VL
T5:2	60	180	0.07	1.1	S39	33	5	6	1.5	26.7	1.9	1000	VL
T5:3	60	180	0.07	0.9	S20	33	5	12.5	1.5	55.6	4.2	1000	VL

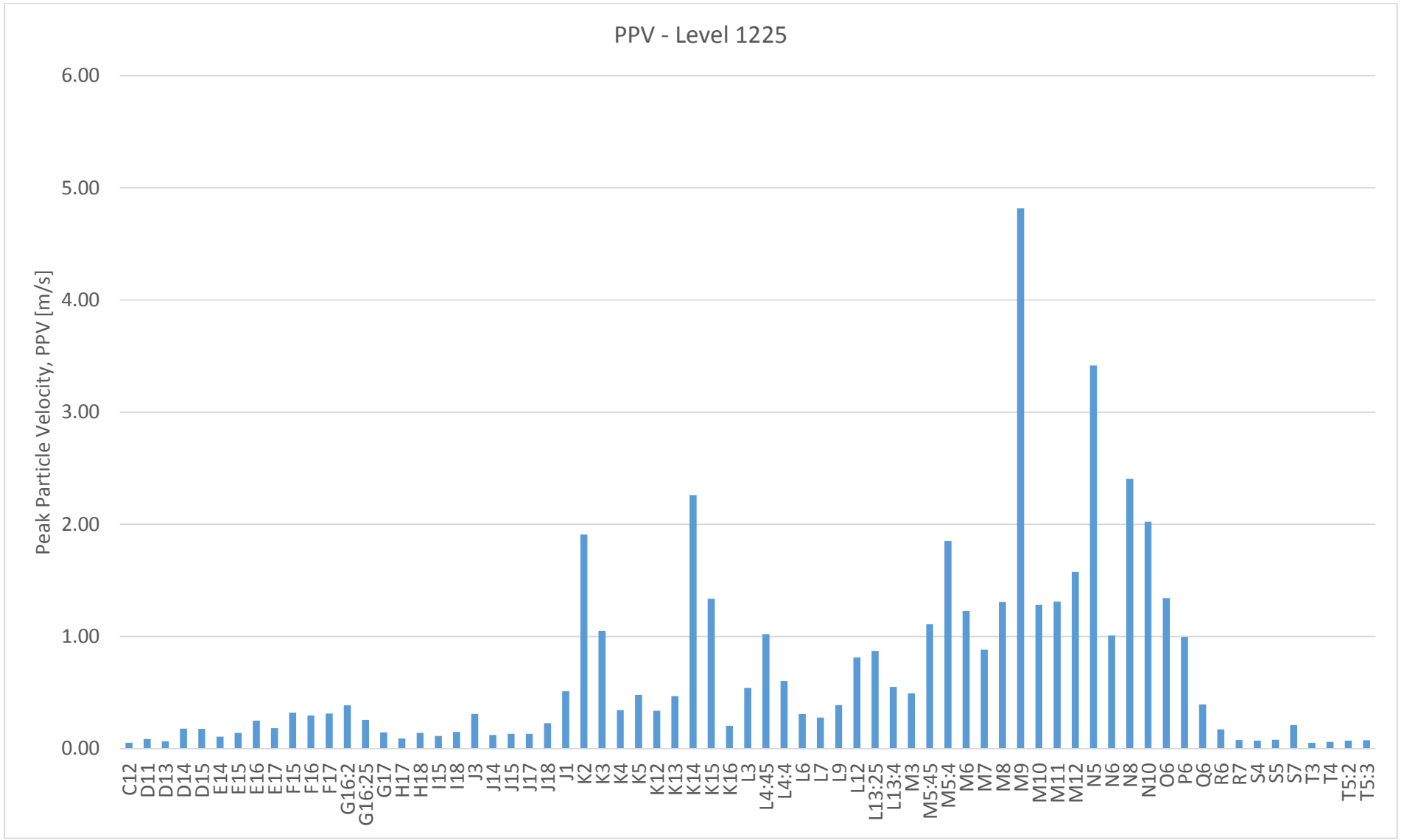
PPV - Level 1225
Peak Particle Velocity, PPV [m/s]
6.00
5.00
4.00
3.00
2.00
1.00
0.00
C12
D11
D13
D14
D15
E14
E15
E16
E17
F15
F16
F17
G16:2
G16:25
G17
H17
H18
I15
I18
J3
J14
J15
J17
J18
J1
K2
K3
K4
K5
K12
K13
K14
K15
K16
L3
L4:45
L4:4
L6
L7
L9
L12
L13:25
L13:4
M3
M5:45
M5:4
M6
M7
M8
M9
M10
M11
M12
N5
N6
N8
N10
O6
P6
Q6
R6
R7
S4
S5
S7
T3
T4
T5:2
T5:3

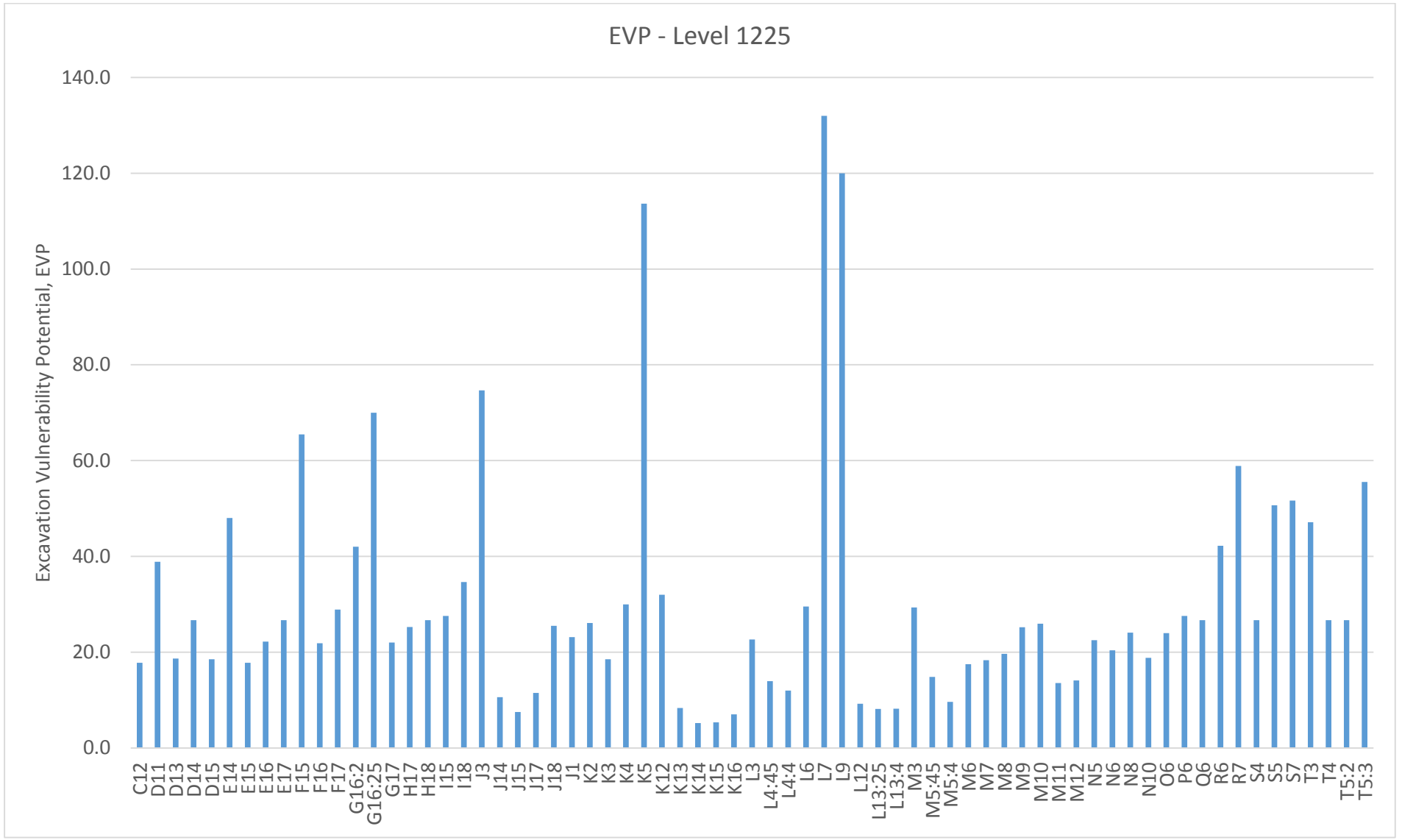
EVP - Level 1225
Excavation Vulnerability Potential, EVP
140.0
120.0
100.0
80.0
60.0
40.0
20.0
0.0
C12
D11
D13
D14
D15
E14
E15
E16
E17
F15
F16
F17
G16:2
G16:25
G17
H17
H18
I15
I18
J3
J14
J15
J17
J18
J1
K2
K3
K4
K5
K12
K13
K14
K15
K16
L3
L4:45
L4:4
L6
L7
L9
L12
L13:25
L13:4
M3
M5:45
M5:4
M6
M7
M8
M9
M10
M11
M12
N5
N6
N8
N10
O6
P6
Q6
R6
R7
S4
S5
S7
T3
T4
T5:2
T5:3

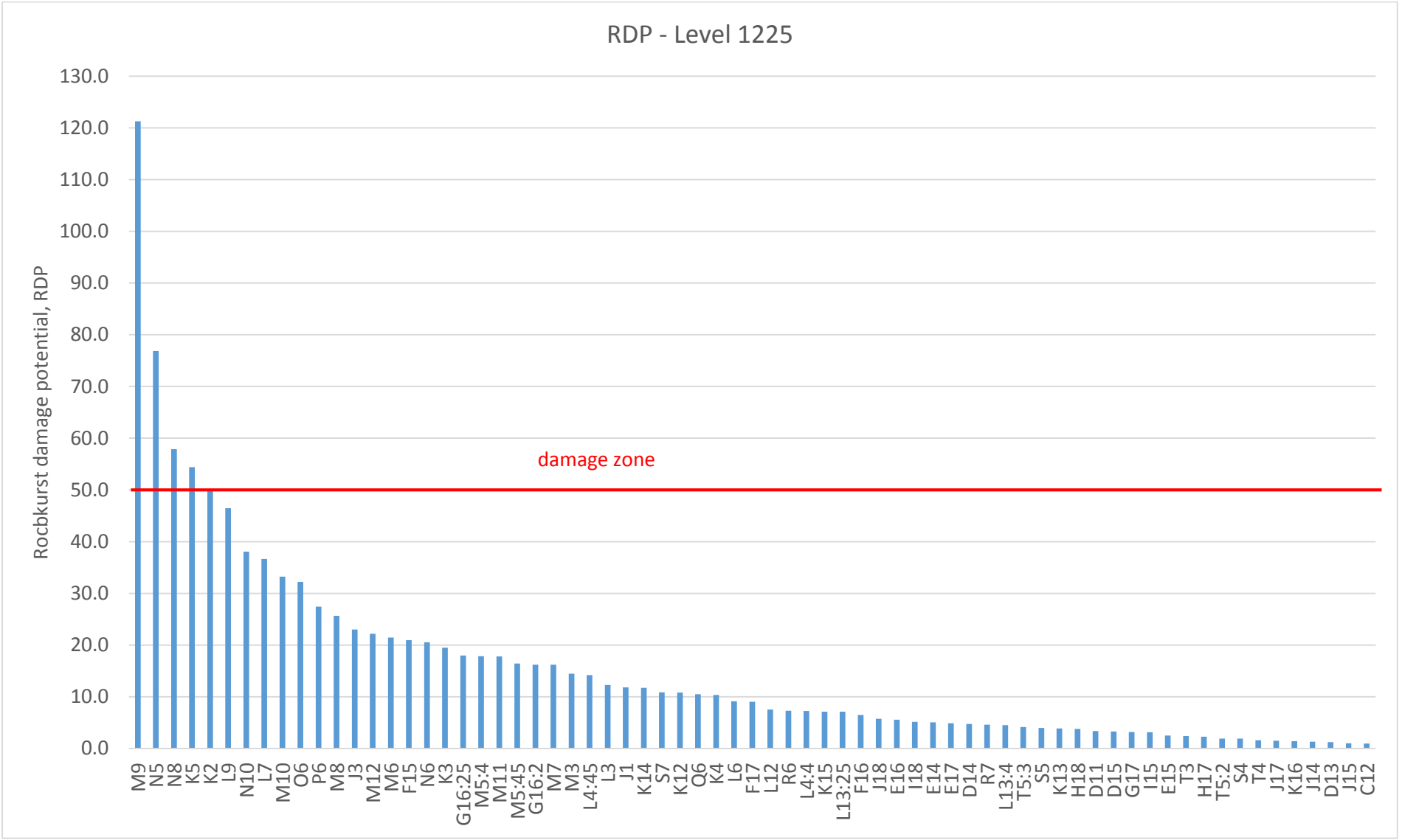
RDP - Level 1225
Rockburst damage potential, RDP
130.0
120.0
110.0
100.0
90.0
80.0
70.0
60.0
50.0
40.0
30.0
20.0
10.0
0.0
damage zone
M9 N5 N8 K5 K2 L9 N10 L7 M10 O6 P6 M8 J3 M12 M6 F15 N6 K3 G16:25 M5:4 M11 M5:45 G16:2 M7 M3 L4:45 L3 J1 K14 S7 K12 Q6 K4 L6 F17 L12 R6 L4:4 K15 L13:25 F16 J18 E16 I18 E14 E17 D14 R7 L13:4 T5:3 S5 K13 H18 D11 D15 G17 I15 E15 T3 H17 T5:2 S4 T4 J17 K16 J14 D13 J15 C12

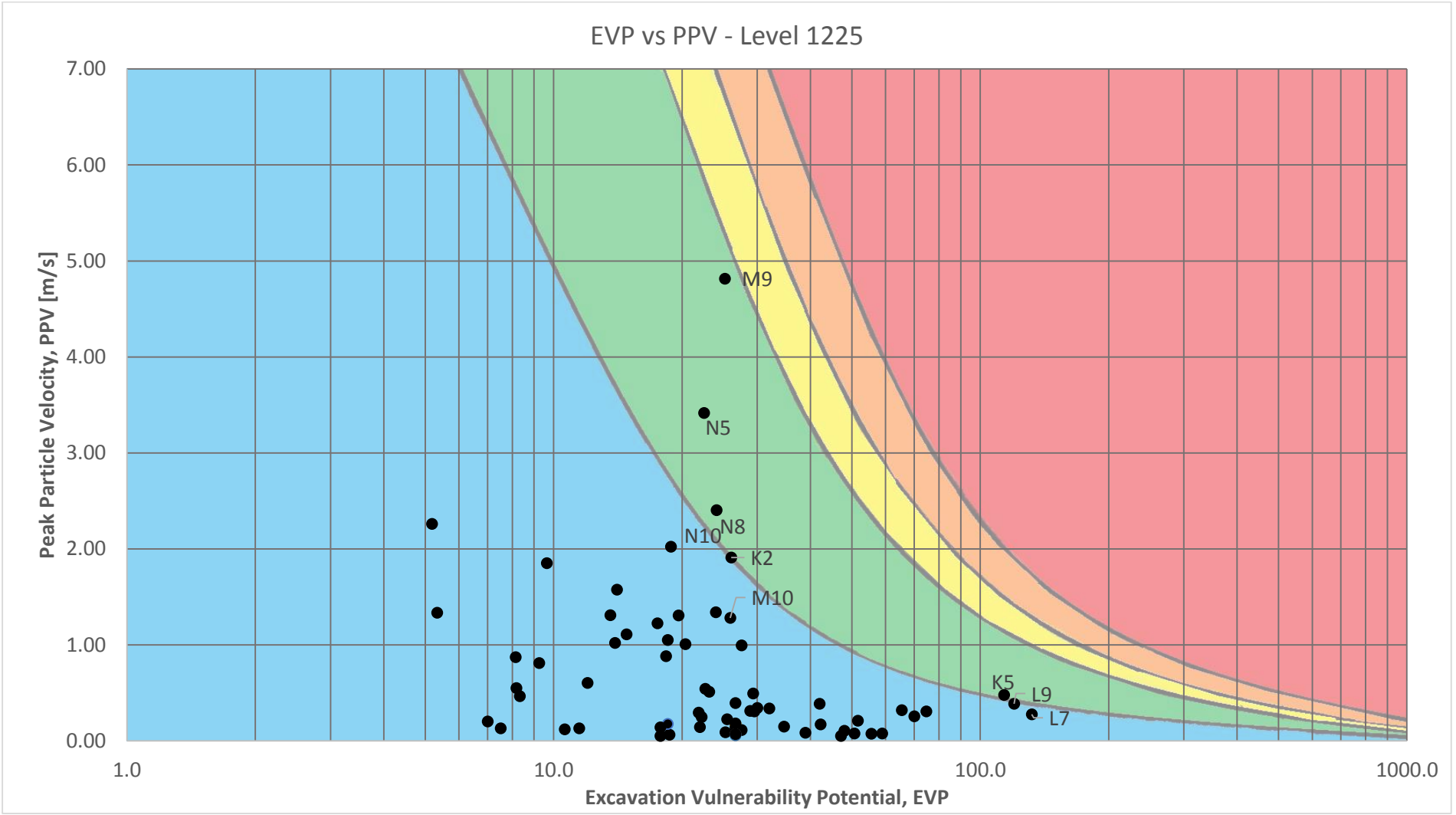
EVP vs PPV - Level 1225
Peak Particle Velocity, PPV [m/s]
7.00
6.00
5.00
4.00
3.00
2.00
1.00
0.00
1.0
10.0
100.0
1000.0
Excavation Vulnerability Potential, EVP
M9
N5
N8
N10
K2
M10
K5
L9
L7

b. Level 1250

Table D-2. Results of seismic risk assessment using QSHRAF for mining level 1250.

GRID	MAX σ [Mpa]	UCS [Mpa]	MAX PPV [m/s]	MAX M_L	Closest cluster group	E_1	E_2	E_3	E_4	EVP	RDP	Exposure	SEISMIC RISK RATING
B7	30	180	0.31	0.1	S33	17	5	6.5	1.5	14.4	4.4	1000	VL
B8	35	180	0.19	0.1	S33	19	5	6.5	1.5	16.9	3.1	1000	VL
B9:2	35	180	0.22	0.3	S62	19	5	9.2	1.5	23.9	5.3	2000	VL
B9:3	35	180	0.42	0.3	S62	19	5	6.5	1.5	16.9	7.1	2000	VL
B10	40	180	0.24	0.3	S62	22	5	10.3	1.5	30.5	7.3	1000	VL
B11	40	180	0.12	0.3	S62	22	5	6	1.5	17.8	2.1	1000	VL
C3	10	110	0.09	0.1	S33	9	10	9	1.5	5.5	0.5	100	VL
C4	5	105	0.18	0.1	S33	5	10	6.4	1.5	2.0	0.4	100	VL
C5	5	110	0.71	0.1	S33	5	10	7	0.5	6.4	4.5	100	VL
C6	5	110	0.20	0.1	S33	5	10	6.4	0.5	5.8	1.2	100	VL
C7	10	110	0.31	0.1	S33	9	5	6.5	1.5	7.9	2.5	1000	VL
C8	10	75	0.39	0.1	S33	13	5	9.6	0.5	51.2	19.9	1000	VL
C9	20	75	0.41	0.3	S62	27	5	6	0.5	64.0	26.4	1000	L
C10	30	180	0.28	0.3	S62	17	5	6	1.5	13.3	3.7	1000	VL
C11	35	180	0.10	0.3	S62	19	6	6	0.5	38.9	4.0	1000	VL
C12:4	40	180	0.05	0.3	S62	22	10	7	1.5	10.4	0.6	1000	VL
C12:2	40	180	0.05	0.3	S62	22	5	9.8	1.5	29.0	1.6	1000	VL
C13	45	180	0.05	0.2	S68	25	5	6.6	1.5	22.0	1.1	1000	VL
C14	50	180	0.08	0.2	S68	28	5	5.2	1.5	19.3	1.6	1000	VL
D2	10	75	0.07	0	S28	13	10	6.6	0.5	17.6	1.2	100	VL
D8	5	110	0.14	0.1	S33	5	10	6.6	0.5	6.0	0.8	100	VL
D8	5	110	0.13	0.1	S33	5	10	7	0.5	6.4	0.8	100	VL
D11	20	110	0.06	0.3	S62	18	10	8.2	0.5	29.8	1.7	100	VL

GRID	MAX σ [Mpa]	UCS [Mpa]	MAX PPV [m/s]	MAX M_L	Closest cluster group	E_1	E_2	E_3	E_4	EVP	RDP	Exposure	SEISMIC RISK RATING
D12:4	20	180	0.05	0.3	S62	11	10	5.5	0.5	12.2	0.7	1000	VL
D12:4	10	75	0.04	0.2	S68	13	10	5.5	0.5	14.7	0.6	1000	VL
D13	35	180	0.06	0.2	S68	19	5	6	1.5	15.6	0.9	1000	VL
D14	40	180	0.10	0.2	S68	22	5	8.6	1.5	25.5	2.7	1000	VL
D15	45	180	0.08	0.2	S68	25	5	9	1.5	30.0	2.4	1000	VL
E1	10	75	0.08	0.3	S04	13	10	6	0.5	16.0	1.3	100	VL
E2	10	75	0.06	0.3	S04	13	10	6.5	0.5	17.3	1.0	100	VL
E14	25	180	0.07	0.2	S68	14	5	6.7	1	18.6	1.2	1000	VL
E15	35	180	0.09	0.2	S68	19	5	9.6	1.5	24.9	2.1	1000	VL
E17	45	180	0.08	0.2	S68	25	5	10.3	1.5	34.3	2.7	3000	VL
F1	10	75	0.10	0.3	S04	13	6	7	0.5	31.1	3.1	1000	VL
F13	10	75	0.06	0.2	S68	13	5	5.6	0.5	29.9	1.8	100	VL
F16	40	180	0.15	0.2	S68	22	5	5.6	1.5	16.6	2.5	1000	VL
F17	50	180	0.11	0.2	S68	28	5	10.2	1.5	37.8	4.1	14000	M
G1	15	180	0.06	0.3	S04	8	5	6.4	1	10.7	0.6	1000	VL
G17	45	180	0.09	0.2	S68	25	5	6.5	1.5	21.7	1.9	1000	VL
H1	30	180	0.05	0.1	S50	17	5	6.8	1	22.7	1.2	1000	VL
H2	10	75	0.06	0.5	S24	13	6	6	0.5	26.7	1.6	1000	VL
H17	50	180	0.19	0.1	S61	28	5	6.4	1.5	23.7	4.5	1000	VL
I1	45	180	0.07	0.5	S24	25	5	6	1.5	20.0	1.4	1000	VL
I2	40	75	0.08	0.5	S24	53	6	6	1	53.3	4.1	1000	VL
I3	10	75	0.09	0.5	S24	13	5	7.6	0.5	40.5	3.5	1000	VL
I17	10	180	0.27	0.1	S61	6	6	7.8	1.5	4.8	1.3	1000	VL
J1:45	50	180	0.12	0.5	S24	28	10	11	1.5	20.4	2.5	1000	VL
J1:2	50	180	0.29	0.5	S24	28	5	5	1.5	18.5	5.3	1000	VL
J3:2	30	180	0.16	0.5	S24	17	5	10.2	0.5	68.0	11.0	1000	VL

GRID	MAX σ [Mpa]	UCS [Mpa]	MAX PPV [m/s]	MAX M_L	Closest cluster group	E_1	E_2	E_3	E_4	EVP	RDP	Exposure	SEISMIC RISK RATING
J3:4	30	180	0.12	0.5	S24	17	10	6	0.5	20.0	2.4	1000	VL
J13	10	75	0.14	-0.2	S16	13	10	8	0.5	21.3	2.9	1000	VL
J16	35	180	0.17	0.1	S61	19	6	6.5	1.5	14.0	2.4	1000	VL
K2	50	180	0.69	0.5	S24	28	6	6.5	1.5	20.1	13.8	1000	VL
K3:2	35	180	0.47	0.5	S24	19	5	6.5	1.5	16.9	7.9	1000	VL
K3:25	35	180	0.37	0.5	S24	19	6	10	1.5	21.6	8.1	1000	VL
K5	20	110	0.28	-0.3	S22	18	5	8	0.5	58.2	16.4	1000	VL
K12	10	75	0.42	0.2	S12	13	10	9.6	0.5	25.6	10.7	1000	VL
K15	10	75	0.16	-0.2	S16	13	6	5.6	1.5	8.3	1.3	1000	VL
L2	55	180	0.69	0.5	S24	31	5	7	1.5	28.5	19.7	3000	VL
L3	60	180	1.00	0.5	S24	33	6	10	1.5	37.0	37.2	3000	L
L4	60	180	1.55	0.5	S24	33	10	10.4	1.5	23.1	35.8	3000	L
L5	30	180	0.57	0.5	S24	17	5	12	0.5	80.0	45.4	1000	L
L7	45	110	1.51	0.9	S20	41	5	6	0.5	98.2	147.8	1000	M
L8	30	110	0.84	0.9	S20	27	10	5.6	0.5	30.5	25.7	1000	L
L9	30	110	0.27	0.9	S20	27	5	12.4	0.5	135.3	36.7	1000	L
L12	10	75	0.70	0.2	S12	13	6	9.1	1.5	13.5	9.4	7000	L
L13	10	75	0.84	0.2	S12	13	5	5.6	1.5	10.0	8.3	1000	VL
L14	10	75	0.26	0.2	S12	13	5	6	1.5	10.7	2.7	1000	VL
M2	50	180	0.55	0.5	S24	28	5	6	1.5	22.2	12.2	3000	VL
M3	55	180	0.80	0.5	S24	31	5	6.5	1.5	26.5	21.1	3000	VL
M4	55	180	1.73	0.5	S24	31	5	6.5	1.5	26.5	45.8	3000	L
M5:2	45	180	0.72	0.5	S24	25	5	5.6	1.5	18.7	13.5	1000	VL
M5:4	45	180	0.92	0.5	S23	25	10	9.8	1.5	16.3	15.0	1000	VL
M6	40	180	2.23	0.5	S24	22	5	5.8	1.5	17.2	38.3	1000	L
M7	40	180	1.28	0.9	S20	22	10	9.6	1.5	14.2	18.2	1000	VL

GRID	MAX σ [Mpa]	UCS [Mpa]	MAX PPV [m/s]	MAX M_L	Closest cluster group	E_1	E_2	E_3	E_4	EVP	RDP	Exposure	SEISMIC RISK RATING
M8	40	180	1.29	0.9	S20	22	5	9.2	1.5	27.3	35.2	4000	L
M9:4	35	180	1.12	0.9	S20	19	10	10.6	1.5	13.7	15.4	3000	VL
M9:2	35	180	2.38	0.9	S20	19	5	10	1.5	25.9	61.6	3000	L
M10	35	180	2.61	0.2	S12	19	5	5.2	1.5	13.5	35.2	2000	L
M11	35	180	0.92	0.2	S12	19	6	5.8	1.5	12.5	11.6	2000	VL
M12	30	180	2.57	0.2	S12	17	10	10.2	1.5	11.3	29.1	4000	L
M13	10	75	0.70	0.2	S12	13	5	5.5	1.5	9.8	6.9	1000	VL
N5	50	180	6.12	0.5	S24	28	4	5.2	1.5	24.1	147.3	100	M
N8	50	180	6.08	0.9	S20	28	4	5.6	1.5	25.9	157.6	100	M
N9	50	180	1.55	0.9	S20	28	6	5.6	1.5	17.3	26.8	3000	L
N12	60	180	0.94	1.1	S39	33	6	7.8	1.5	28.9	27.2	4000	L
N13	65	180	0.32	1.1	S39	36	5	11	1.5	53.0	16.9	4000	VL
O12	65	180	0.92	0.9	S20	36	5	7	1.5	33.7	31.0	4000	L
O13	70	180	0.28	0.9	S20	39	6	11	1.5	47.5	13.5	4000	VL
P10	60	180	1.17	0.9	S20	33	4	5	1.5	27.8	32.6	4000	L
P11	65	180	0.97	0.9	S20	36	4	6	1.5	36.1	35.2	4000	L

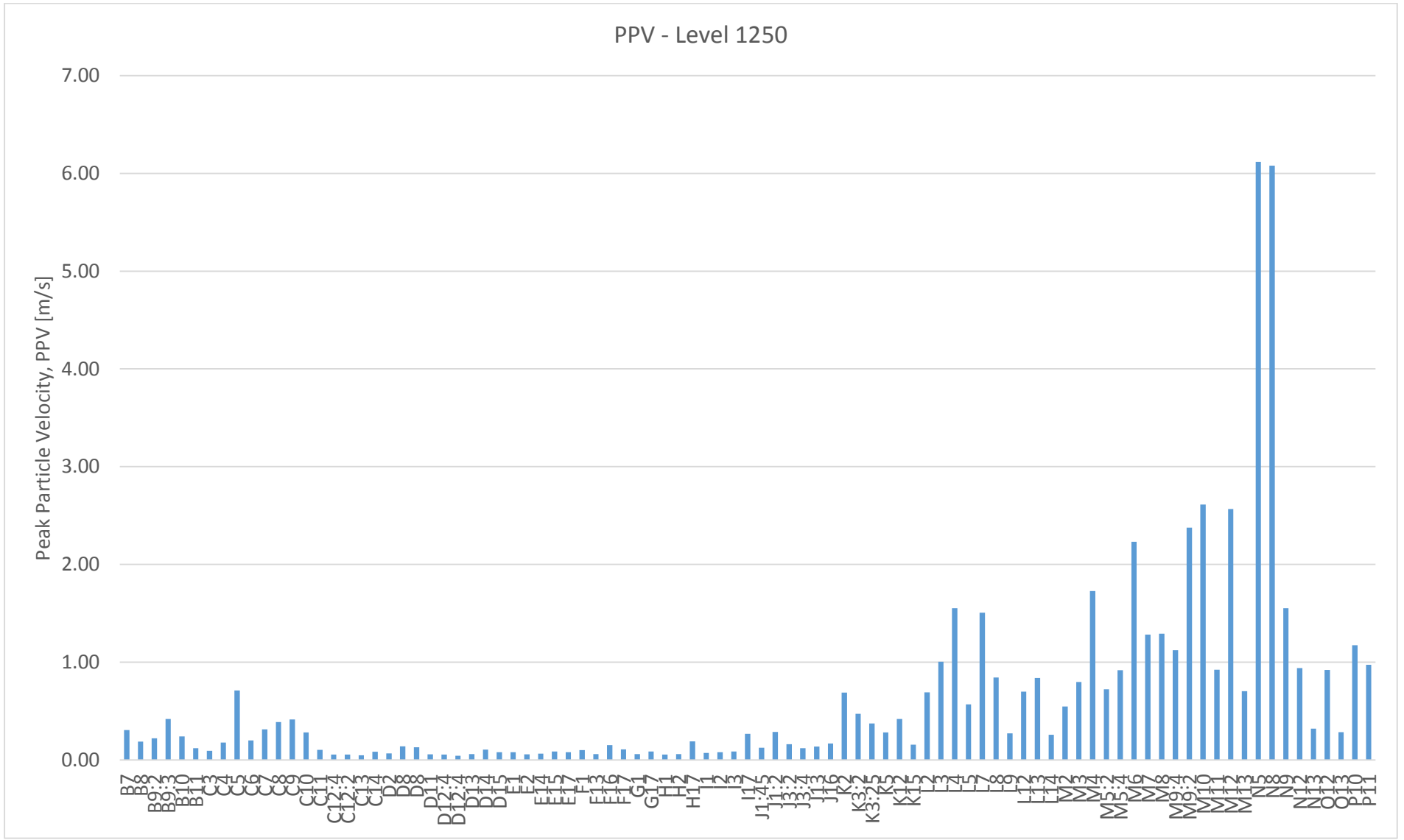
PPV - Level 1250
Peak Particle Velocity, PPV [m/s]
7.00
6.00
5.00
4.00
3.00
2.00
1.00
0.00
B7
B8
B9:2
B9:3
B10
B11
C3
C4
C5
C6
C7
C8
C9
C10
C11
C12:4
C12:5
C13
C14
D2
D8
D8
D11
D12:4
D12:4
D13
D14
D15
E1
E2
E14
E15
E17
F1
F13
E16
F17
G1
G17
H1
H2
H17
I1
I2
I3
I12
J1:45
J1:2
J3:5
J3:2
J13
J16
K2
K3:2
K3:25
K5
K12
K15
L2
L3
L4
L5
L7
L8
L9
L12
L13
L14
M2
M3
M4
M5:2
M5:4
M6
M7
M8
M9:4
M9:2
M10
M11
M12
M13
N5
N8
N9
N12
N13
O12
O13
P10
P11

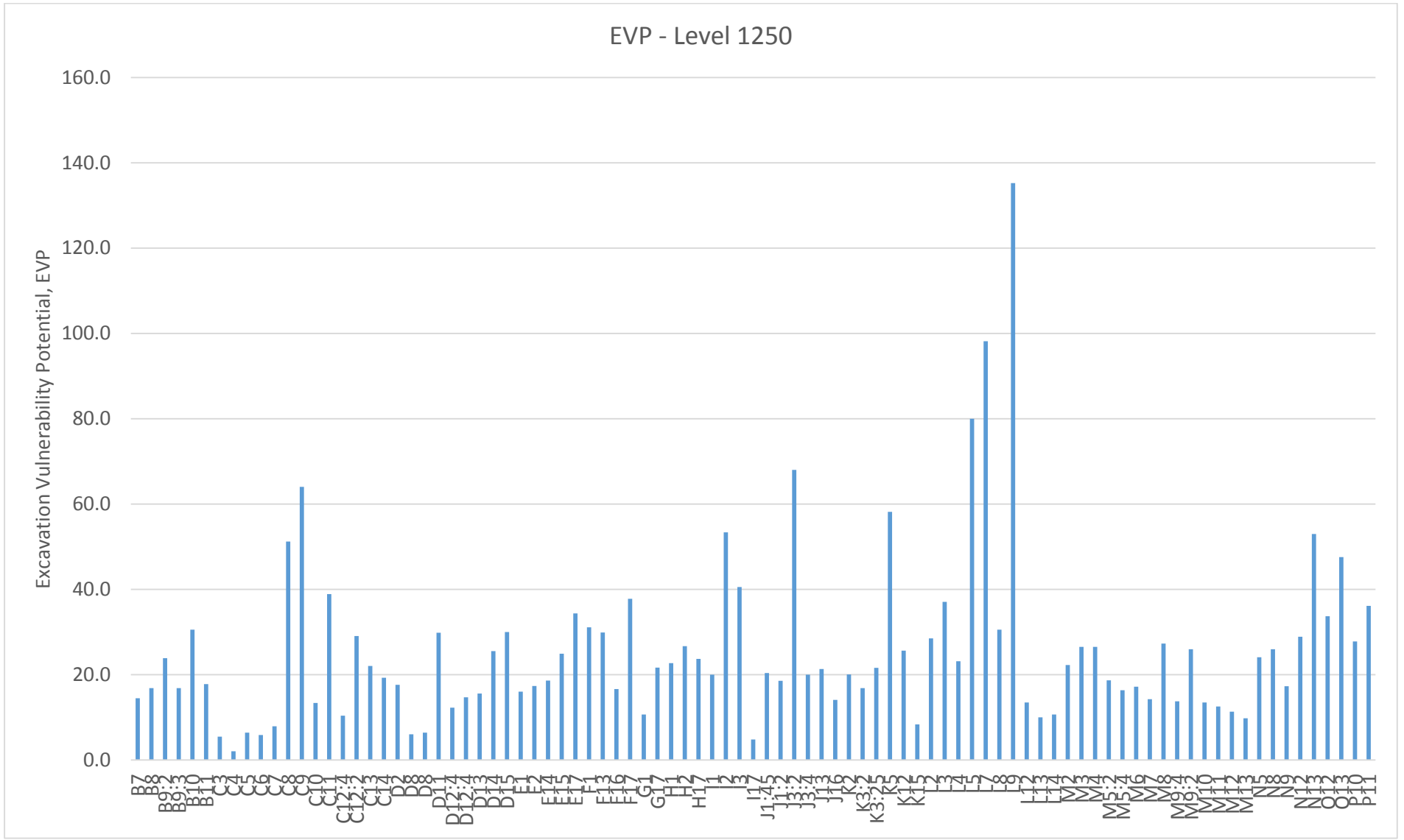
EVP - Level 1250
Excavation Vulnerability Potential, EVP
160.0
140.0
120.0
100.0
80.0
60.0
40.0
20.0
0.0
B7
B8
B9:2
B9:3
B10
B11
C3
C4
C5
C6
C7
C8
C9
C10
C11
C12:4
C12:3
C13
C14
D6
D8
D9
D11
D12:4
D12:3
D13
D14
D15
E1
E2
E14
E15
E17
F1
F13
F16
F17
G1
G17
H1
H2
H17
I1
I2
I3
I17
J1:4
J1:3
J3:2
J3:4
J13
J16
K2
K3:2
K3:25
K5
K12
K15
L3
L4
L5
L7
L8
L9
L2
L13
L14
M2
M3
M4
M5:3
M5:4
M6
M9
M8
M9:4
M9:3
M10
M11
M12
M13
N5
N8
N9
N12
N13
O13
P10
P11

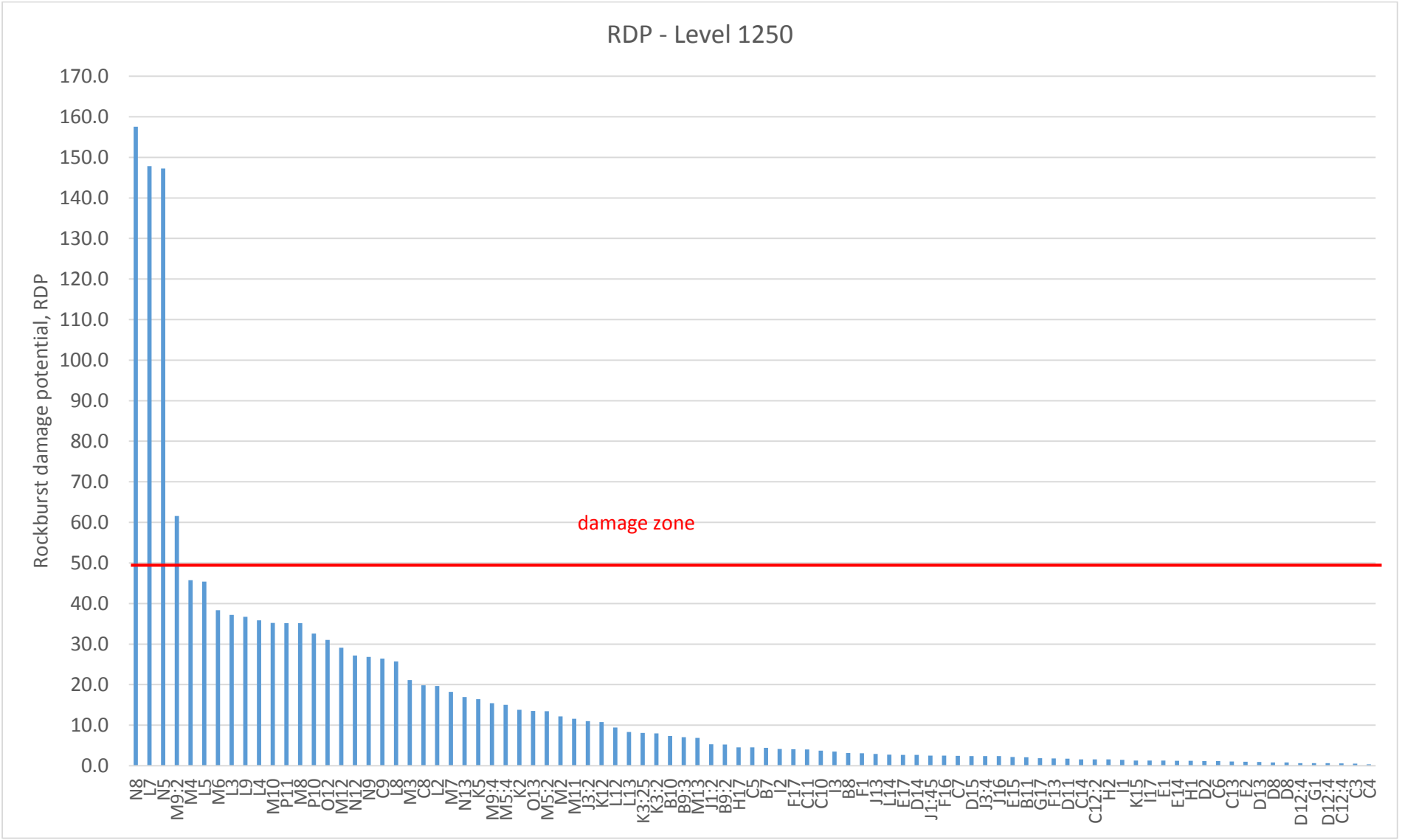
RDP - Level 1250
Rockburst damage potential, RDP
170.0
160.0
150.0
140.0
130.0
120.0
110.0
100.0
90.0
80.0
70.0
60.0
50.0
40.0
30.0
20.0
10.0
0.0
damage zone
N8 L7 N5 M9:2 M4 L5 M6 L3 L9 L4 M10 P11 M8 P10 O12 M12 N12 N9 C9 L8 M3 C8 L2 M7 N13 K5 M9:4 M5:4 K2 O13 M5:2 M2 M11 J3:2 K12 L12 L13 K3:2:5 K3:2 B10 B9:3 M13 J1:2 B9:2 H17 C5 B7 I2 F17 C11 C10 I3 B8 F1 J13 L14 E17 D14 J1:45 F16 C7 D15 J3:4 J16 E15 B11 G17 F13 D11 C14 C12:2 H2 I1 K15 I17 E1 E14 H1 D2 C6 C13 E2 D13 D8 D8 D12:4 G1 D12:4 C12:4 C3 C4

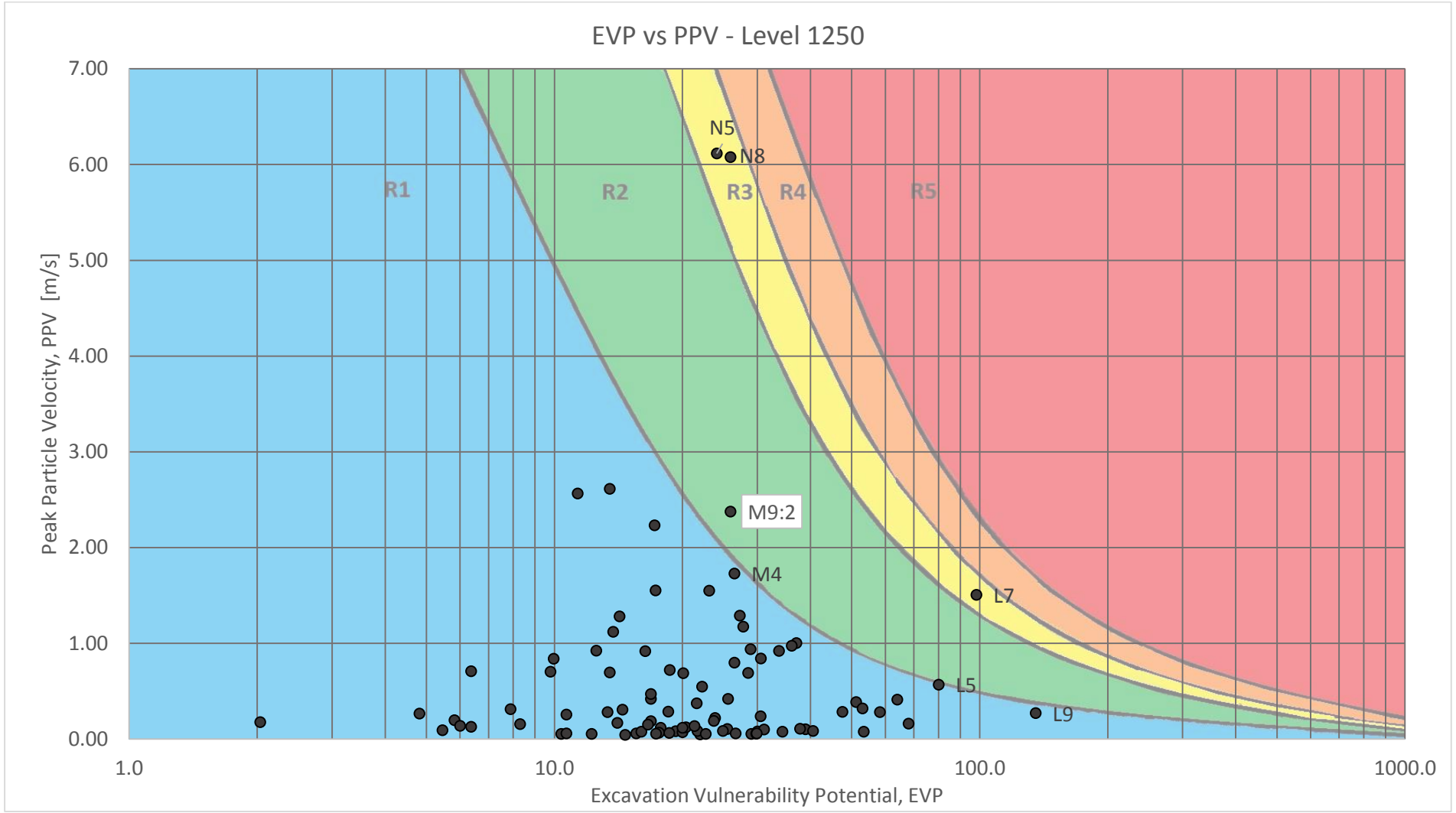
EVP vs PPV - Level 1250
Peak Particle Velocity, PPV [m/s]
7.00
6.00
5.00
4.00
3.00
2.00
1.00
0.00
1.0
10.0
100.0
1000.0
Excavation Vulnerability Potential, EVP
R1
R2
R3
R4
R5
N5
N8
M9:2
M4
L7
L5
L9

c. Level 1275

Table D-3. Results of seismic risk assessment using QSHRAF for mining level 1275.

GRID	MAX σ [MPa]	UCS [MPa]	MAX PPV [m/s]	MAX M_L	Closest cluster group	E_1	E_2	E_3	E_4	EVP	RDP	Exposure	SEISMIC RISK RATING
E0	15	75	0.08	0.3	S04	20	6	6.6	0.5	44.0	3.6	1000	VL
F0	25	180	0.08	0.3	S04	14	6	6.2	1.5	9.6	0.8	1000	VL
F1	35	75	0.07	0.3	S04	47	5	6.6	0.5	123.2	8.0	1000	VL
G0	35	180	0.05	0.3	S04	19	6	11	1.5	23.8	1.3	1000	VL
H0	40	180	0.04	0.6	S10	22	5	6.5	1.5	19.3	0.8	1000	VL
H1	25	110	0.05	0.1	S41	23	5	5.6	0.5	50.9	2.7	1000	VL
I0	40	180	0.06	0.1	S41	22	5	11	1.5	32.6	1.9	1000	VL
I1:2	25	180	0.07	0.1	S41	14	5	6.3	1.5	11.7	0.8	1000	VL
I1:25	25	180	0.23	0.1	S41	14	6	6.2	0.5	28.7	6.7	1000	VL
J1:2	50	180	0.26	0.1	S41	28	5	5.2	1.5	19.3	5.0	1000	VL
J1:45	45	180	0.38	0.1	S41	25	10	11	1.5	18.3	7.0	1000	VL
J2:25	30	180	0.36	0.1	S41	17	6	6.4	0.5	35.6	12.7	1000	VL
J2:2	30	180	0.17	0.1	S41	17	5	6	0.5	40.0	6.6	1000	VL
J13	15	75	0.08	1.1	S39	20	6	7	0.5	46.7	3.7	100	VL
K2	50	180	0.31	0.1	S41	28	10	9.4	0.5	52.2	16.4	1000	VL
K3	65	110	0.51	0.5	S24	59	6	6.5	0.5	128.0	64.8	1000	L
K4	30	110	0.38	0.5	S24	27	6	6	0.5	54.5	20.9	1000	VL
K5	35	110	0.21	0.5	S24	32	10	6.1	0.5	38.8	8.1	1000	VL
K10	25	110	0.82	0.2	S12	23	10	6	0.5	27.3	22.3	1000	VL
K12	15	75	0.25	0.2	S12	20	10	6.3	0.5	25.2	6.2	1000	VL
K13	15	75	0.10	1.1	S39	20	6	6	1.5	13.3	1.3	1000	VL
L2:2	65	180	0.39	0.5	S24	36	5	7	1.5	33.7	13.3	1000	VL

GRID	MAX σ [MPa]	UCS [MPa]	MAX PPV [m/s]	MAX M_L	Closest cluster group	E_1	E_2	E_3	E_4	EVP	RDP	Exposure	SEISMIC RISK RATING
L2:45	85	180	0.69	0.5	S24	47	10	6.6	1	31.2	21.5	1000	VL
L3	85	180	1.21	0.5	S24	47	10	9.4	1	44.4	53.6	2000	L
L4:45	65	180	0.85	0.5	S24	36	10	10	1.5	24.1	20.5	1000	VL
L4:25	60	180	0.47	0.5	S24	33	6	6	1	33.3	15.7	1000	VL
L5:45	50	180	0.42	0.5	S24	28	10	10.7	0.5	59.4	24.9	1000	VL
L5:2	50	180	0.27	-0.1	S27	28	5	6	0.5	66.7	17.9	1000	VL
L6	45	180	0.35	0.9	S20	25	6	5.4	0.5	45.0	15.6	1000	VL
L9:4	45	180	0.22	0.9	S08	25	10	10.6	0.5	53.0	11.4	2000	VL
L9:45	40	180	0.33	0	S76	22	10	6.4	0.5	28.4	9.5	2000	VL
L10	45	180	0.34	0.2	S12	25	10	6.2	1	15.5	5.3	2000	VL
L11	25	180	0.72	0.2	S12	14	10	6.1	1	8.5	6.1	1000	VL
L13	15	180	0.14	0.2	S12	8	5	7.6	1.5	8.4	1.2	1000	VL
M2	65	180	1.03	0.5	S24	36	5	12	1.5	57.8	59.5	2000	L
M3	65	180	2.47	0.5	S24	36	5	6.5	1.5	31.3	77.3	2000	M
M4	80	180	0.76	0.5	S24	44	5	5.2	1.5	30.8	23.3	2000	VL
M5	60	180	0.36	-0.1	S27	33	10	5.5	1.5	12.2	4.4	2000	VL
M6	60	180	1.49	0.9	S20	33	10	12	1.5	26.7	39.8	4000	L
M7:45	60	180	0.98	0.9	S20	33	10	9.4	1.5	20.9	20.4	2000	VL
M7:4	60	180	1.98	0.9	S20	33	10	5.2	1.5	11.6	22.9	2000	VL
M8	55	180	0.42	0.9	S20	31	6	5.4	1.5	18.3	7.7	2000	VL
M9:45	50	180	0.60	0.2	S12	28	10	13	1.5	24.1	14.3	2000	VL
M9:25	45	180	0.45	0.2	S12	25	6	13	1.5	36.1	16.4	2000	VL
M10	50	180	0.85	0.2	S12	28	10	10.5	1.5	19.4	16.4	3000	VL
M11	60	180	0.93	0.2	S12	33	10	12.2	1.5	27.1	25.3	3000	L
M12	45	180	0.30	0.2	S12	25	10	5.4	1.5	9.0	2.7	1000	VL

GRID	MAX σ [MPa]	UCS [MPa]	MAX PPV [m/s]	MAX M_L	Closest cluster group	E_1	E_2	E_3	E_4	EVP	RDP	Exposure	SEISMIC RISK RATING
N2	60	180	0.66	0.5	S24	33	5	6.3	1.5	28.0	18.4	1000	VL
N6	60	180	1.67	0.9	S20	33	5	5.5	1.5	24.4	40.9	4000	L
N7	60	180	1.57	0.9	S20	33	4	8.6	1.5	47.8	75.2	100	L
N9	60	180	1.15	0.2	S12	33	6	6	1.5	22.2	25.7	1000	L
N10	60	180	1.51	0.2	S12	33	6	8.5	1.5	31.5	47.5	1000	L
N11	65	180	0.70	0.2	S12	36	10	6	1.5	14.4	10.2	3000	VL
O6	60	180	0.60	0.9	S20	33	5	6	1.5	26.7	16.1	4000	VL
O10	65	180	1.13	0.2	S12	36	10	6	1.5	14.4	16.3	3000	VL
P6	65	180	0.19	1.1	S39	36	5	6.1	1.5	29.4	5.5	4000	VL
Q6	65	180	0.16	1.1	S39	36	5	6	1.5	28.9	4.5	4000	VL
R6	65	180	0.10	1.1	S39	36	5	6.6	1.5	31.8	3.3	4000	VL
R7:2	65	180	0.13	0.9	S20	36	5	11	1.5	53.0	7.1	4000	VL
R7:1	65	180	0.16	0.9	S20	36	4	10	1.5	60.2	9.8	4000	VL
R8	65	180	0.09	0.9	S08	36	4	5.8	1.5	34.9	3.3	4000	VL
S6	65	180	0.12	0.9	S20	36	5	7.2	1.5	34.7	4.0	4000	VL
S7	65	180	0.20	0.9	S20	36	4	10.8	1.5	65.0	12.8	4000	VL
T6	65	180	0.10	0.9	S20	36	5	6.4	1.5	30.8	3.2	4000	VL

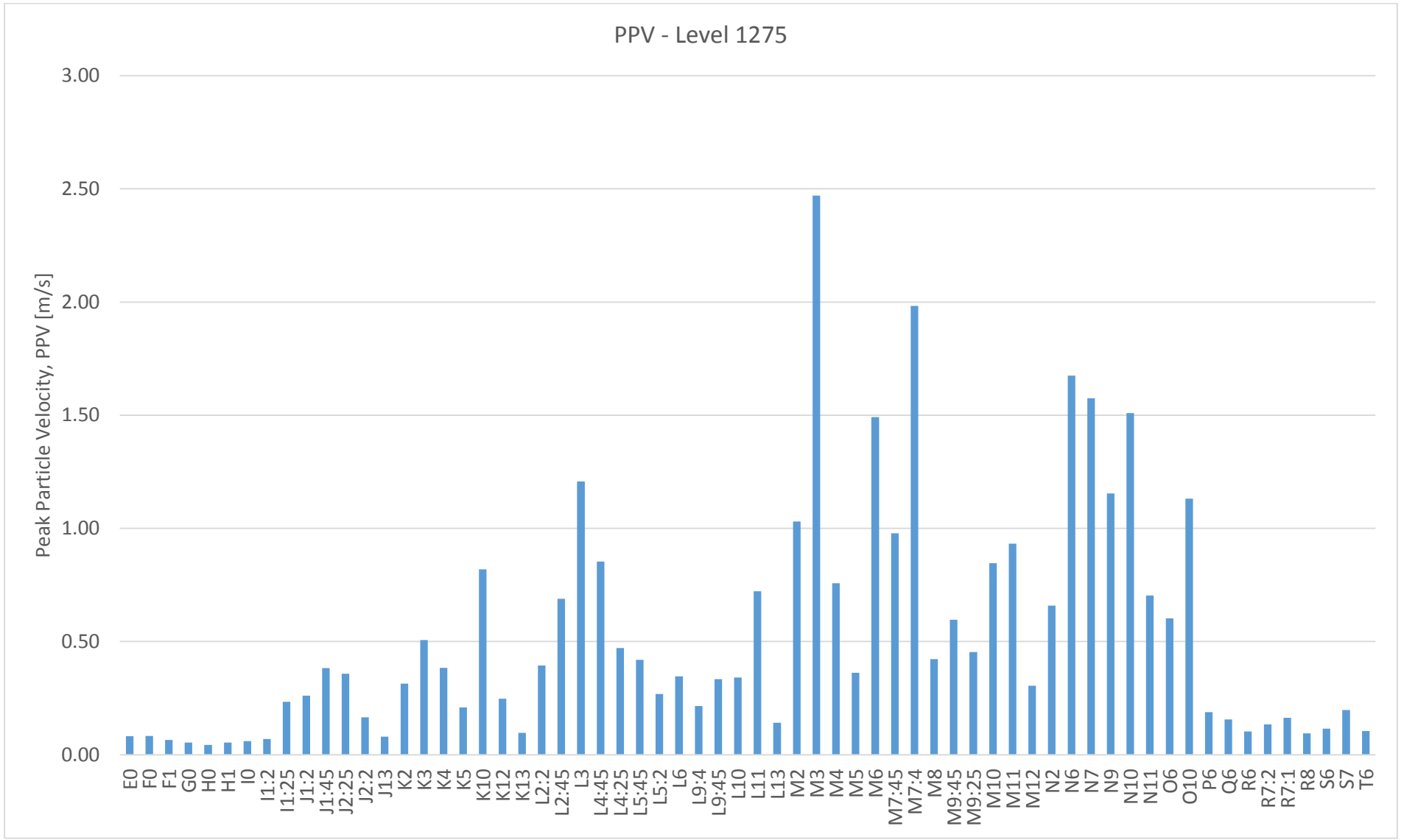
PPV - Level 1275
Peak Particle Velocity, PPV [m/s]
3.00
2.50
2.00
1.50
1.00
0.50
0.00
E0
F0
F1
G0
H0
H1
I0
I1:2
I1:25
J1:2
J1:45
J2:25
J2:2
J13
K2
K3
K4
K5
K10
K12
K13
L2:2
L2:45
L3
L4:45
L4:25
L5:45
L5:2
L6
L9:4
L9:45
L10
L11
L13
M2
M3
M4
M5
M6
M7:45
M7:4
M8
M9:45
M9:25
M10
M11
M12
N2
N6
N7
N9
N10
N11
O6
O10
P6
Q6
R6
R7:2
R7:1
R8
S6
S7
T6

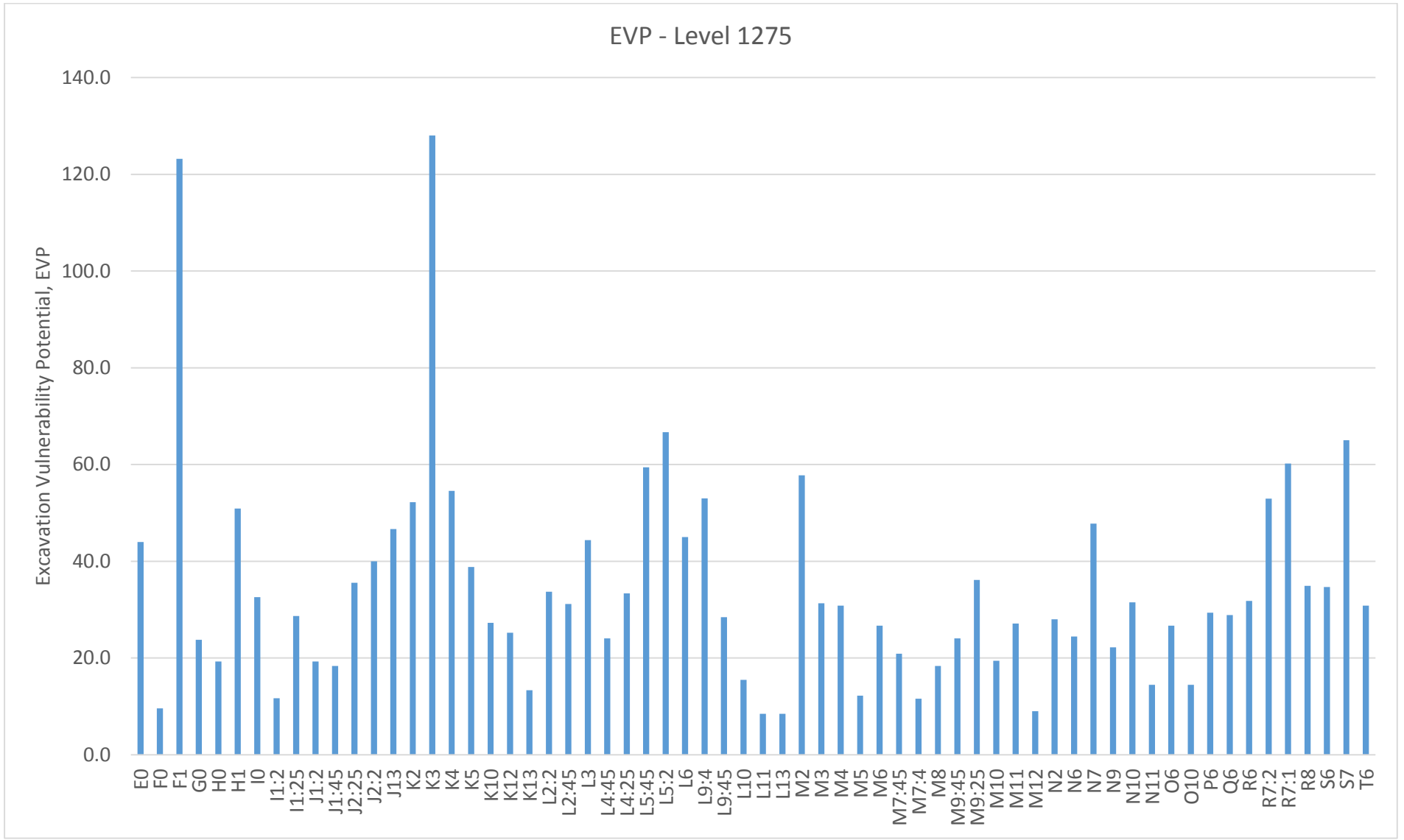
EVP - Level 1275
Excavation Vulnerability Potential, EVP
140.0
120.0
100.0
80.0
60.0
40.0
20.0
0.0
E0
F0
F1
G0
H0
H1
I0
I1:2
I1:25
J1:2
J1:45
J2:25
J2:2
J13
K2
K3
K4
K5
K10
K12
K13
L2:2
L2:45
L3
L4:45
L4:25
L5:45
L5:2
L6
L9:4
L9:45
L10
L11
L13
M2
M3
M4
M5
M6
M7:45
M7:4
M8
M9:45
M9:25
M10
M11
M12
N2
N6
N7
N9
N10
N11
O6
O10
P6
Q6
R6
R7:2
R7:1
R8
S6
S7
T6

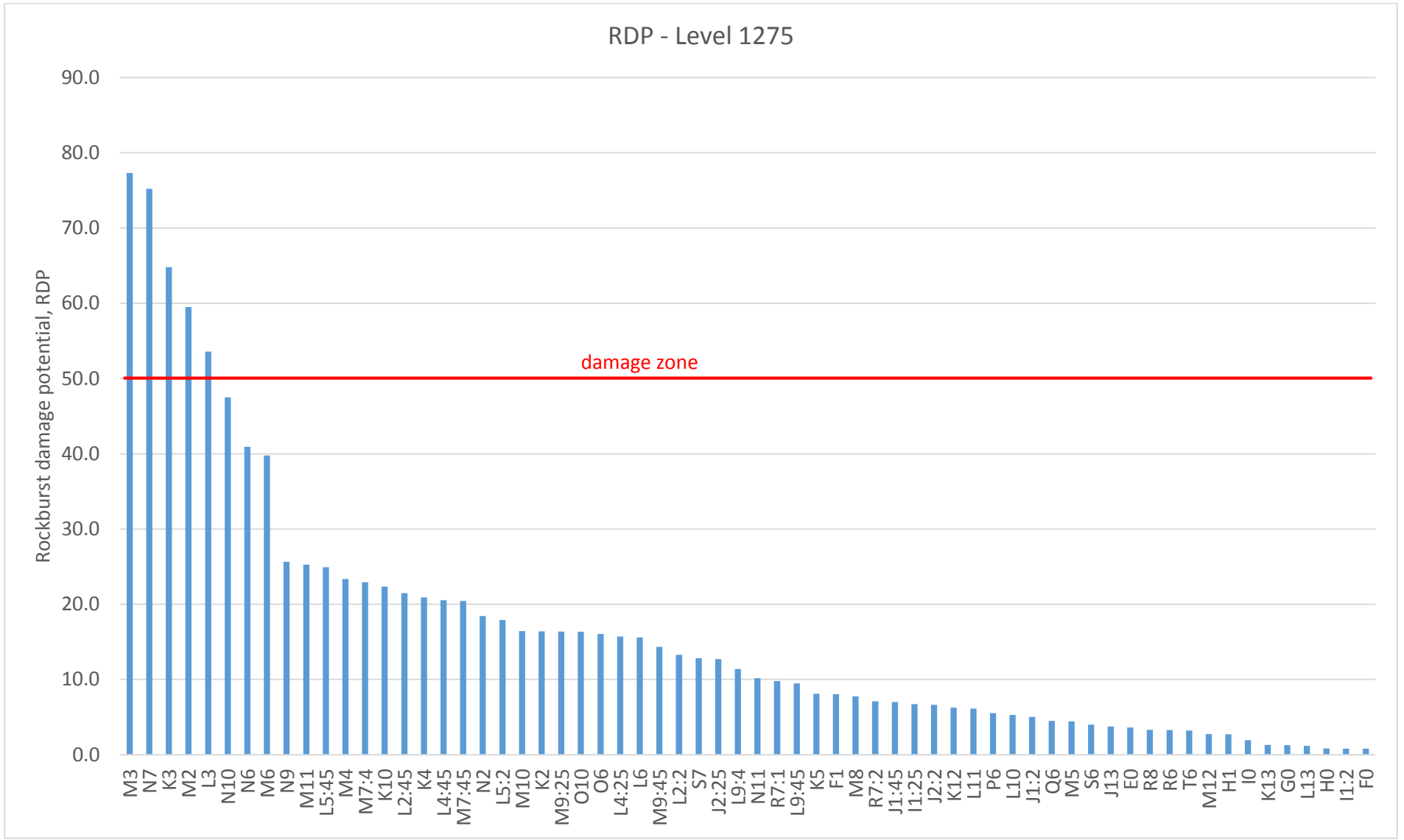
RDP - Level 1275
Rockburst damage potential, RDP
90.0
80.0
70.0
60.0
50.0
40.0
30.0
20.0
10.0
0.0
damage zone
M3
N7
K3
M2
L3
N10
N6
M6
N9
M11
L5:45
M4
M7:4
K10
L2:45
K4
L4:45
M7:45
N2
L5:2
M10
K2
M9:25
O10
O6
L4:25
L6
M9:45
L2:2
S7
J2:25
L9:4
N11
R7:1
L9:45
K5
F1
M8
R7:2
J1:45
I1:25
J2:2
K12
L11
P6
L10
J1:2
Q6
M5
S6
J13
E0
R8
R6
T6
M12
H1
I0
K13
G0
L13
H0
I1:2
F0

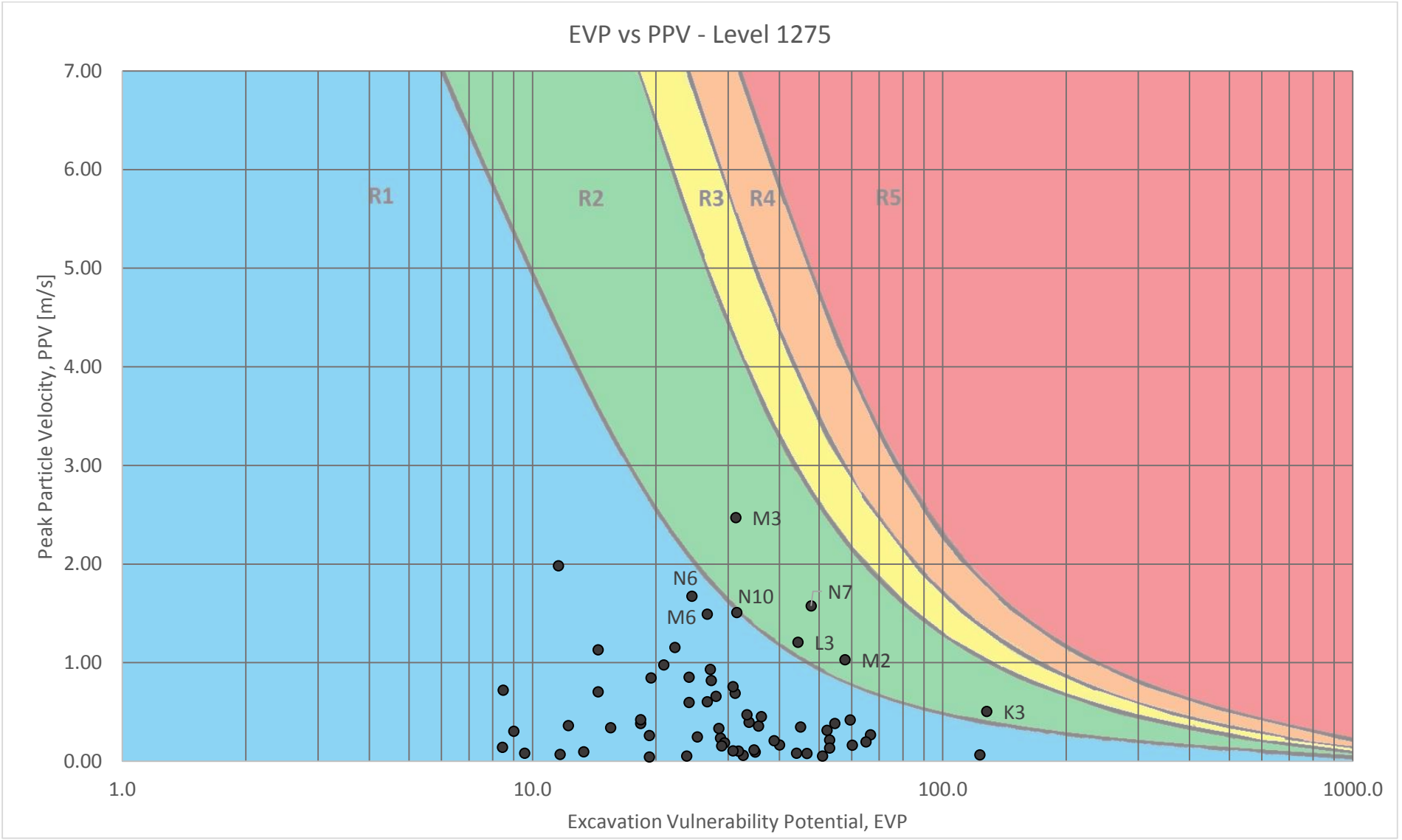
EVP vs PPV - Level 1275
Peak Particle Velocity, PPV [m/s]
7.00
6.00
5.00
4.00
3.00
2.00
1.00
0.00
R1
R2
R3
R4
R5
M3
N6
N10
N7
M6
L3
M2
K3
1.0
10.0
100.0
1000.0
Excavation Vulnerability Potential, EVP

E Seismic risk mitigation

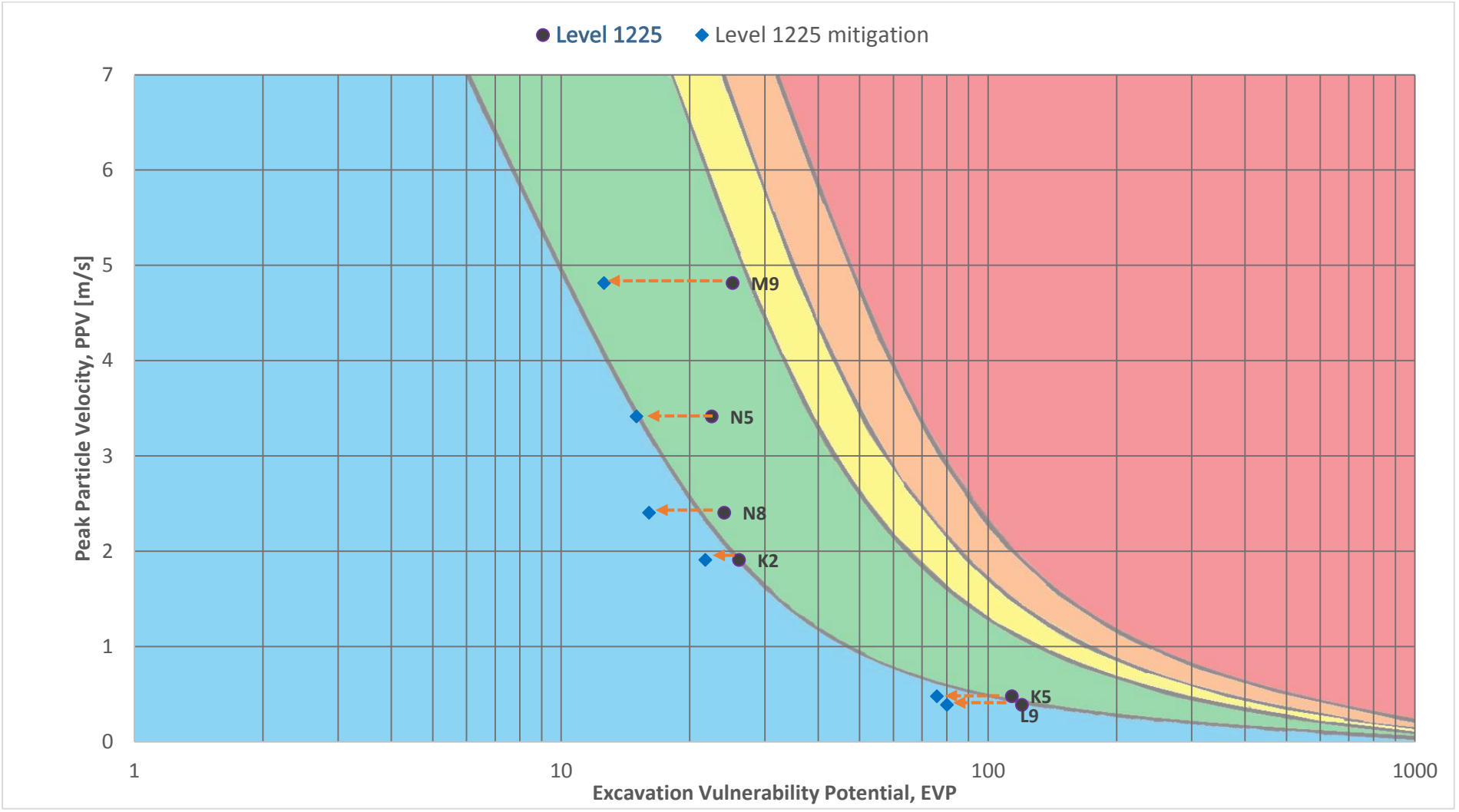

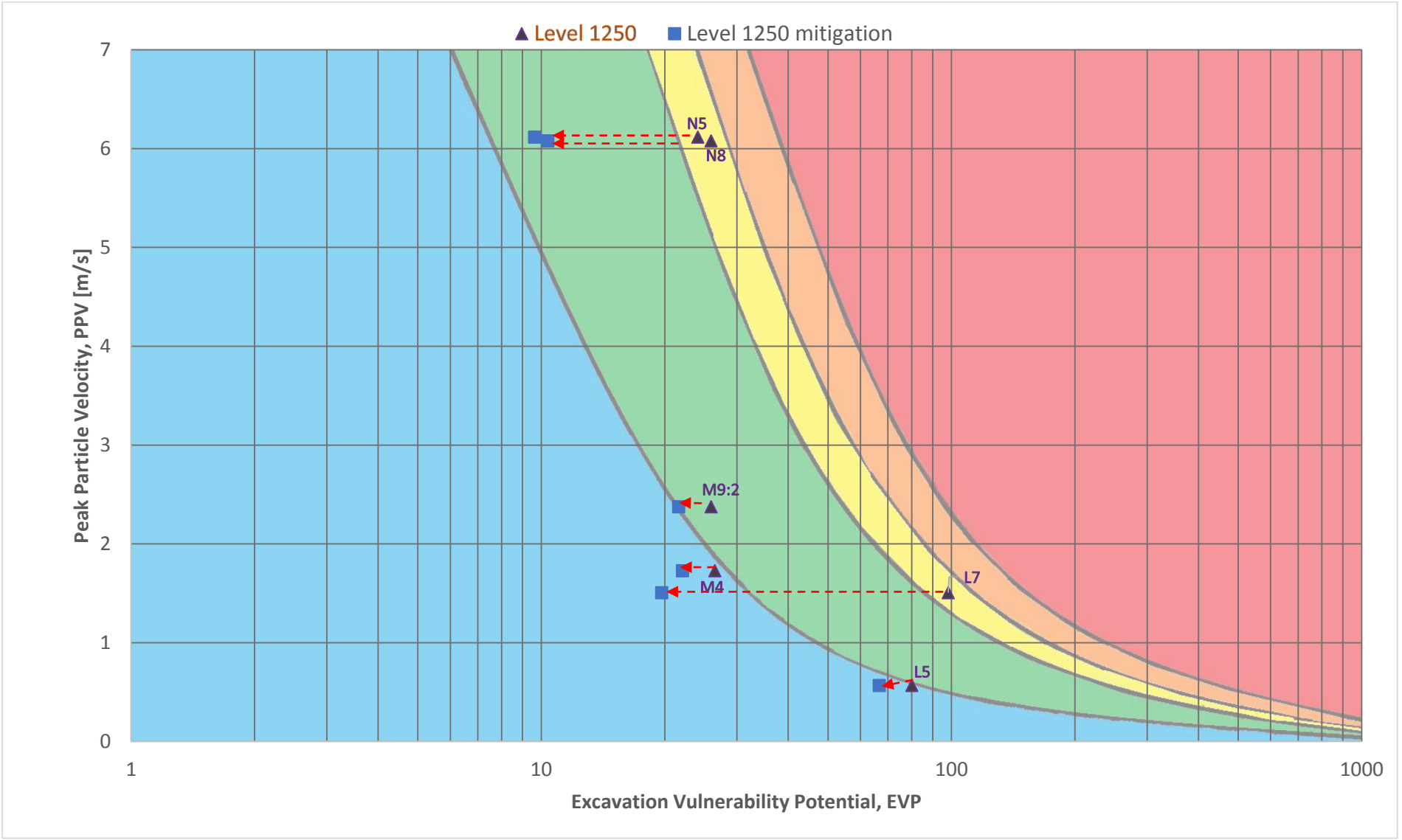
Level 1250
Level 1250 mitigation
N5
N8
M9:2
M4
L7
L5
Peak Particle Velocity, PPV [m/s]
Excavation Vulnerability Potential, EVP
0
1
2
3
4
5
6
7
1
10
100
1000

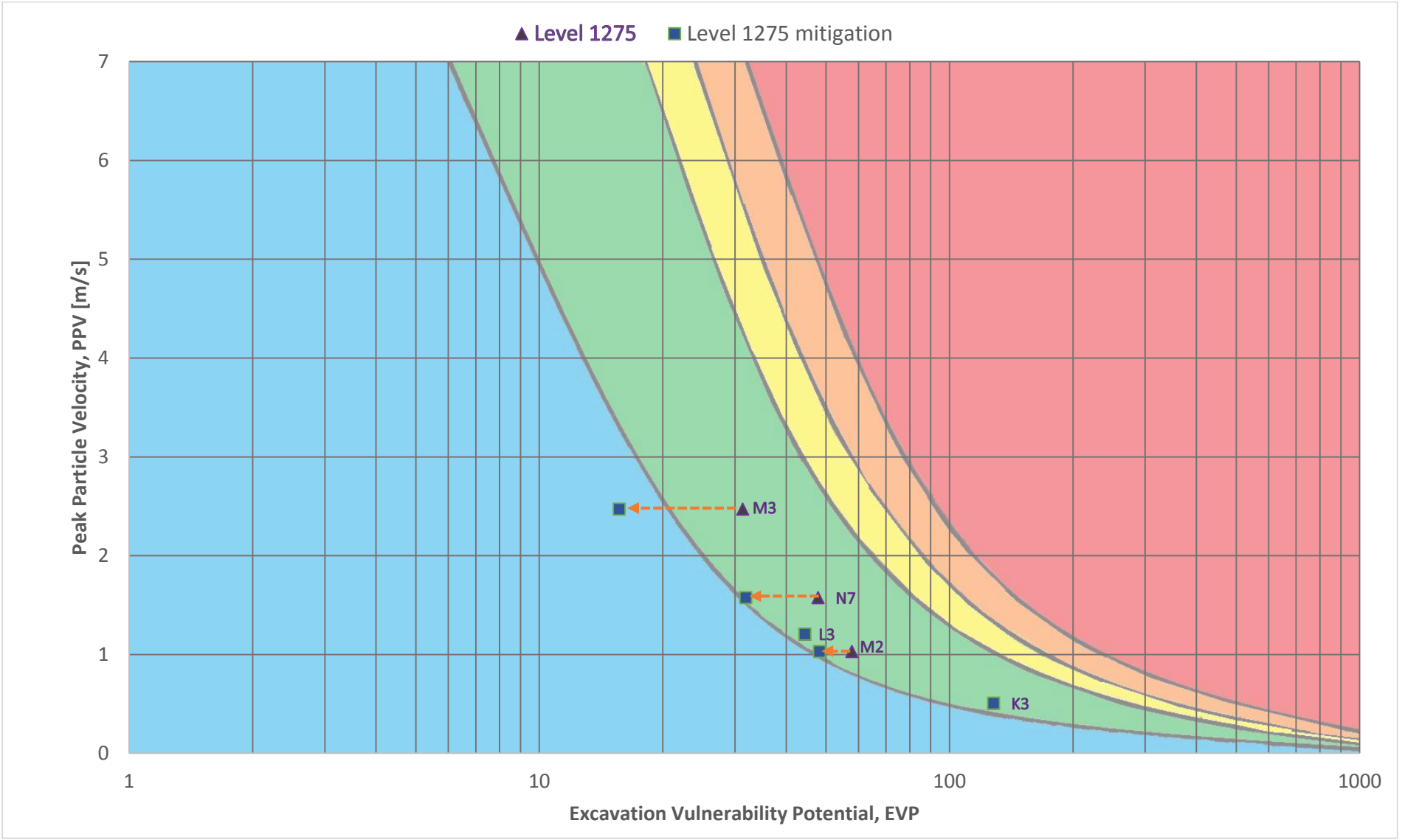
Level 1275
Level 1275 mitigation
Peak Particle Velocity, PPV [m/s]
0
1
2
3
4
5
6
7
1
10
100
1000
Excavation Vulnerability Potential, EVP
M3
N7
L3
M2
K3